FEDERAL UNIVERSITY OF ITAJUBÁ
POSTGRADUATE PROGRAM IN
ELECTRICAL ENGINEERING

STUDY OF ARTIFICIAL INTELLIGENCE AND COMPUTER VISION METHODS FOR TRACKING TRANSMISSION LINES WITH THE AID OF UAVs

WANDER MENDES MARTINS

Itajubá, December 14, 2023

FEDERAL UNIVERSITY OF ITAJUBÁ
POSTGRADUATE PROGRAM IN ELECTRICAL ENGINEERING

WANDER MENDES MARTINS

STUDY OF ARTIFICIAL INTELLIGENCE AND COMPUTER VISION METHODS FOR TRACKING TRANSMISSION LINES WITH THE AID OF UAVs

Thesis submitted to POSTGRADUATE PROGRAM IN ELECTRICAL ENGINEERING as part of the requirements for obtaining the Title of Doctor in ELECTRICAL ENGINEERING.

Concentration Area: Automation and Industrial Electrical Systems

Supervisor: Prof. DSc. Tales Cleber Pimenta
Co-supervisor: Prof. DSc. Alexandre Carlos Brandão Ramos

2023
Itajubá

FEDERAL UNIVERSITY OF ITAJUBÁ
POSTGRADUATE PROGRAM IN
ELECTRICAL ENGINEERING

STUDY OF ARTIFICIAL INTELLIGENCE AND COMPUTER VISION METHODS FOR TRACKING TRANSMISSION LINES WITH THE AID OF UAVs

WANDER MENDES MARTINS

Thesis evaluated by an examining board in 11 of December of 2023.

Examining Board:
Prof. DSc. Tales Cleber Pimenta, UNIFEI (Supervisor)
Prof. DSc. Alexandre Carlos Brandão Ramos, UNIFEI (Co-supervisor)
Prof. DSc. Elcio Hideiti Shiguemori, external member - IEAv
Prof. DSc. Hildebrando Ferreira de Castro Filho, external member - Acelen
Prof. DSc. Gabriel Antonio Fanelli de Souza, member - UNIFEI
Prof. DSc. Robson Luiz Moreno, member - UNIFEI

Itajubá
2023

WANDER MENDES MARTINS
STUDY OF ARTIFICIAL INTELLIGENCE AND COMPUTER VISION METHODS FOR TRACKING TRANSMISSION LINES WITH THE AID OF UAVs/ WANDER MENDES MARTINS. – Itajubá, December 14, 2023-
115 p. : il. (some color.) ; 30 cm.

Supervisor: Prof. DSc. Tales Cleber Pimenta

Thesis (Doutorado)
Federal University of Itajubá
POSTGRADUATE PROGRAM IN ELECTRICAL ENGINEERING, December 14, 2023.

1. Computer Vision. 2. Object Tracking. 3. Artificial Intelligence. I. Supervisor Prof. PhD. Tales Cleber Pimenta. II. Co-supervisor Prof. PhD. Alexandre Carlos Brandão Ramos. III. Federal University of Itajubá. IIV. PPG-EE. V. STUDY OF ARTIFICIAL INTELLIGENCE AND COMPUTER VISION METHODS FOR TRACKING TRANSMISSION LINES WITH THE AID OF UAVs
CDU 07:181:009.3

WANDER MENDES MARTINS

STUDY OF ARTIFICIAL INTELLIGENCE AND COMPUTER VISION METHODS FOR TRACKING TRANSMISSION LINES WITH THE AID OF UAVs

Thesis submitted to POSTGRADUATE PROGRAM IN ELECTRICAL ENGINEERING as part of the requirements for obtaining the Title of Doctor in ELECTRICAL ENGINEERING.

Approved work. Itajubá, 11 of December of 2023:

Prof. DSc. Tales Cleber Pimenta
Supervisor

Prof. DSc. Alexandre Carlos Brandão Ramos Co-supervisor

Prof. DSc. Elcio Hideiti Shiguemori, external member - IEAv

Prof. DSc. Hildebrando Ferreira de Castro Filho, external member - Acelen

---

Prof. DSc. Gabriel Antonio Fanelli de Souza, member - UNIFEI

Prof. DSc. Robson Luiz Moreno, member - UNIFEI

Itajubá
December 14, 2023

Acknowledgements

I dedicate this work to my dear mother Maria Aparecida Domingues Pinto Alves (*in memoriam*), my maternal grandparents, Joaquim Domingues Pinto and Maria José Pinto, my sisters Walkíria and Waleska, my nephews Gustavo and Julliano, whom I thank for their support in all aspects of my life.

I also dedicate it to my wonderful children Brena, Fernanda, Ana Paula, Bárbara, Geovana, Jean, Isabela, Gabriel, Beatriz, Nícolas, Lavínia and Rebeca, and to my lovely ex-wife Yolanda Daniela, and I thank them for giving me time with them to carry out this work.

I thank my great friend Jefferson Muniz Canto for supporting commercial issues in Rio de Janeiro during my master's and doctorate studies in Minas Gerais.

For the encouragement and financial support, I would like to thank my friends, the couple Aprígio Pereira do Carmo and Maria de Fátima Simplício do Carmo, businesswoman Silvana Teixeira de Figueiredo Tavares, and businessman Nilson Henrique Batista de Souza.

With special affection given to my unforgettable friend, philosophical conversations, fights, laughter and great moments together, José Antônio "Teixeira" (in memorian).

Thank you to the teachers and friends who helped me with the first steps in the direction that brought me to this moment, Carlos Honório Areas Pinheiro (UAM), Paulo Cesar Guimarães (UNIFEI) (in memorian), Henrique Otavio Queiroz de Aquino (EEL-USP), João Bosco Schumann Cunha (UNIFEI), Edison Oliveira de Jesus (UNIFEI), Sdnei de Brito Alves (in memorian) and Denise Pinheiro.

I thank all my colleagues from the Multimedia and Interactivity Laboratory (LMI) and the Black Bee team, both from the Federal University of Itajubá (UNIFEI) and, in particular, my friends Antonio Josivaldo Dantas Filho, Leandro Diniz de Jesus and Nicole Monteiro, for all the help and support in the experiments carried out.

To my supervisors, Prof. DSc. Tales Cleber Pimenta and Prof. DSc. Alexandre Carlos Brandão Ramos, I thank you for your friendship, trust, attention, reviews and suggestions for this dissertation, and for all your generous support during this learning journey.

I thank the members of the Examining Board for their willingness to analyze, evaluate and enrich this work with their experience and valued professional opinion.

I woukd also thank the Coordination of the National Council for Scientific and Technological Development (CNPq), for the extremely important financial support granted, without which it would have been impossible to even begin this endeavor.

Finally, but with the same gratitude and affection, I thank all those who in some way contributed to the completion of this work, directly or indirectly, such as UNIFEI public servants, outsourced workers and others.

Thank you!

"A wise person is someone who knows the limits of their own ignorance."
(Socrates)

Abstract

Currently, Unmanned Aerial Vehicles (UAVs) have been used in the most diverse applications in both the civil and military sectors. In the civil sector, aerial inspection services have been gaining a lot of attention, especially in the case of inspections of high voltage electrical systems transmission lines. This type of inspection involves a helicopter carrying three or more people (technicians, pilot, etc.) flying over the transmission line along its entire length which is a dangerous service especially due to the proximity of the transmission line and possible environmental conditions (wind gusts, for example). In this context, the use of UAVs has shown considerable interest due to their low cost and safety for transmission line inspection technicians. This work presents research results related to the application of UAVs for transmission lines inspection, autonomously, allowing the identification of invasions of the transmission line area as well as possible defects in components (cables, insulators, connection, etc.) through the use of Convolutional Neural Networks (CNN) for fault detection and identification. This thesis proposes the development of an autonomous system to track power transmission lines using UAVs efficiently and with low implementation and operation costs, based exclusively on rea-time image processing that identifies the structure of the towers and transmission lines durin the flight and controls the aircraft´s movements, guiding it along the closest possible path. A sumary of the work developed will be presented in the next sections.

Keywords: *UAV Application; Convolutional Neural Network; Aerial Inspection.*

Resumo

Atualmente, os Veículos Aéreos Não Tripulados – VANTs têm sido utilizados nas mais diversas aplicações tanto no setor civil quanto militar. No setor civil, os serviços de inspeção aérea vêm ganhando bastante atenção, principalmente no caso de inspeções de linhas de transmissão de sistemas elétricos de alta tensão. Este tipo de inspeção envolve um helicóptero transportando três ou mais pessoas (técnicos, pilotos, etc.) sobrevoando a linha de transmissão em toda a sua extensão, o que constitui um serviço perigoso principalmente pela proximidade da linha de transmissão e possíveis condições ambientais (rajadas de vento, por exemplo). Neste contexto, a utilização de VANTs tem demonstrado considerável interesse devido ao seu baixo custo e segurança para técnicos de inspeção de linhas de transmissão. Este trabalho apresenta resultados de pesquisas relacionadas à aplicação de VANTs para inspeção de linhas de transmissão, de forma autônoma, permitindo a identificação de invasões da área da linha de transmissão bem como possíveis defeitos em componentes (cabos, isoladores, conexões, etc.) através do uso de Convolucional. Redes Neurais - CNN para detecção e identificação de falhas. Esta tese propõe o desenvolvimento de um sistema autônomo para rastreamento de linhas de transmissão de energia utilizando VANTs de forma eficiente e com baixos custos de implantação e operação, baseado exclusivamente no processamento de imagens em tempo real que identifica a estrutura das torres e linhas de transmissão durante o voo e controla a velocidade da aeronave. movimentos, guiando-o pelo caminho mais próximo possível. Um resumo do trabalho desenvolvido será apresentado nas próximas seções.

Palavras-chaves: Aplicações com VANT; Rede Neural Convolucional; Inspeção Aérea;

List of Figures

List of Tables

List of Algorithms

*

List of symbols

A	- ampere
C	- discharge rate C-rate
cm	- centimeter
D	- distance between two colors
g	- gram
GB	- giga byte
GHz	- giga hertz
Hz	- hertz
kg	- Kilogram
kV	- Kilovolt
L	- degree of luminosity
m	- meter
M	- mega
mm	- milímeter
Mp	- mega pixels
mAh	- miliampere-hour
t	- width
%	- percentage
$*$	- multiplication
$<-$	- assignment

Acronyms

2D With two dimensions, two-dimensional. 38

3D With three dimensions, three-dimensional. 36, 38

4D With four dimensions, four-dimensional. 36

A Ampere. 90

AI Artificial Intelligence. 46

AIS Artificial Immune Systems. 46

ANAC Agência Nacional de Aviação Civil. 40–42

Anatel Brazilian National Telecommunications Agency. 47

ANEEL Brazilian National Electric Energy Agency. 25

ANN Artificial Neural Network. 54

API Application Programming Interface. 52, 54

CBM Condition Based Maintenance. 25

CEMIG Minas Gerais State Energy Company. 24

CIACO Cluster-enhanced Ant-colony Optimization Algorithm. 36

CNN Convolutional Neural Network. 54, 55

DCNN Deep Convolutional Neural Network. 39

DECEA Departamento de Controle do Espaço Aéreo. 40–42, 47

DL Deep Learning. 32

DOF Degree of Freedom. 92

DRL Deep Reinforcement Learning. 12, 70, 82

ED Edge Detection. 65

EPE Energy Research Company. 24

ESCs Electronic Speed Controllers. 88

ETI Information Technology Equipment. 103

FC Flight Controller. 50–52

FOB Forward Operating Airbase. 39

FPN Feature Pyramid Network. 68, 78

FPV First Person View. 56, 85

GCS Ground Control Station. 32, 52, 79

GPS Global Positioning System. 26, 27, 32, 33, 38, 51, 71

GUI Graphical User Interface. 52

GWh Giga Watt hour. 24

H2020 European Commission under the Horizon. 24

HDMI High-Definition Multimedia Interface. 95

HIL Hardware in the Loop. 53

HT Hough Transform. 57, 65–67

Hz Hertz. 90

IAC Instrução de Aviação Civil. 42, 47

ICAO International Civil Aviation Organization. 42

IMU Inertial Measurement Unit. 26, 27, 33, 50, 92

KCF Kernelized Correlation Filter. 32

kV A thousand . 24

LBDM Local Screw Detection Module. 39

LIDAR Light Detection and Ranging. 95

LL Lower threshold limit. 67

LSD Line Segment Detector. 57, 65–67

MLP Multi layer Perceptron. 54

MRS Multi-Robot Systems. 44

MTDS Multi-task Distributed Scheduling. 37

NED North, East and Down. 48

ONS Brazilian National Electric System Operator. 24, 25

OSHW Open Source Hardware. 96

PC Personal Computer. 95

PHT Probabilistic Hough Transform. 57, 65–68

PI Performance Impact. 37

PID Proportional Integral Derivative Controller. 49, 52

PSO Particle Swarm Optimization. 45

PWMLs Pulses Width Modulation. 88

RAM Random Access Memory. 95

RELU Rectified Linear Unit. 68

ResNet Residual Networks. 68

RL Reinforcement Learning. 66, 69, 70

ROI Automatic region of interest. 82

RPA Remotely Piloted Aircraft. 14, 39–42, 46

RPS Remote Piloting Station. 41

RTH Return-to-Home. 92

RTL Return-to-Launch. 92

SAA South Atlantic Magnetic Anomaly. 27

SDaaS Swarm-based Drone-as-a-Service. 36

SDK Software Development Kit. 52

SI Swarm Intelligence. 45, 46

SISANT Unmanned Aircraft System. 47

SLR Systematic Literature Review. 14, 29–31, 36

SSD Single Shot Multibox Detector. 14, 68, 78

TBM Time-Based Maintenance. 25

TL Transmission Line. 12, 24, 27, 34, 35, 47, 59, 75–78, 81, 82

TLs Transmission Lines. 24, 26–31, 34–39, 55, 57, 67, 69, 80, 81

UA Unmanned Aircraft. 42

UAS Unmanned Aircraft Systems. 42

UAV Unmanned Aerial Vehicle. 12, 28–30, 32–40, 42, 47, 48, 50–53, 55, 56, 58, 61, 64, 66, 69–72, 74, 76, 79–82, 86, 89

UAVs Unmanned Aerial Vehicles. 12, 26, 29, 36–39, 42, 47–49, 52, 56–58, 71, 74, 75, 77, 78, 80, 82

UBDDM Ultra-small Screw Defect Detection Model. 39

UL Upper threshold limit. 67

UNIFEI Federal University of Itajubá. 47

UOPM Ultra-small Object Perception Module. 39

USB Universal Serial Bus. 95

UUV Underactuated Unmanned Underwater Vehicle. 38

VLOS Visual Line Of Sight. 47

VS Vision-based Robot Control. 34

Contents

1 Introduction

1.1 Context and Motivation

Electric power transmission are huge infrastructures with great importance for the electricity supply of a country, as they support the cables that transmit energy from the generation site to the final consumer. Distribution reliability continues to be one of the most important topics in the electric power sector, due to the direct correlation with customer satisfaction. The rupture or even damage of these structures can have significant consequences for the economy (KIRTLEY JAMES L, 2020).

Transmission Lines (TLs) carry electric power at high voltages. Typically transmission voltage is more than 69kV, whereas distribution lines generally operate at lower voltage (less than 69kV). These voltages may pose life threatening hazards to anyone nearby a Transmission Line (TL) and TLs towers. For example, the National Grid Corporation of the Philippines, previously launched a campaign stressing the dangers of various activities such as kite flying, planting trees, or parking vehicles near transmission towers (GONZALES, 2013).

TLs also distribute electricity over long distances, supplying electricity from big power plants to smaller power distribution lines to end users and any attacks such on infrastructure could cause a nationwide harm and/or distress (HARRELL, 2016).

In 2016, the European Commission under the Horizon (H2020) framework initiated a Call for Proposals (H2020-CIP-01) towards the protection of critical infrastructures including, but not limited, to Energy Infrastructure (COMMISSION, 2017).

According to the Brazilian National Electric System Operator (ONS), in 2025 the extension of the length of electricity transmission, using high voltage lines, in Brazil, will reach 184,054km in length, with the current number being 145,600km. Electricity consumption in Brazil totaled 474,231GWh in 2020, an increase of 38% compared to the previous 10 years, according to Energy Research Company (EPE) (MACHADO G, 2021). Furthermore, Minas Gerais State Energy Company (CEMIG) will count on a government investment from the Program More Energy worth 5 billion Brazilian Reals, creating 200 new energy distribution substations, increasing to 615 units and 3,100 kilometers of new high voltage lines by 2027 in Minas Gerais state (BIANCHETTI, 2021).

Aerial Inspection of TLs have several challenges such as covering predefined and known areas, avoiding obstacles, recognizing objects of interest, identifying faults in transmission line components, identifying risks of erosion or landslides, identifying unauthorized occupation on the ground etc. In all these cases, corrective actions for identified anomalies

will be defined and planned by technicians involved in the inspection process according to their degree of severity.

In order to guarantee the continuity and quality of this complex system, maintenance and inspection activities are regulated by the ONS and supervised by Brazilian National Electric Energy Agency (ANEEL), which determines a minimum plan of action and frequency (DANTAS, 2021).

These measures are necessary because transmission structures that are long in length are subject to damage caused by nature and aging, therefore requiring thorough checks periodically or after major environmental catastrophes. Furthermore, it is the responsibility of the concessionaires to put together an inspection plan for these cases, so that maintenance occurs regularly in a specialized preventive and predictive way, and according to the characteristics of their structures. Preservation strategies can be Time-Based Maintenance (TBM), defined by fixed calendar intervals, operating hours or operating cycles, or Condition Based Maintenance (CBM), which is an extension of the TBM strategy and use non-invasive testing techniques to assess the condition of the equipment (KIRTLEY JAMES L, 2020). Figure 1.1 presents real examples of the occurrence of some of these problems.

Figure 1.1 – Common faults in power transmission line structures
(**a**) Loose wire structure, (**b**) Corroded structure, **(c)** Cable damaged by shock absorber, (**d**) Corroded cable, (**e**) Loose and damaged cable and (**f**) Broken cable.
Sources: (ADAMI, 2008; RIBEIRO, 2019)

Problems related to the structure can be identified during regular inspections and maintenance. They consist of occurrences in the environment that pose future risks to people nearby or to the regular operation of power transmission, problems that can be presented

by: trees close to the structure or conductors, irregular suppression on half a slope, undue invasions in the right-of-way, natural erosion or removal to landfill, among others. Figure 1.2 shows the most common situations that can compromise structures or people's safety.

Figure 1.2 – Occurrences in the transmission line area.
(**a**) Trees close to the lines; (**b**) Erosion on the ground; and (**c**) Intrusions into the service lane.
Sources: (SILVA, 2011; G1, 2021; GLOBO, 2019)

In general, simple routine inspections can be carried out with a pedestrian patrol or land vehicle, composed of a group of electricians, located on on-site platforms with the aid of forklift trucks, or on isolated platforms with the aid of binoculars. The more specific inspections are carried out by a conventional helicopter containing sensors for data acquisition, flying parallel to the transmission line and an operator filming the line (SILVA G. C. DA; MUNARO, 2008). These methods, although functional, have many disadvantages: the first is restricted due to the limitation of the observation point and equipment, while the second due to the availability of the equipment and vehicles used. Both solutions require high investment per course and also pose a high risk of accidents to operators (SILVA G. C. DA; MUNARO, 2008; RESENDE, 2017a).

Unmanned Aerial Vehicles (UAVs), commonly known as drones, have already been successfully used in many traditional civil and military applications. Recently, UAVs have been used in inspections of TLs in a manual and reduced way, to the detriment of their limitation in terms of restricted field of vision, scarcity of specialized operators and operating time (BRITO, 2019).

An emerging application is the replacement of traditional means of inspecting power transmission lines with autonomous UAVs, however new questions are raised, including how to operate with lower cost, better performance and greater safety, in compliance with current legislation. Therefore, the use of UAVs to track the path of a power transmission line is currently carried out by a highly trained pilot or by simple programmed missions, using way-points based on Inertial Measurement Unit (IMU) coupled to the aircraft, such as accelerometers, gyroscopes , compass, in addition to Global Positioning System (GPS) coordinates with prior knowledge of the environment to carry out the mission (PAUL, 2006). Figure 1.3 shows some kind of TLs used nowadays.

Figure 1.3 – TL Inspection currently.
(**a**)With helicopters, (**b**) Visual and (**c**) Using drones.
Sources: (RESENDE, 2017b; RANGEL; KIENITZ; BRANDÃO, 2009)

Identifying elements to assist in inspection using a navigation and altitude control environment accurately is a major challenge for this application, especially in situations where the GPS signal and IMU data may not be reliable, or the operator's driving may be affected. Precision failures in measuring instruments, external interference, such as the level of absorption of electromagnetic energy, South Atlantic Magnetic Anomaly (SAA) and adverse weather conditions are common. The limitation of the operator's perspective, limited or incorrect information on the coordinates of TLs towers, particular characteristics characteristics of the soil and structure also make the use of this technique difficult. Achieving a low-cost, broad, efficient and safe solution, especially in a country with large areas and limited financial resources in infrastructure, is a major challenge (TRIVEDI, 2005).

In addition to the issues raised, TLs structures are installed in different environments, and there may be corridors in urban centers, mountainous regions, bridges, rivers, among others. Similarly, it is common for these structures to intersect with other power line corridors, which can be of different categories and formats. Figure 1.4 shows areas related to photo and video collection.

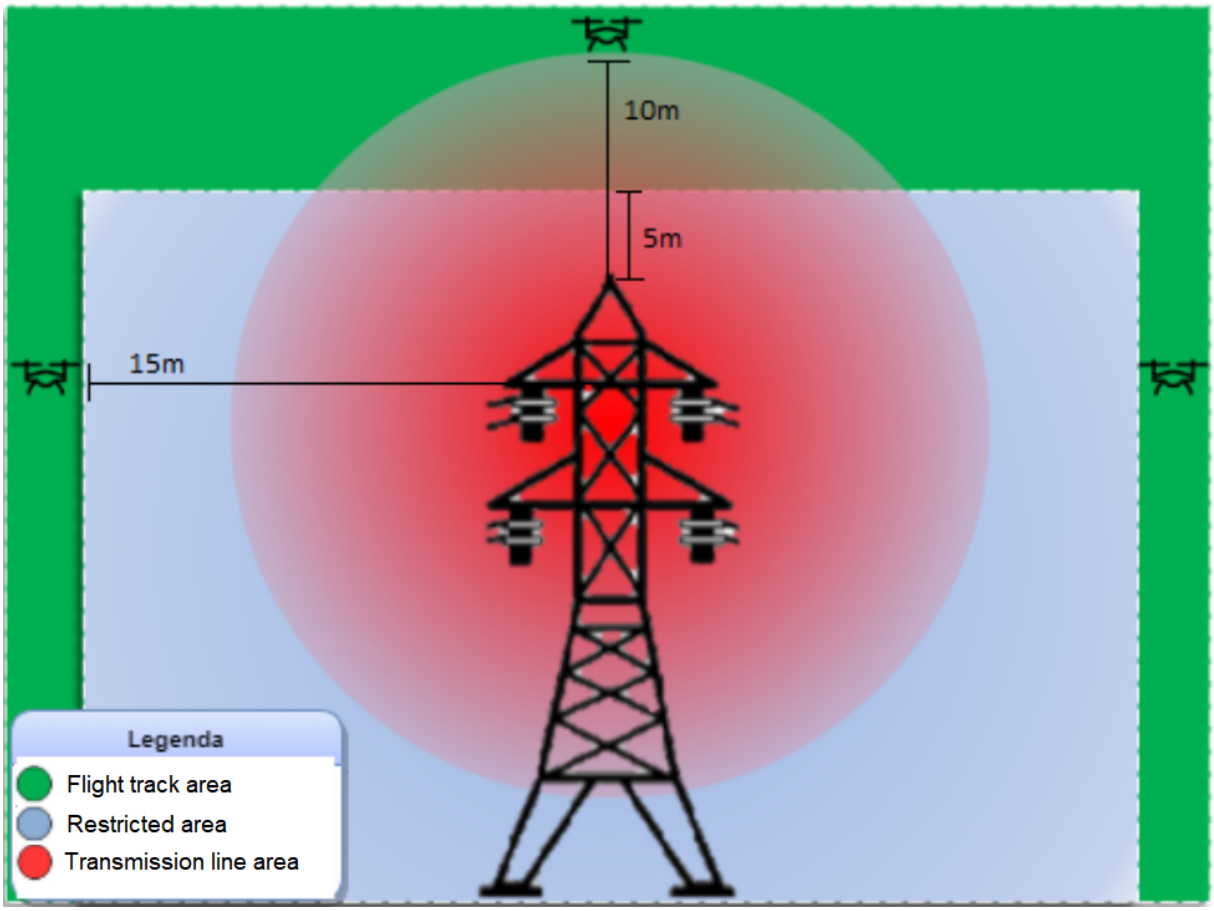

Figure 1.4 – Areas related to photo and video collection.
Source: (DANTAS, 2021)

With this background we believe that here is an increased need for protection against any encroachment or unauthorized activity nearby TLs.

1.2 Objectives and Scope of Work

The main hypothesis that led the authors to carry out this work was: is the integration of cooperative swarm algorithms with image inferences using deep learning for autonomous power TL tracking possible?

In order to prove the aforementioned hypothesis, this work begins with the objective to provide a detailed analysis of the use of autonomous and cooperative UAV in the inspection of TLs, with an emphasis on aircraft trajectory control during flight, using exclusively monovision, in simulated and real environments. To meet the main objective of this thesis it is necessary that the following specific objectives are achieved.

- Know and master the ways of recognizing objects using monovision;
- Know and master the ways of tracking objects, specifically TLs;
- Know and master the ways of processing images in real time;

- Know and master the ways of controlling the trajectory of groups of UAVs;
- Present the different components of a UAV;
- Simulate UAVs flights;
- Implement a simulated UAVs environment containing TLs that can be tracked;
- Propose and implement a solution for controlling the trajectories of groups and UAVs using exclusively monovision;
- Verify the efficiency of the proposed solution through simulations.

1.3 Literature review

For this research, 184 academic works, books, websites and other sources published in the period from 1982 to 2023 were consulted, a range of 4 decades, with the most of sources (61.41%) up to five years of publication, with 44.24% of these being from last two years (Figure 1.5).

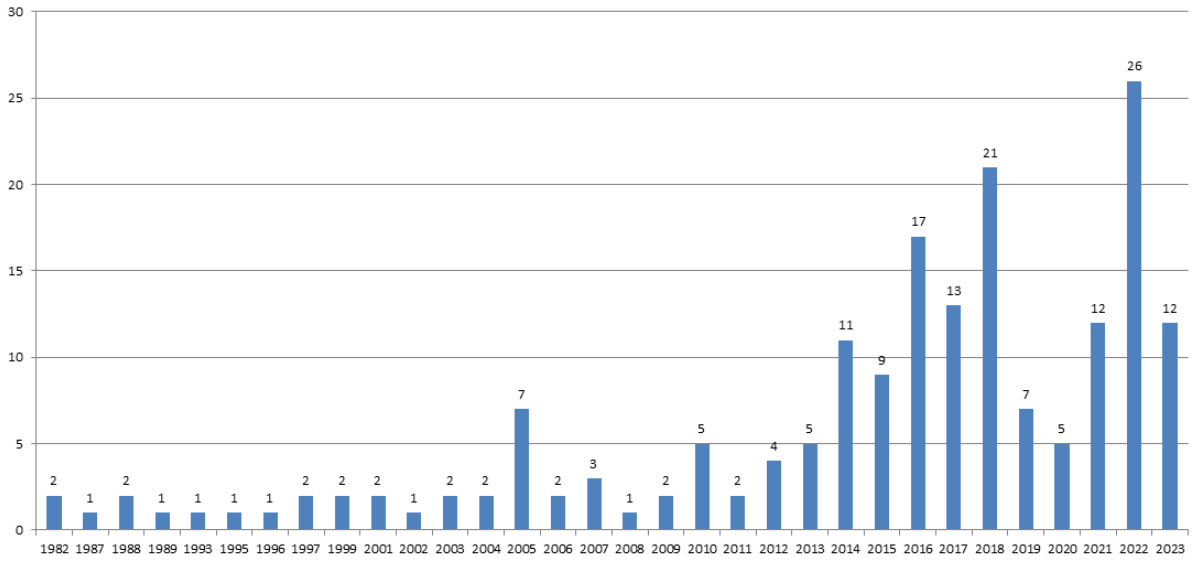

Figure 1.5 – Number of references per year of publication
Source: Author

This thesis produced a Systematic Literature Review (SLR) (MARTINS et al., 2020) that considered scientific works that answered the research questions (Table 1.1) on techniques used for the use of autonomous UAV in the inspection of TLs, identifying the materials and methods used.

To answer these questions the search expression *("Autonomous" OR "Self-navigation" OR "Self navigation" OR Automatic OR Autopilot) AND ("Remotely Piloted" OR "RPA" OR "Aerial Unmanned" OR "UAV" OR "DRONE" OR "Airplane") AND ("Image" OR "Inspection" OR "Maintenance") AND ("Transmission Power" OR "Transmission Line"*

N.	Research Question
1	What is the cost of implementing the materials and techniques used to inspect TLs using UAV?
2	What is the computational and energy efficiency of the techniques used to guide the UAV?
3	What is the level of security and location of the solutions implemented for tracking TLs using UAV?

Table 1.1 – SLR's Research Question

OR "Power Grid" OR "Power Line") (Table 1.2) in online search engines in the IEEE, Scopus and Compendex databases.

After applying some inclusion criteria (Table 1.3) and exclusion criteria (Table 1.4) to the articles found, the quantitative result is shown in Table 1.5.

The quality of the proposals presented in the articles evaluated by SLR was measured according to the criteria listed in Table 1.6.

The systematic mapping resulting from SLR containing evidence from the 15 selected and evaluated studies, is presented in Table 1.7.

N.	Link	String	Link
1		Autonomous	OR
2		Self-Navigation	OR
3		Self Navigation	OR
4		Automatic	OR
5		AutoPilot	
6	AND		
7		Remotely Piloted	OR
8		RPA	OR
9		Unmanned aerial	OR
10		UAV	OR
11		UAS	OR
12		DRONE	OR
13		Airplane	
14	AND		
15		Imaging	OR
16		Inspection	OR
17		Maintenance	
18	AND		
19		Transmission Power	OR
20		Transmission Line	OR
21		Power Network	OR
22		Power Line	

Table 1.2 – SLR's Search Expression

N.	Selected Publication
1	Use unmanned aircraft to inspect TLs autonomously.
2	Have different techniques for autonomous tracking of TLs.

Table 1.3 – Criteria adopted in SLR for inclusion of articles

N.	Discarded publications
1	Do not contain the exact keywords of the search phrase or its variations.
2	Do not use unmanned aircraft.
3	Do not aim to inspect TLs.
4	Do not use autonomous mode.
5	Do not describe all the processes used in the proposed solution.
6	Have not been applied at least in the simulation environment.

Table 1.4 – Criteria adopted in SLR for excluding articles

N.	Phase	Articles Found	Duplicate Articles	Included Articles	Excluded Articles
1	Search	223	85	140	
2	Selection			30	110
3	Evaluation		4	15	10

Table 1.5 – Result of the SLR article selection process

N.	Quality criterion
1	Was the study described clearly and adequately?
2	Were the methods or techniques used clearly reported?
3	Was the virtual environment used clearly reported?
4	Has the proposed solution been evaluated/validated?
5	Were the results stated clearly?

Table 1.6 – Criteria adopted in SLR to measure the quality of the proposed solutions.

Table 1.7: Features identified in other solutions

N	Reference	Material	Methods	Tests[1]	UAV	Cost[2]	QLT[3]
1	(ZHANG et al., 2016)	Laser	DL Binocular vision	Real flight	Uni[4]	Average	4.0
2	(HUI et al., 2019)	Camera	DL KCF Tracking	Real flight	Multirotor	Low	5.0
3	(LUQUE-VEGA et al., 2014)	Infrared camera	GCS GPS	Real flight	Multirotor	Average	4.0
4	(ZORMPAS et al., 2018)	Camera	Edge detection[5]	Real flight	Multirotor	Very low	3.0
5	(DENG et al., 2016)	Laser	Adaptive algorithm[6]	Laboratory	Multirotor	Average	4.0
6	(HAMELIN et al., 2019)	Camera and lidar	Discrete Time Control	Real flight	Hybrid multirotor[7]	Average	4.5

Continued on next page

Table 1.7: Features identified in other solutions (Continued)

N	Reference	Material	Methods	Tests[1]	UAV	Cost[2]	QLT[3]
7	(WU et al., 2019)	Magnetic sensors	Meta-heuristic algo-rithm	Labora-tory	Multirotor	Ave-rage	4.5
8	(ZHOU et al., 2016)	Camera	Edge de-tection[5]	Real flight	Multirotor	Low	4.5
9	(XIE et al., 2017)	Manifold	Multi-sensor ajust-ment	Real flight	Helicopter	Very high	4.5
10	(DENG(B) et al., 2014)	GPS IMU	Adjust-able way-points	Real flight	Fixed wing and multi-rotor	Low	3.0
11	(MENENDEZ et al., 2016)	Camera	Edge de-tection[5]	Labora-tory	Uni[4]	Ave-rage	4.5
12	(GERKE; SEIBOLD, 2014)	Camera	Edge de-tection[5]	Labora-tory	Airship	Low	3.0
13	(ARAAR; AOUF, 2014)	Camera	Visual servoing[8]	Labora-tory	Multirotor	Low	4.5
14	(GAO et al., 2018)	Magnetic sensors	Inverse model al-gorithm[9]	Simula-tion	Uni[4]	Low	3.0
15	(CHANG et al., 2017)	Laser	Adaptive algo-rithm[6]	Labora-tory	Hybrid multiro-tor[7]	High	4.5

[1]Test environment.

[2]Costs reported subjectively by the authors of the articles, making it not possible to compare them with each other.

[3]Quality measured according to criteria listed in the Table 1.6

[4]Uni: uninformed

[5]Edge detection includes mathematical methods that aim at identifying edges, defined as curves in a digital image.

[6]Adaptive algorithms is an algorithm that changes its behavior at the time it is run, based on information available and on a priori defined reward mechanism (or criterion) (GUI; LI; FANG, 2023).

[7]A hybrid multirotor combines the advantages of both fixed-wing (airplane) and rotary-wing (multirotor) systems in one and the same UAV

[8]Visual Servoing, also known as Vision-based Robot Control (VS), is a technique which uses feedback information extracted from a vision sensor to control the motion of a robot (CENTER; AGIN, 1979).

[9]Inverse modeling with deep learning algorithms involves training a deep architecture to predict device parameters from its static behavior. Inverse device modeling is suitable for reconstructing changed physical parameters of temporarily degraded devices or for recovering the physical configuration (SPATA et al., 2023).

An unmanned aerial system based on a quadcopter for TLs inspection is proposed by (LUQUE-VEGA et al., 2014), where the main interest, according to the authors, is to equip the quadcopter with the necessary payload to be able to carry out a qualitative inspection, and the hardware architecture of the aerial robotic system was presented.

(ZHANG et al., 2016) developed an embedded navigation system based on binocular laser vision (or binocular stereo vision), when two laser beams work at the same time. The binocular stereo vision system is based on bionic theory. Just like a person's two eyes, two devices are installed in a UAV. The distance between the laser camera and the object can be calculated based on the optical laws between the images taken by the left and right cameras. The distance and direction of the object can then be determined. In this work, during the UAV flight, the distance between the TLs and the onboard binocular ranging device and the angle between the yaw direction and the line direction could be obtained, functioning as auxiliary navigation for the UAV and improving the success rate of landing. Once the distance is obtained, the angle between the UAV yaw direction and the line direction can be calculated using a simple mathematical model. The results showed that the relative error of binoculars measuring distance was 2 – 3%.

A hardware and software system design for UAV-based TL inspection is proposed by

(DENG et al., 2016) using real-time data processing and Kalman filter for TL detection and tracking. In the work, the authors apply the solution in a real environment.

(ZHOU et al., 2016) use specific knowledge about TLs to build a model that achieves predictive and continuous parameters of selection so that the best limits are selected when there are changes in the scenarios. According to the authors, experimental studies show that the proposed solution is much better than existing ones. They would have built the first fully automated UAV that successfully tracks TL in the real world.

(XIE et al., 2017) present a multi-sensor solution for the inspection of TLs based on the use of a large unmanned helicopter, where multiple sensors can perform synchronized inspection on all components of the TL and surrounding objects. The authors present in detail the planning method for the unmanned helicopter flight path and sensor tasks before inspecting the TLs, and the method used to automatically track power lines and insulators during the inspection process. According to the authors, the results obtained show that the proposed method is effective for inspection of TLs.

(ZORMPAS et al., 2018) examined the effectiveness of using TL image processing acquired by a UAV and proposed two methodologies differing in the pre-processing required to detect the location of lines in video images. Both proposed methodologies were tested in real-world cases, with the image background in each case being characterized by non-uniform texture, i.e. natural rough terrain in some places, wooded terrain in others and roads. According to the authors, the experiment was successful and the proposed work offers a robust and low-cost way to inspect TLs, being able to locate where a cable failure occurred.

The work of (HUI et al., 2019) presents a monocular (one camera) vision-based navigation approach for continuous inspection by a UAV along one side of the TL. Object detection based on deep learning and a fast and smooth tracking algorithm based on kernelized correlation filter were combined to locate the transmission tower. The distance between the UAV and the transmission tower was measured by triangulation in multiple views. The proposed navigation approach and the designed UAV platform were tested in a real-world environment.

(WU et al., 2019) propose a new parameter reconstruction method for TL overloading, which deals with the challenge as a non-linear optimization problem, building an algorithm that combines metaheuristic algorithm and interior point method, where the position and the current parameters of the lines were reconstructed from the magnetic field data.

(HAMELIN et al., 2019) present the design of a discrete-time control algorithm system for the TL tracking and assisted landing of the Hydro-LineDrone robot, a UAV designed to land and traverse energized power lines. The algorithm automatically aligns the UAV with the cable while the pilot remains in control of the vertical and longitudinal positions, thus

facilitating landing by having fewer degrees of freedom on which the pilot must focus. The emphasis of the project is placed on the discrete time control law. The proposed control system is also designed to meet the requirements for operation near lines, which means the system is immune to electromagnetic interference. The proposed control algorithm is experimentally validated on the LineDrone hybrid UAV under real outdoor conditions.

In addition to the work handled by SLR, others that deal with the inspection of TLs or the control of groups of drones will be described below.

(MAZA et al., 2010) present a work on cooperation and control of multiple UAVs capable of detecting and acting using an architecture to carry out cooperative missions where interactions between UAVs are not only exchanges of information, but also physical couplings necessary for the joint transport of a single charge. The work also presents a control system for transporting suspended cargo using one or more helicopters, as well as results from cargo transport experiments with one and three helicopters.

A multi-layer control model comprised of an interplay of decentralized algorithms for perception and swarming that enables information propagation and multitasking in swarms using only local interactions and without explicit communication or prescribed formations, causing variations in individual speed to be implicitly propagated through the swarm, causing a change in the group's direction almost immediately, was proposed by (AL-ABRI; MAXON; ZHANG, 2019).

Three algorithms to select the best option in a framework for allocating swarms of UAV for delivery services known as Swarm-based Drone-as-a-Service (SDaaS), in order to guarantee a minimum cost (or maximum profit) for UAV swarm suppliers meeting the requirement of shorter response time, were presented and evaluated by (ALKOUZ; BOUGUETTAYA, 2021a).

In a scenario where a swarm of UAVs must visit some locations and build a map in a disaster area, assuming that UAVs can only communicate with their neighbors and manage partial mission information, a work proposed by (ALKOUZ; BOUGUETTAYA, 2021b) analyzes two game theoretical algorithms: one competitive and one cooperative. The competitive algorithm proposes games between each UAV and its neighbors and seeks the Nash Equilibrium, while the cooperative one defines electoral systems in which UAVs vote on their preferred task allocations to their neighbors. After the experiments, the authors conclude that, in a swarm, robots must cooperate and not compete.

A 4D path planning for swarm-based drone operations is proposed by (WU et al., 2021), applying 3D path planning for a single drone and inter-drone conflict resolution. A Cluster-enhanced Ant-colony Optimization Algorithm (CIACO) is employed to solve the multi-path planning problem.

(LI et al., 2021) states that currently the method of using UAVs with traditional navigation

equipment to inspect TLs has the limitations of expensive sensors, difficult data processing and vulnerable to climatic and environmental factors, which cannot guarantee the safety of aircraft and energy systems. To minimize these problems, it presents a mathematical model of spatial distribution of TLs to study the field intensity distribution information around the TLs. Based on this, it suggests a navigation and positioning algorithm where data collected by the positioning system are inserted into the mathematical model to complete the identification, positioning and diagnosis of the field source safety distance. The detected data and processing results can provide reference for obstacle avoidance navigation and UAV security warnings.

(LI; CHEN, 2022) proposes a solution for Multi-task Distributed Scheduling (MTDS) in the form of an improved Performance Impact (PI) algorithm integrating a new task removal strategy and inclusion conflict prediction.

Other topics of interest in this thesis are image recognition and obstacle avoidance, as they pose challenges to be overcome in the inspection of TLs and in controlling the trajectory of UAVs.

A navigation system for indoor UAVs, using computer vision, was proposed by (JONES; ANDRESEN; CROWLEY, 1997). The system required advance knowledge of the environment being flown over. This knowledge was provided through images acquired and stored previously to be processed during the flight. In this type of solution, the images captured by UAV are compared with those in the stored image database. The algorithm seeks to identify common points (anchors) in the images that may indicate the location of the aircraft, acting as physical spatial references (SHIGUEMORI; MARTINS; MONTEIRO, 2007).

A real-time solution using stereo computer vision (using two cameras) was developed by (NISTER; NARODITSKY; BERGEN, 2006). The solution applied to the autonomous navigation of a terrestrial robot, locating and making the robot avoid objects in its path. This solution used an algorithm to detect the contours of images and identify obstacles and options for avoiding these obstacles in the robot's path.

Another solution for autonomous obstacle avoidance is proposed by (SAUNDERS; BEARD; MCLAIN, 2007), using several circular paths, obtained using a laser that, combined, defined the presence or absence of obstacles in the environment and measured the distance between the robot and the obstacles identified.

A solution using Python programming language is proposed by (HERMíNIO et al., 2010). A small mobile prototype traveled a pre-defined route, avoiding obstacles using a video camera from an on-board cell phone. The images were transmitted in real time to a computer, via the wi-fi network, which processed them and sent movement commands to a microcontroller embedded in the prototype.

The use of several sensors is the solution proposed by (WAGSTER et al., 2012) to make a UAV avoid obstacles flying at a constant speed through the environment. The combination of multiple sensors increases efficiency in pose definition (aircraft positioning) and object identification and location.

The use of UAV to scan building facades, using a high-resolution digital camera, is presented by (ESCHMANN et al., 2012). In this solution, initially 2D images are acquired by UAV in horizontal and vertical flights. Afterwards, the collected images are joined and looked for signs of cracks. Similar work to detect cracks using 3D images was presented by (TOROK; GOLVARPAR-FARD; KOCHERSBERGER, 2014).

A solution for avoiding obstacles through a UAV using graphs was proposed by (WEISS et al., 2014). Connectivity between nodes indicated the presence or absence of obstacles.

A solution that uses onboard GPS and a laser device is created by (STUBBLEBINE et al., 2015) to make a UAV avoid obstacles in real time.

According to (NETO, 2016), one of the sectors of the Brazilian economy that can take great advantage of UAV technology with computer vision capable of carrying out some programmed tasks is commercial agriculture, as with the use of aircraft it is possible to map cultivated soil, verify which individuals (plants) need more nutrients and also check their health. In his solution, (NETO, 2017) used monovision to guide a ground robot around obstacles.

Obstacle avoidance in real time by UAVs finds applications in the inspection of urban areas, as proposed by (MOTA et al., 2014) and (FELIZARDO; RAMOS; CAMINO, 2015), including the inspection of TLs. An analysis of the effectiveness of using mini-helicopters for this purpose was presented by (HRABAR; MERZ; FROUSHEGER, 2010).

In the oceanic area, autonomous obstacle avoidance has also been explored, as in work to control the trajectory of unmanned underwater vehicles (Underactuated Unmanned Underwater Vehicle (UUV)) (YAN et al., 2015) including multiple vehicles (CAI; ZHANG; ZHENG, 2017), and can be applied to inspections of cables and submerged oil pipelines (YAN et al., 2018).

(LUO; BAI; ZHANG, 2021) proposed a novel formation control strategy to address the target tracking and circumnavigating problem of multi-UAV formation, using two sets of definitions, space angle definition and space vector definition, to describe the flight state and construct the desired relative velocity establishing the moving target by the relative kinematic model between the UAV and the moving target.

The problem of cooperative circular formation with limited target information for multiple UAV systems is addressed in (HUO; DUAN; FAN, 2021). A pigeon-inspired circular formation control method is proposed to form the desired circular distribution in a plane based on the intelligent behavior of the pigeon during hovering flight. Each UAV rotates

around a specified circle at the same angular speed using only the relative position between the UAV and the target.

(LUO et al., 2023) proposed a Ultra-small Screw Defect Detection Model (UBDDM) based on a Deep Convolutional Neural Network (DCNN), including a Ultra-small Object Perception Module (UOPM) and a Local Screw Detection Module (LBDM) to structure inspections using UAV.

(OLSSON, 2023) investigated an approach of using a swarm/team of drones, able to cooperate, to autonomously deal with unauthorized trespassing of a restricted area. In that instance, the critical infrastructure object was set to be an aircraft hangar such as a part of a Forward Operating Airbase (FOB). And the area was continuously patrolled in search for trespassing objects by a single drone equipped with high performance camera and processing equipment.

1.4 Thesis Structure

This work is organized as follows.

Chapter 1 presents the context of the problem addressed by this thesis and the motivation for investing efforts in solving it. It presents a review on the typical TLs inspection approach using autonomous UAVs, briefly describes the main technique of this thesis and lists some relevant works in which it stood out. It also presents the objectives and scope of the work.

Chapter 2 presents the concept and formal definitions of RPA in Brazil according to official control and aviation bodies.

Chapter 2.3 presents the concept of swarm and RPA group.

Materials and Methods are presented in Chapter 3.

The results obtained from this work are discussed in Chapter 4.

Chapter 5 presents the conclusions, difficulties, and contributions.

Finally, Chapter 6 proposes future works.

2 Remotely Piloted Aircraft - RPA

2.1 Introduction

Although the term Unmanned Aerial Vehicle (UAV) is the most used around the world, according to the official Brazilian bodies use the term Remotely Piloted Aircraft (RPA).

RPAs are small aircraft that, without any direct physical contact, have the ability to perform tasks such as monitoring, mapping, among others (MEDEIROS, 2017). According to (MEDEIROS, 2017), these aircraft are characterized by two basic aspects: not having a pilot on board and carrying equipment, usually sensors, that allow them to carry out certain missions. These RPAs are piloted or controlled remotely through electronic and computational means, supervised by humans. Currently, more than 40 (forty) countries are working on the development of RPAs aimed at different markets (JORGE, 2001).

This intends to present the concept and formal definitions of this term in Brazil according to these official control and aviation bodies.

2.2 Official Definition of ARP in Brazil

This section presents the official definitions of the term RPA according to the official Brazilian regulatory bodies, Agência Nacional de Aviação Civil (ANAC) and Departamento de Controle do Espaço Aéreo (DECEA).

2.2.1 Definition of RPA According to ANAC

Agência Nacional de Aviação Civil (ANAC) published in May 2017 a special regulation with general rules for the civil use of unmanned aircraft in Brazil and published it in the form of Guidelines for Drone Users (ANAC, 2020), where it defines Remotely Piloted Aircraft (RPA) as an unmanned aircraft used for purposes other than recreation (commercial, corporate or experimental use) (Table 2.1).

ANAC also defines, in this same regulation, the figures of the Remote Pilot and the Observer (Table 2.2) and the types of operations with RPAs (Table 2.3 and Figure 2.1).

Regarding the definition of RPA, ANAC also, on its online page (ANAC, 1999), provides two other definitions for Remotely Piloted Aircraft:

- Definition 01: ”It is one in which the pilot is not on board, but controls the aircraft remotely through an interface (computer, simulator, digital device, remote control, etc.). Unlike another subcategory of UAVs, the so-called ’Autonomous Aircraft’,

N.	Term	Definition
1	Drone	Popular name for unmanned aircraft
2	Model Aircraft	Unmanned aircraft used for recreation
3	Remotely Piloted Aircraft (RPA)	Unmanned aircraft used for purposes other than recreation (commercial, corporate, or experimental use)
4	Remotely Piloted Aircraft (RPA)s	Set formed by the aircraft (RPA), the Remote Piloting Station (RPS), the command and control link and any other component that is part of the aircraft design

Table 2.1 – Glossary of technical terms about RPAs (ANAC, 2020).

N.	Actor	Definition
1	Pilot Remote	Person who manipulates the controls and directs the flight of an aircraft unmanned
2	Observer	Person who, without the aid of equipment, assists the remote pilot in safely conducting the flight by maintaining direct visual contact with the UAV

Table 2.2 – ANAC definition for people involved in a flight with UAV. Source: Author with data obtained in (ANAC, 2020)

N.	Operating	Definition
1	BVLOS	Operation in which the pilot is unable to keep the UAV within his visual range, even with the help of an observer.
2	VLOS	Operation in which the pilot maintains direct visual contact with UAV (without the aid of lenses or other equipment)
3	EVLOS	Operation in which the remote pilot is only able to maintain direct visual contact with the UAV with the aid of lenses or other equipment and RPA observers.

Table 2.3 – Types of flight with UAV in relation to the remote pilot's and observer's vision (ANAC, 2020).

which, once programmed, does not allow external intervention during the flight and which in Brazil has its use prohibited. The so-called RPA[1] , Finally, it is the correct terminology when we refer to non-recreational remotely piloted aircraft";

- Definition 02: "Unmanned aircraft, flown from a remote pilot station".

2.2.2 Definition of ARP According to DECEA

Brazilian Departamento de Controle do Espaço Aéreo (DECEA), organization responsible for controlling Brazilian airspace, provider of air navigation services that enable flights and the ordering of air traffic flows in the country (DECEA, 2023b), offers the following definitions applicable to the concept of RPAs:

[1] ANAC assigns the acronym RPA to designate 'Remotely Piloted Aircraft' even when, in Portuguese, it would be ARP, an acronym for Remotely Piloted Aircraft.(sic) (ANAC, 1999).

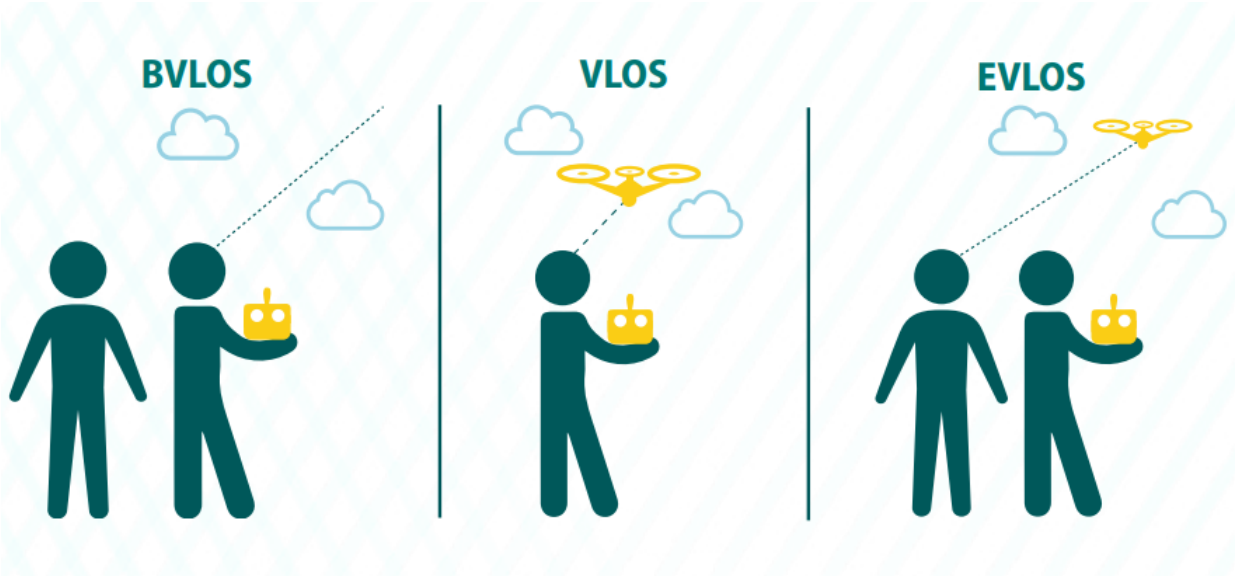

Figure 2.1 – Types of Operation with UAVs.
Source: (ANAC, 2020)

- UNMANNED AIRCRAFT: "Any device that can sustain itself in the atmosphere, based on air reactions other than air reactions against the earth's surface, and which is intended to operate without a pilot on board";
- AUTONOMOUS UNMANNED AIRCRAFT: "Unmanned aircraft that does not allow pilot intervention in flight management";
- REMOTELY PILOTED AIRCRAFT: "Subset of Unmanned Aircraft, piloted from a remote piloting station, with purposes other than recreation, that is capable of interacting with Air Traffic Control in real time".

While ANAC uses the acronym RPA to refer to Remotely Piloted Aircraft (Aeronave Remotamente Pilotada, in portguese), DECEA uses two acronyms, ARP and UA (Unmanned Aircraf).

In accordance with Instrução de Aviação Civil (IAC) 100-40/2023 - "Unmanned Aircraft and Access to Brazilian Airspace" (DECEA, 2023a), Unmanned Aircraft Systems (UAS) are a new component of global aviation that operators, industry and several international organizations are studying and working to understand, define and, finally, promote their complete integration into Airspace.

In Brazil, Unmanned Aircraft are still widely known as drones, UAV, or RPA.

According to the International Civil Aviation Organization (ICAO), UA, covers a wide spectrum of aircraft, from unmanned free balloons and model aircraft to highly complex aircraft. According to DOC 100-19, UAs are subdivided into: *Remotely Piloted Aircraft (RPA)*, *Small Unmanned Aircraft*, Model Aircraft and Autonomous Aircraft. The first three have similar characteristics, as they are Unmanned Aircraft and flown from a remote pilot station. Unmanned and Definitive Aircraft as Innovative have the characteristic of

not allowing human intervention, once the flight has started. With the publication of the Brazilian Special Civil Aviation Regulation nº 94, A basic difference was established between Remotely Piloted Aircraft and Model Aircraft, the latter being used only for recreational purposes. and define:

- MODEL AIRCRAFT: Unmanned aircraft, used for exclusively recreational purposes;
- AIRCRAFT: Any device that can sustain itself in the atmosphere from air reactions other than air reactions against the earth's surface;
- UNMANNED AIRCRAFT: Any device that can sustain itself in the atmosphere, based on air reactions other than air reactions against the earth's surface, and that is intended to operate without a pilot on board;
- AUTONOMOUS UNMANNED AIRCRAFT: Unmanned aircraft that does not allow pilot intervention in flight management;
- REMOTELY PILOTED AIRCRAFT: Subset of Unmanned Aircraft, piloted from a remote piloting station, with purposes other than recreation, that is capable of interacting with Air Traffic Control in real time;
- REMOTE PILOT STATION: Component of the Unmanned Aircraft system that contains the equipment used to pilot the aircraft;
- AUTOMATED OPERATION: Operation in which the unmanned aircraft automatically fulfills the programmed flight plan and during which, under normal operating conditions of the UAS components, it is possible for the Remote Pilot to intervene in the conduct of the operation in all its phases.

  NOTE: Under normal conditions, the Remote Pilot must be able to interfere in the flight of the unmanned aircraft, the piloting of which is under his responsibility and supervision;
- OPERATION AROUND A STRUCTURE: Operation carried out around any structure or obstacle, whether artificial or natural, limited vertically to 5 m (five meters) above the height of the structure or obstacle and horizontally distanced up to 30 m (thirty meters) of this;
- SMALL UNMANNED AIRCRAFT: Subset of Unmanned Aircraft with maximum takeoff weight (PMD) less than or equal to 25kg;
- RPA: Remotely Piloted Aircraft;
- RPAS: Remotely Piloted Aircraft System;
- UNMANNED AIRCRAFT SYSTEM: System composed of the Aircraft and its associated elements, which can be remotely piloted or fully autonomous;
- REMOTELY PILOTED AIRCRAFT SYSTEM: Subset of the Unmanned Aircraft System, which is capable of interacting with Air Traffic Control in real time, consist-

ing of the remotely piloted aircraft (RPA), its remote piloting station(s), the piloting link and any another component associated with its operation;

- UA: Unmanned Aircraft;
- UAS: Unmanned Aircraft System;
- UAV: Unmanned Aerial Vehicle (obsolete term)

2.3 RPA Swarm

The term swarm was introduced by Beni and Wang in their studies on Cellular Robotic Systems (ZAVALA-RIO; SOERENSEN, 2013; SAHIN, 2004).

Multi-Robot Systems (MRS) allow members of a group of robots to cooperate with each other to complete a given task more quickly than a single robot would be able to do, and with greater tolerance to failures due to robot redundancy (GUZZONI et al., 1997).

A group of robots is not just a group, but has some special characteristics that are found in swarms of insects such as decentralized control, lack of synchronization and having simple and almost identical members (BENI; WANG, 1993).

Swarm robotics is the study of how large numbers of relatively simple, physically embedded agents can be designed so that a desired collective behavior emerges from local interactions between the agents and between the agents and the environment (SAHIN, 2004; ZAVALA-RIO; SOERENSEN, 2013).

One of the largest swarms brought together 1,024 microrobots, just a few centimeters tall and wide, called kilobots, and was presented at the Wyss Institute for Biological Inspection Engineering at Harvard University, in the United States, and was published in Science magazine in 2014 (JÚNIOR; NEDJAH, 2016).

The study of drones grouped cooperatively to perform a specific task is often based on the observation of biological systems, such as flocks of birds and schools of fish, that operate collectively to achieve objectives. The idea is that multiple drones operating together can overcome challenges that would be difficult or impossible for a single drone (FLOREANO D., 2015).

Swarm optimization approaches seek to apply known Particle Swarm optimized solutions (KENNEDY; EBERHART, 1995).

Producing a system made up of several autonomous aircraft that come together as a cohesive group to perform a certain task is challenging. In this type of system, each individual needs to take care of themselves in order to achieve their individual goals; avoid colliding with obstacles in the environment, including other members of the group and not becoming an obstacle to others; collaborate with the group's mission; signal at all times

your position and where you are in your specific mission; everyone has an understanding of where the group's mission is; obtain and process data from the environment and the group itself, decide what actions to take and act in accordance with these decisions; produce and transmit data in real time in a scenario called swarm intelligence.

The technological capacity to control a vehicle in a constantly uncertain environment has always been a limiting factor in the construction of unmanned systems (SHIMA; RASMUSSEN, 2009).

Different approaches can be found in the literature, combining software and hardware solutions, applied to simulated and real environments. Behavior-based approaches inspired by nature allow drones to operate based on simple rules, which combined result in complex and cohesive group behavior (BAYıNDıR, 2016) of aircraft, such as avoiding collisions between individuals in the group and possible obstacles during flight.

Despite these challenges, swarm intelligence and bioinspired computing have become very popular in recent years, providing the basis for modern solutions in different applications (MATARIĆ, 2007).

Swarm Intelligence (SI) can be defined, from the point of view of Robotics and AI, as a collection of Evolutionary Algorithms based on populations of individuals cooperating with each other, inspired by groups of animals observed in nature, which have improved their behavior over time generations thanks to continuous training, adaptations and learning (GOLDBERG; HOLLAND, 1988a; PANIGRAHI; SHI; LIM, 2011).

Research on SI is divided into three categories: Algorithms, Challenges and Applications (PANIGRAHI; SHI; LIM, 2011). In SI algorithms, there are studies to create or modify solutions for use in groups of robots, such as Particle Swarm Optimization (PSO) algorithms, which are easy to implement computationally compared to other population algorithms inspired by nature (SILVA; LEMONGE; LIMA, 2014) and its classic variants (GOLDBERG; HOLLAND, 1988a) or others arising from these studies (SMITH; SIMONS, 2013). Challenges in SI in turn, deal with the types of problems that these algorithms, originally designed for single and unrestricted objectives, would be capable of solving when applied to multi-objective optimizations with constraints such as combinatorial optimization problems and others. A trend of swarm intelligence research is on hybrid algorithms (GOLDBERG; HOLLAND, 1988b). Evolutionary Algorithms are based on biological evolution as Genetic Algorithms have been extensively investigated in this context due to their ability to solve complex optimization problems by working efficiently in evaluating specific variations of the problems studied (GOLDBERG; HOLLAND, 1988b). Among the most used evolutionary algorithms are those based on Darwin's theories on natural selection, genetic reproduction and evolution of species. We can also mention Memetic Algorithms, which combine concepts such as search based on populations of evolutionary algorithms and local improvement, as in gradient tracking techniques

(MOSCATO, 2003), Artificial Immune Systems (AIS) a branch of Computational Intelligence oriented mainly by mammalian immunology, which evolved from the proposition of using theoretical immunological models for machine learning and automated problem solving (BORUAH, 2023) and Ant Colony, a popular meta-heuristic based on ant behavior that is used to solve traveling salesman problems (THONG-IA; CHAMPRASERT, 2023).

Finally, all research on AI applied to solving a wide variety of real-world problems would be Applications in SI, which would be, according to (PANIGRAHI; SHI; LIM, 2011), "very difficult, if not impossible , for traditional algorithms to solve", and which would be attracting the attention of engineers in all areas to the successful applications of swarm intelligence algorithms in the real world.

Autonomous obstacle perception and avoidance also have applications in swarms of RPAs, where several aircraft fly together cooperatively to perform tasks, as (BRAGA et al., 2018a) proposes, in an approach in which aircraft constantly attract each other (to maintain formation) and retract (to avoid collisions) through calculations resulting from vectors of weighted virtual physical forces, without losing focus on the task to be performed together.

3 Materials and Methods

The next sections present the resources used to develop the research, in particular, the hardware, that is, the drone and the sensors and electronic devices necessary for mapping the TL; as well as the software used for monitoring, trajectory control and identification of objects of interest.

3.1 The Proposed Hardware

The performance of any field test flight must be in line with the current regulatory framework, presented in the legislation for access to Brazilian airspace. Initially, it is necessary to have exclusive documentation for the UAV duly registered in the Unmanned Aircraft System (SISANT), where information on the characteristics of the aircraft will be defined, and explicitly indicates the suitability for carrying out non-recreational flights, with the specific branch of activity for training, research and development. For this study, radio frequency equipment was used that has a large market in Brazil, and is approved by the Brazilian National Telecommunications Agency (Anatel).

The missions carried out for this study always operated in a TL system under construction, therefore de-energized. The flight missions took place outside the delimitation around the structure and above 5 meters in height and 30 meters from the surroundings, thus also avoiding the action of the electromagnetic field produced by the transmission lines, as represented in Figure 1.4.

The flights reached a maximum height of 130 feet above the ground, and always in Visual Line Of Sight (VLOS) conditions. Specific issues of proximity to aerodromes are not addressed as they do not exist in proximity to Federal University of Itajubá (UNIFEI), however this and other variables can directly influence the deadline and decision for flight authorization by Departamento de Controle do Espaço Aéreo (DECEA). The conditions presented here for this study are in accordance with the Instrução de Aviação Civil (IAC) 100-40 standard.

With the rapid development of technology, autonomous vehicle projects are highlighted in the computational academic research scene, and have made rapid progress in the last decade. For UAVs, the possibilities are great considering their dynamics, depending on the application it is possible to use multirotors or fixed wings autonomously and safely (MAANYU K. N.; RAJ, 2020).

One of the proposals is to build a small UAV with enough hardware to complete the flight proposal, and at the lowest possible cost (FILHO A. J. D.; RAMOS, 2020). Using

data from manufacturers and calculations based on information about motors, batteries, maximum climbing speed, battery time in stationary mode and average price units (considering US$1,000) were organized in Table 3.1, comparing with other types and costs of UAVs of different structures.

Table 3.1 – Characteristics and costs of the drones.

Structure	**Maximum Load (g)**	**Ascending Speed (m/s)**	**Baterry Time(s)**	**Price (US$)**
Q250	1,000	5	720	200
F450	1,600	4	880	200
Glider	300	2	3,110	1,000
Mavic	900	4	1,440	1,000

The UAV used in the research was an F450 quadcopter (45 cm), which encompasses the mini UAV category, weighing between 2 and 25 kg (GUPTA, 2013). It was chosen due to the low cost of construction material, load capacity of up to 1,600g free, low battery consumption, ease of maintenance, total freedom of movement, good stability, speed and flight time autonomy when compared to other similar UAVs.

Figure 3.1 shows the Euler angles, movements in relation to space and coordinate orientations, in North, East and Down (NED) in relation to UAV (MAANYU K. N.; RAJ, 2020).

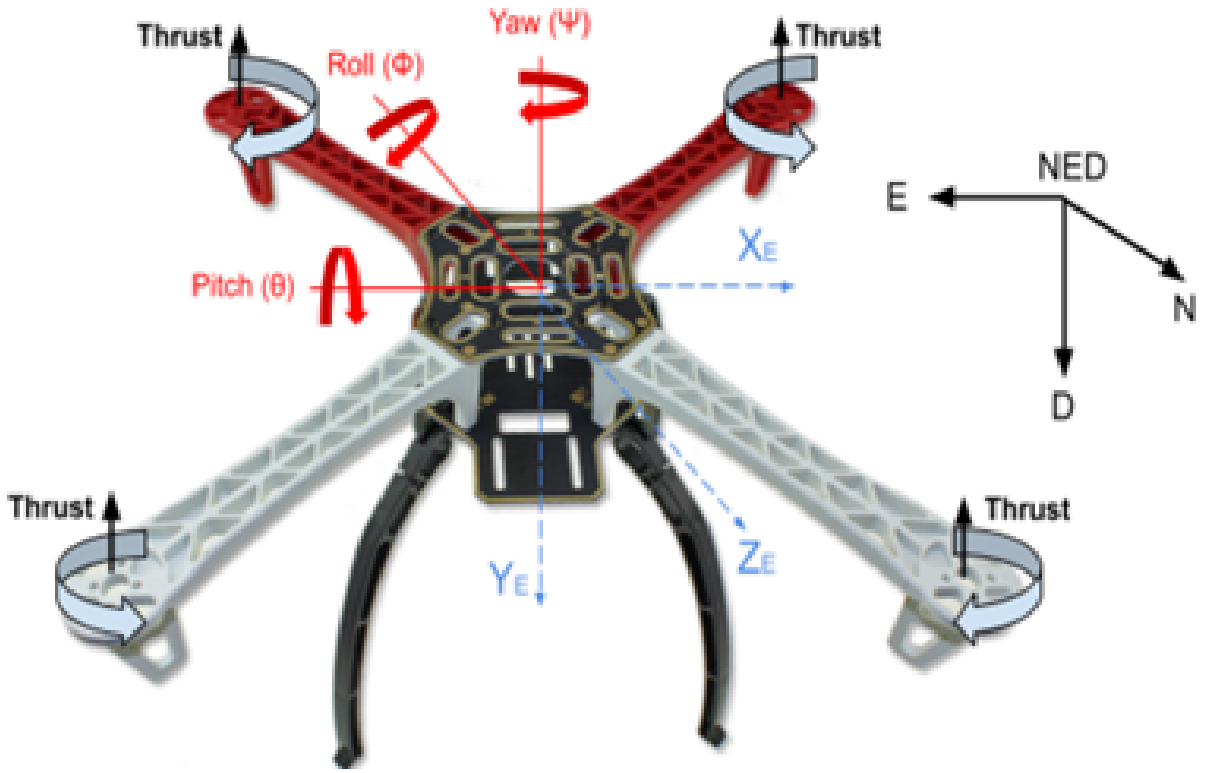

Figure 3.1 – A F450 drone frame used in the research.
Source: Author

Two or more independent UAVs generally are called swarms, and can act at the same time carrying out different tasks, with a final global objective that would be difficult to execute individually. Swarms are highly scalable and self-organizing (SHRIT, 2017). In this study, a swarm subdivided into a pair of well-defined tasks was used.

Another important issue in the construction of UAVs is stabilization, which is why calibration modes and adjustments will be evaluated Proportional Integral Derivative Controller (PID). For image stabilization generally a gimbal stabilizer installed at the bottom of the frame structure. However, to save money, it is possible to install fixed directional cameras with impact absorbers.

The main ground controller operating system can be easily changed to an on-board computer in this type of UAVs, for example Raspberry Pi, for algorithm processing. Figure 3.2 below presents the architecture of the system as a whole, detailing its communications and integrations between the main components.

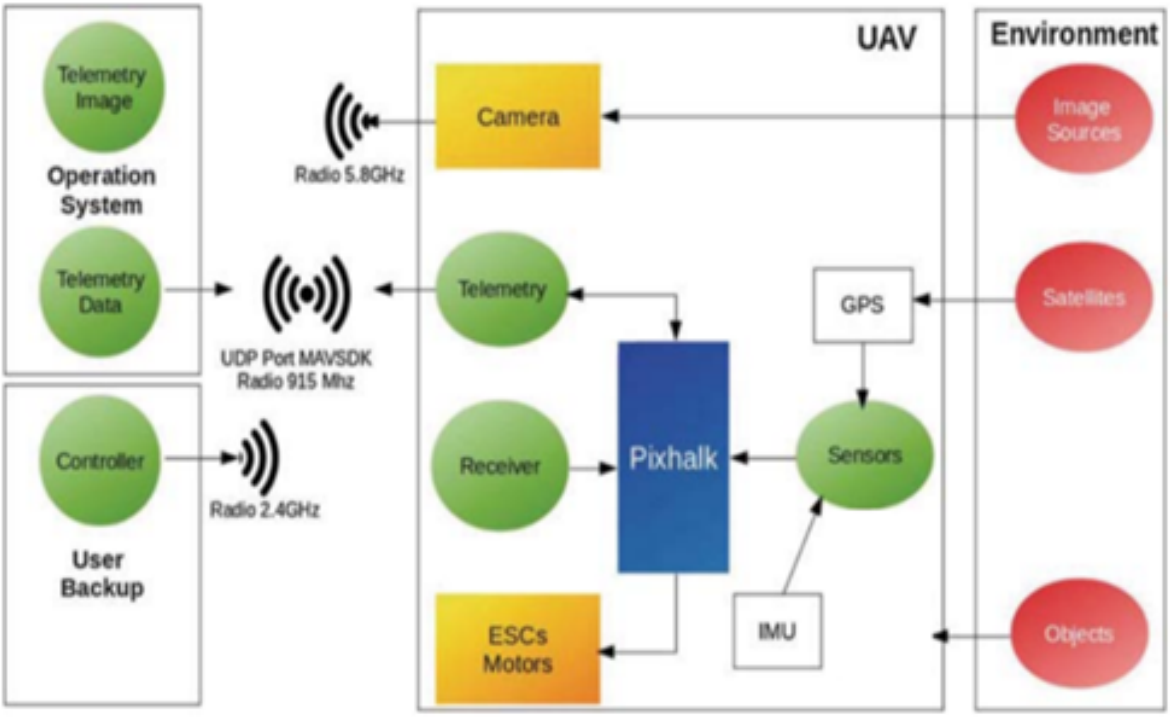

Figure 3.2 – Hardware and communication architectures.
Source: Author

3.2 Control Flight System

To guarantee flight stability, it is necessary to use a range of sensors that detect the movement of the UAV and the environment in which it is inserted, such as the IMU, so that they converge, applied to a data processing algorithm. This function is performed by the Autopilot Flight Controller (FC), which is a circuit board, which in addition to ensuring flight stability also records user parameters and commands. The low-cost Autopilot analyzed was determined by availability in the research laboratory, their details described below, and also presented in Figure 3.3.

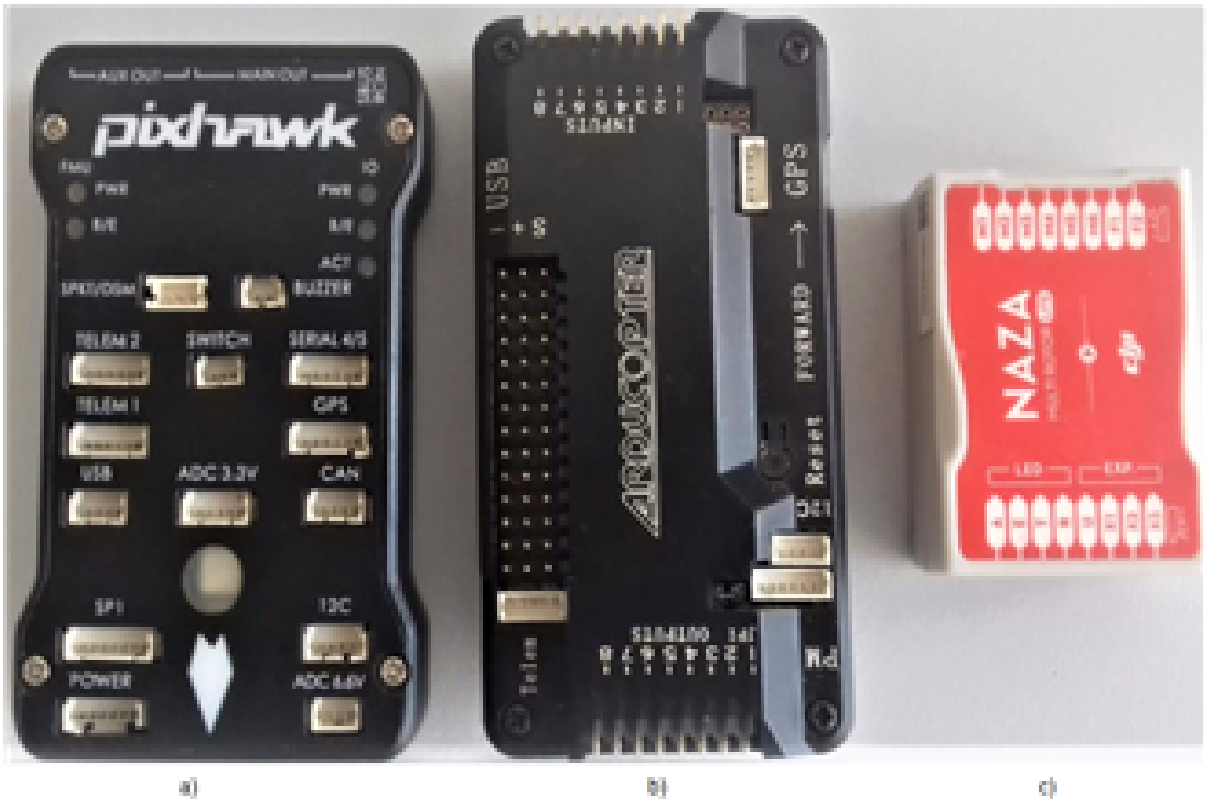

Figure 3.3 – Low cost Autopilots.
(a) Pixhawk, **(b)** Arducopter, and **(c)** DJI Naza.
Source: Author

The Pixhawk 4 FC board (a) contains, in addition to the common components for UAV stabilization, an FMU-STM32F765 main processor that also allows programming of parameters and movement commands flexibly. Pixhawk is one of the most stable and low-cost controllers, has open code, protocols and standards, in addition to continuous interaction with the community of professional computer and aeronautical engineers, ensuring quality, safety and efficiency of products for modern autonomous systems. According to analyses carried out by (YANG Z.; LIN, 2016) and the facts presented previously, Pixhawk 4 was the choice for this research.

Arducopter (b) is one of the pioneering autopilots to enable the use of reliable autonomous vehicle systems. It has a basic set of tools suitable for almost any vehicle and application. It has an extensive community to support open source implementations, but was disregarded in the study due to its limited, outdated hardware and recurring firmware problems.

The NAZA-M Lite (c) FC system has high reliability and stability, the autopilot contains internal damping, controllers, 3-axis gyroscope, 3-axis accelerometer and barometer. It also has an advanced attitude stabilization algorithm, hovering accuracy is approximately 2.5 m horizontally and 0.8 m vertically (DJI, 2019). However, it is poorly adaptable to GPS failures, thus being dependent on its sensors and significantly increasing the error rate. It has a certain limitation in accessing parameters and sending commands to the

aircraft, requiring the use of specific software, and was therefore disregarded from the study.

3.3 Frameworks

Control frameworks are tools that help in programming algorithms and organizing packages, versions, sharing, among other facilities, Control frameworks are tools that help in programming algorithms and organizing packages, versions, sharing, among other facilities, the frameworks used in this project were chosen based on the authors' affinity.

Once the control algorithms for the drone swarm systems were developed, computer simulations of the operation of these systems began. For this purpose, the authors choose the MAVSDK because it is a Software Development Kit (SDK) originally implemented in C++, but currently has a collection of libraries for integration with other languages, such as Python. It is easy to adapt to Pixhawk and interact with MAVLink (OES, 2019).

The data stream is also published as peer-to-peer topics with relay. The way vehicles are managed in MAVSDK is through a simple Application Programming Interface (API), with easy and intuitive access, enabling faster implementation.

3.4 Graphical User Interface

FC software for UAVs assists in configuring, obtaining data, planning, and executing a flight plan, thus optimizing time and reducing costs. The Ground Control Station (GCS) is a ground FC center that provides these functions, this allows greater monitoring of the actions being carried out both in real time and offline (WILLEE, 2019). Therefore, a GCS must contain: mission planning, display of equipment data, telemetry schedule, data terminal on the ground, communication equipment and its protection device, possibility of PID adjustment, and integration with other sensors and equipment. All of this using a Graphical User Interface (GUI) (HAQUE S. R.; KORMOKAR, 2017).

The QgroundControl (Figure 3.4) is a GCS compatible with Ardupilot and Pixhawk, is open source and has integration with various systems such as Windows, Mac OSX, Linux, iOS and Android. Allows complete modifications to the PID controller even with UAV in the air. Enables the integration of multiple UAVs for easy configuration or use in parallel. This GCS was defined for this study due to its versatility in terms of interface, being the most intuitive of those analyzed. In this way, it serves both beginners offering a great GUI, and also, for the more experienced, it allows total modification of the parameters and the software as a whole.

Figure 3.4 – QgroundControl interface.
Source: (QGC, 2023)

3.5 Simulation

Simulation plays a fundamental role during research, it allows tests to be carried out on different algorithm models that would be carried out in the field, but safely and quickly. Tests in real environments must first go through a simulation with the greatest possible similarity. In the case of using a real UAV in tests in a real environment, if there is any complication, an accident for example, the costs increase considerably.

The environment simulators considered for analysis have open source, compatibility with previously defined tools, proximity to real-world physics with regard to the position of the ground and objects, applied angular and linear forces, lighting, collisions, and visual proximity. Furthermore, it is necessary that all these characteristics are controllable and auditable to collection and subsequent analysis of data.

The AirSim simulator (Figure 3.5) was defined for use in this study, because it is a photorealistic simulator developed exclusively for machine learning development, it is available for Windows and Linux, and was developed by the Microsoft research team. The graphic is based on Unreal Engine 4, is previously interconnected with the Mavlink interface, making it possible to run Hardware in the Loop (HIL) Simulation (SHAH, 2018).

Figure 3.5 – AirSim simulator.
Source: (MICROSOFT, 2019)

It has its own APIs with a modular design for retrieving data and controlling vehicles easily and independently with various sensors such as monocular and depth cameras. Although APIs are limited, they are sufficient for most machine learning simulations, and accessible through several programming languages, including C++, C#, Python and Java (HENTATI, 2018).

3.6 Convolutional Neural Networks

This research work used a Convolutional Neural Network (CNN) (Figure 3.6), that is a variation of Multi layer Perceptron (MLP) biologically inspired Artificial Neural Network (ANN), for image processing, in this way, several classes of different layers of deep neural networks apply filters at various levels to manage, extract, and classify visual information from a digital source (BRITO, 2019).

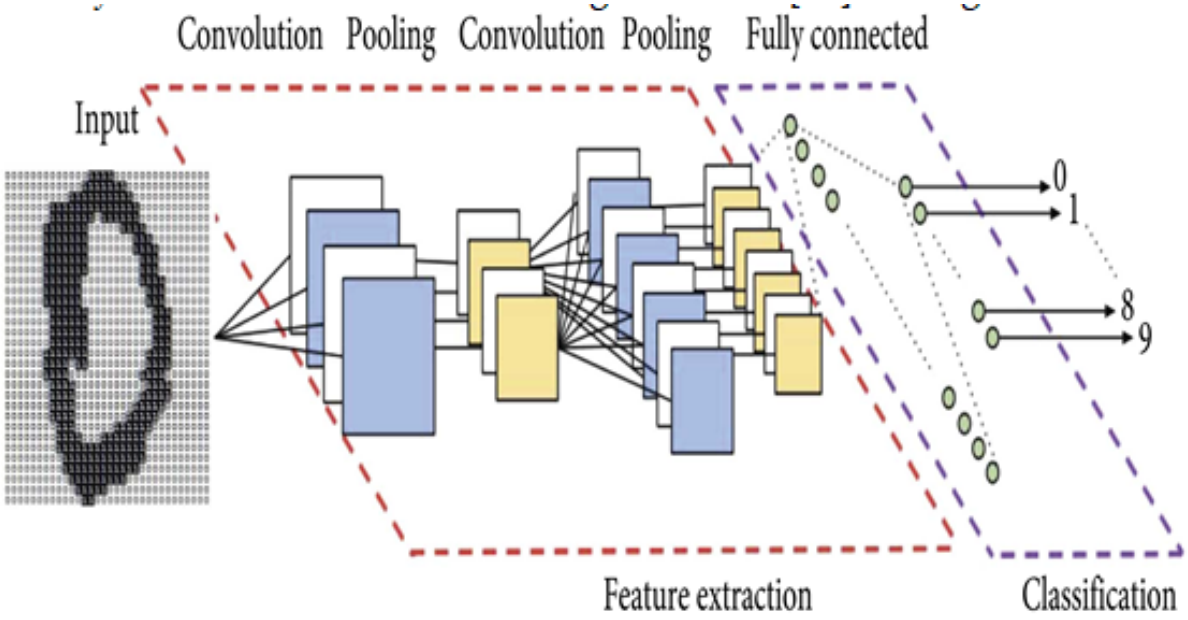

Figure 3.6 – Convolutional Neural Network simplified architecture.
Source: (VARGAS, 2016)

The CNN architecture can have different combinations of layers according to the proposed solution. The initial and middle layers generally have a convolution function, where neurons are mapped according to a subdivided kernel and an operation on a group of pixels within the image. The image is then filtered and classified according to important features and condensed to process the current set and increase network speed. Finally, the fully connected layers provide the network output (ZEILER M. D.; FERGUS, 2014).

3.7 Transmission Line Tracking

To track power TLs in detail, it is necessary to obtain images as close as possible to the structure and line segment, avoiding collisions and respecting legislation, thus allowing a detailed inspection of the target elements. For this purpose, the planning of ideal trajectories for continuous tracking was determined.

From the Figure 3.7 it can be seen the UAV trajectories, let be **p** the position in relation to the view of two or more towers by an external observer, **b** the distance in meters from two points between two segments defined between two towers, and **s** the line segment between two towers. Assuming an image parallel to the plane, the horizontal distance between the UAV trajectory (in the upper position) and the center of the two towers must be as small as possible, Equation 3.1 refers to the central tracking of the power transmission lines between the towers.

$$d_1 p_1 = s_1 \tag{3.1}$$

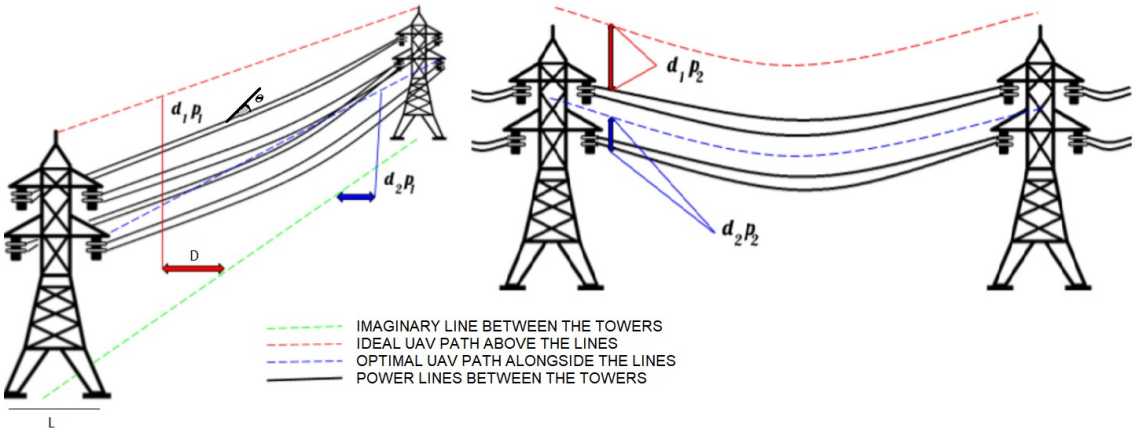

Figure 3.7 – Proposed tracking solution.
Source: Author

Likewise, assuming an image perpendicular to the plane, the distance between the UAV in the lateral position and the line segments must be centered at Equation 3.2, which is responsible for viewing all the wires on one side of the power transmission towers.

$$d_2p_2 = (s_2 - s_3)/2 \tag{3.2}$$

The other distances require a constant **c** so that current legislation is met and a complete view of the wires is obtained. In Equations 3.3 and 3.4 the upper and lateral distances from the UAV are presented respectively.

$$d_2p_1 = c_1.s_1 \tag{3.3}$$

$$d_1p_2 = c_2.s_1 \tag{3.4}$$

After determining the values, if necessary, a simple correction process begins for the UAV trajectory in relation to the difference obtained by these distances. To guarantee this situation, UAVs must be equipped with a camera guide and stabilizer, known as a gimbal, as the movement of the UAV is not constant, and this can influence the results. For the purpose of comparing model results, a camera orientation and 3 movements will be considered for the following two positions of the UAV:

1. Drone above the lines: Forward Yaw (+Y) and YAW Turn in both directions, with camera facing downwards (+90º First Person View (FPV) in PITCH);
2. Drone from the side of the lines: Forward yaw (+Y) and Z axis in both directions, with camera oriented sideways (+90º left or -90º right FPV in YAW)

Both UAVs will act simultaneously and can also be used in a mirrored position, totaling four collaborative UAVs with different activities. Acting together and in constant com-

munication, the movement decisions of each intelligent agent specializing in their actions can be shared between them in a collaborative way. Furthermore, it is possible to provide complete coverage of the structure and obtain more detailed images for inspection of specific points.

3.8 TL Tracking Algorithm

To track the TLs, initially, the parameters of the UAVs initial position, availability and frequency of obtaining images, length of the path to be covered, and standard speed of defined movements are defined. After obtaining the first image, resizing is carried out to convert the image to shades of gray, thus allowing the optimization of subsequent processes that involve the use of the following three algorithms:

1. The Hough Transform (HT), that is an algorithm that receives a binary image with candidates that can belong to a certain straight line, in this way it is possible to find contours that can be parameterized by a well-defined equation as straight lines (BELTRAMETTI M.C., 2021). Representing the perpendicular distance from the straight line to the origin of the image coordinate system and its inclination, based on a predefined number of curve intersections between two different points intersecting in a plane, it is possible to conclude that both points belong to the same line (HUAMÁN, 2019).
2. The Probabilistic Hough Transform (PHT), is more efficient in solutions that need to consider the image as a whole, because its output is the extremes of the lines detected in relation to the dimensions of the image (KIRYATI N.; ELDAR, 1991).
3. The Line Segment Detector (LSD), was designed to work with few external parameters, automatically adjusting the number of false detections. This technique uses a validation approach in reverse. LSD has a execution time proportional to the number of pixels in the image, that is, its detection takes linear time to return accurate results to the subpixel (GIOI R. G. VON; JAKUBOWICZ, 2012).

An image processing determined to be closest to the ideal for the general situation is carried out to facilitate the identification of straight line segments according to the images obtained, thus, the noise filter with a kernel size of 3 or 5 is applied for experiments. In edge detection, a threshold of [50,300] is used to classify any gradient edges with this range as valid (MARTINS, 2020).

After these processes, all sets of accepted parallel lines are found. This restriction is defined by the minimum size defined by the average of the results obtained, to disregard small lines belonging to towers or external elements.

If none are found, the process must be restarted, the selected set is the one with the largest straight line segment sizes. This value is used to determine the direction of rotation, or, ascent and descent to be carried out by the upper or lateral UAV respectively.

$$Action(x) = \left.\begin{cases} left & if(0 < x < 1/3) \\ center & if(1/3 \leq x \leq 2/3) \\ right & if(2/3 \leq x \leq 1) \end{cases}\right\}, wherex = Piso(\Theta_{\propto} - \Theta_{last}), \forall \propto \epsilon A \quad (3.5)$$

The angle formed between the central axis of the image with the central space of the parallel lines is obtained through the hyperbolic tangent function, it was chosen because it has a stable behavior to obtain a unique angle in the calculation from a point, in this case the end of the straight line. According to equation 5, if there is more than one adjustment angle $\propto$ identified in set A, related to the results of left, center or right movements of the UAV, the value is defined based on the smallest value of the difference with the previous Θ_{last}.

As a result with a discrete variable, this value must be defined in the range of the most significant third of the total viewing angle, thus determining the action that will transform into the movements of the UAVs.

4 Results

This chapter presents the results obtained by simulated test scenarios and real tests carried out in accordance with current flight regulations and permissions. An analysis of the experiments is performed with each study solution to select the best of each technique.

Finally, with the intention of validating the solutions obtained in this study, some experiments were also analyzed with the execution of the route in the synthetic Airsim environment, and in real images collected from energy transmission towers.

4.1 Object Recognition Result

Image classification involves assigning a class label to an image, whereas object localization involves drawing a bounding box around one or more objects in an image. Object detection is more challenging and combines these two tasks and draws a bounding box around each object of interest in the image and assigns them a class label. Together, all of these problems are referred to as object recognition (BROWNLEE, 2021).

So that the intelligence of UAVs during flight can identify the objects involved in the inspection of TLs, four classes of objects were defined: people, insulators, towers and lines. The images in the dataset went through a manual process called labeling, where these four objects of interest do not receive their respective labels assigned by a human before the images are subjected to training by a neural network. Figure 4.1 shows these four objects classified during training for a practical application in TL.

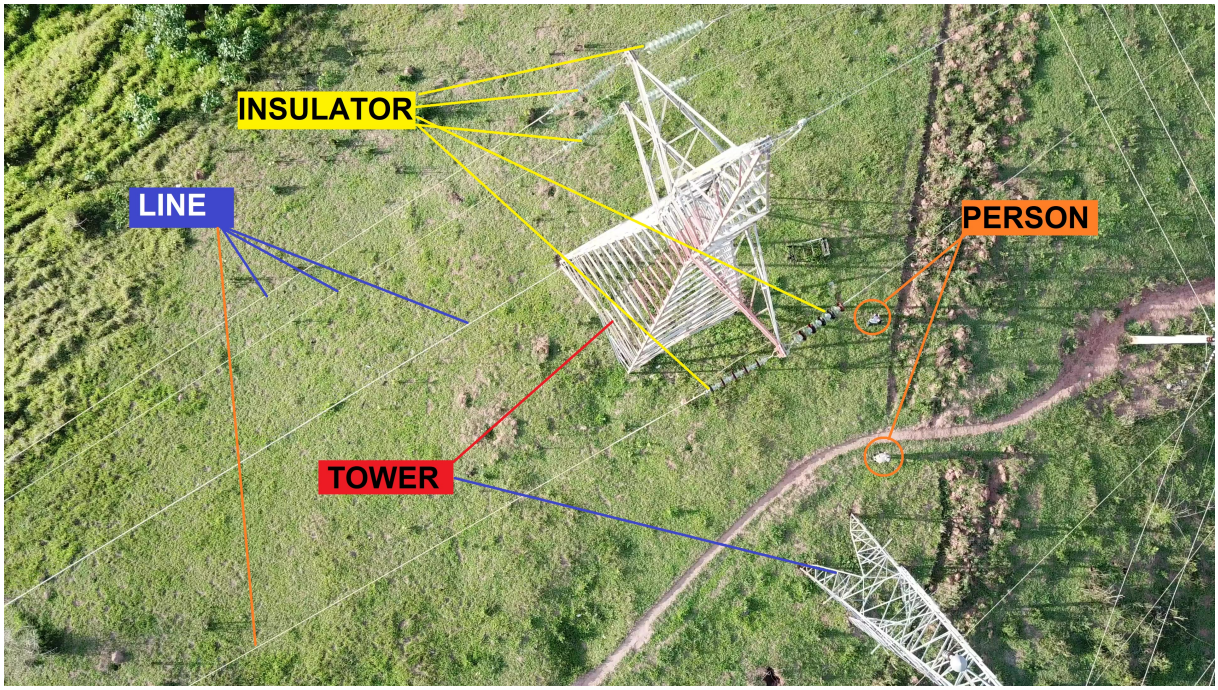

Figure 4.1 – Objects classified during training.
Source: Author

Once trained, an artificial neural network will provide, for each image presented as input, an output containing the degree of confidence that the network has in the detected object belonging to the class inferred by the network.

In this work, for the process of labeling and training the neural networks, the Roboflow dataset manager (ROBOFLOW, 2022) was used, which allows for each input image applied to the input of a trained neural network, based on the output (inference) of the network, to draw the bounding boxes around the detected objects. Figures 4.2 shows the five object classes identified by the trained algorithm. Figure 4.3 shows an image of a video that includes the percentage of certainty that the trained network achieved in each identified object. This video can be watched at (MARTINS, 2023).

Figure 4.2 – Identified objects.
Source: Author

Figure 4.3 – Objects identified and percentages of certainty.
Source: Author

4.2 Simulation Tests

In order to guarantee control of the UAV during the transmission line tracking, a test scenario was set up, containing towers, transmission lines, as well as different scenarios

simulating the area of the towers to have more elements to be tested by the computational vision algorithm.

Three different types of high voltage towers were reproduced in the study, used to transmit energy over long distances, one with 115 kV and two with 230 kV, as shown in Figure 4.4.

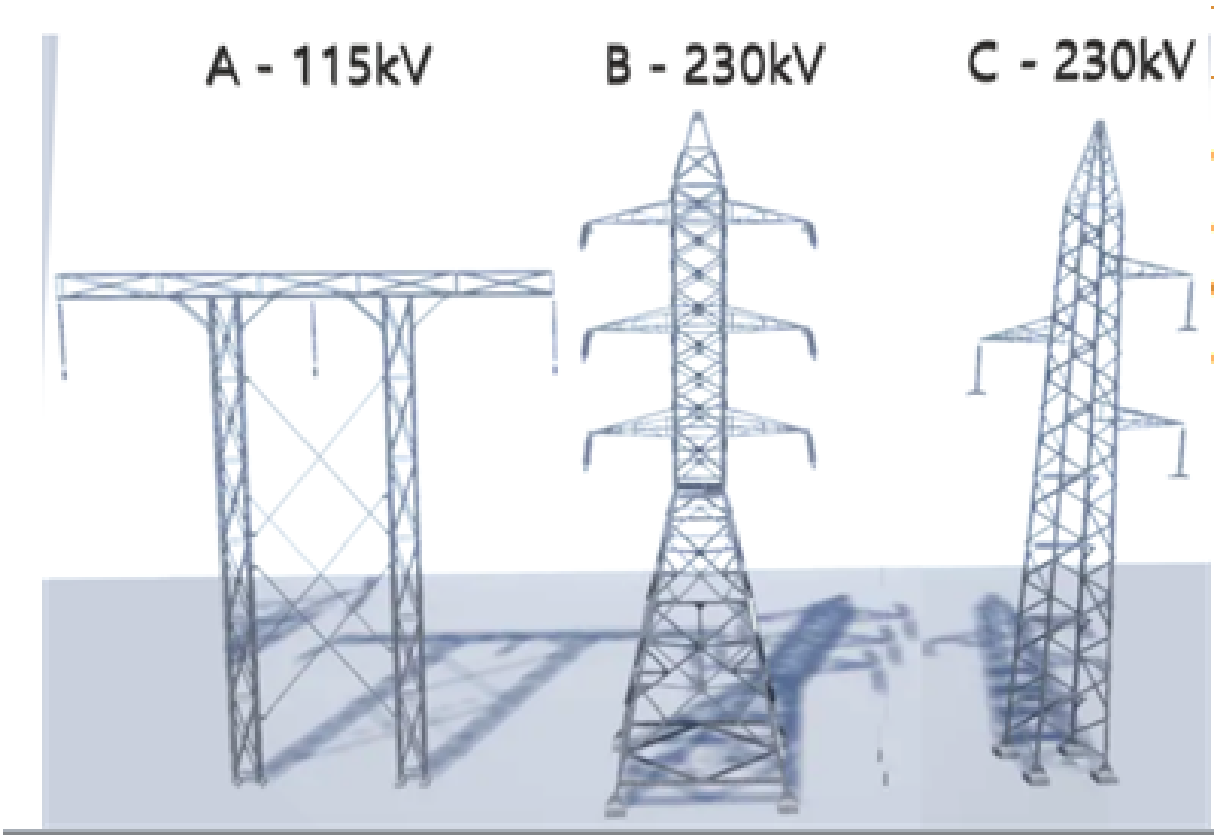

Figure 4.4 – High voltage transmission towers used in simulator.
Source: Author

Two different environments were also reproduced in this study for testing (Figure 4.5). The first depicts a clean simulation, with only the towers and lines connected. The second has a more realistic ground, with differentiation of relief and objects on the ground that do not belong to the structure of power transmission line.

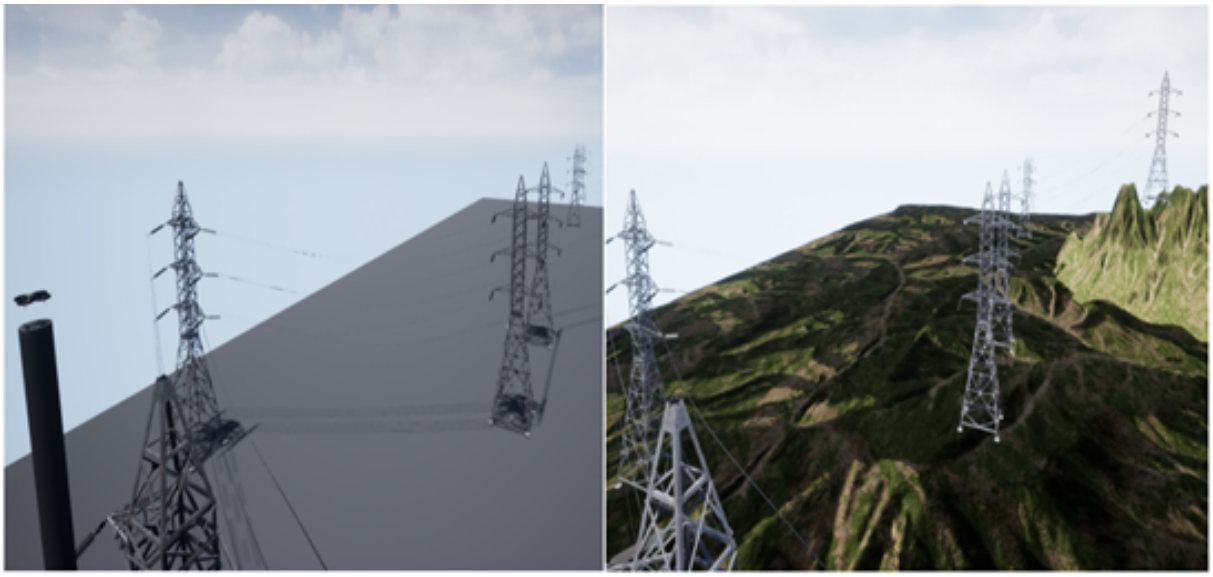

Figure 4.5 – Simulated worlds used in simulation.
Source: Author

Figure 4.6 shows the objects in the simulated environment.

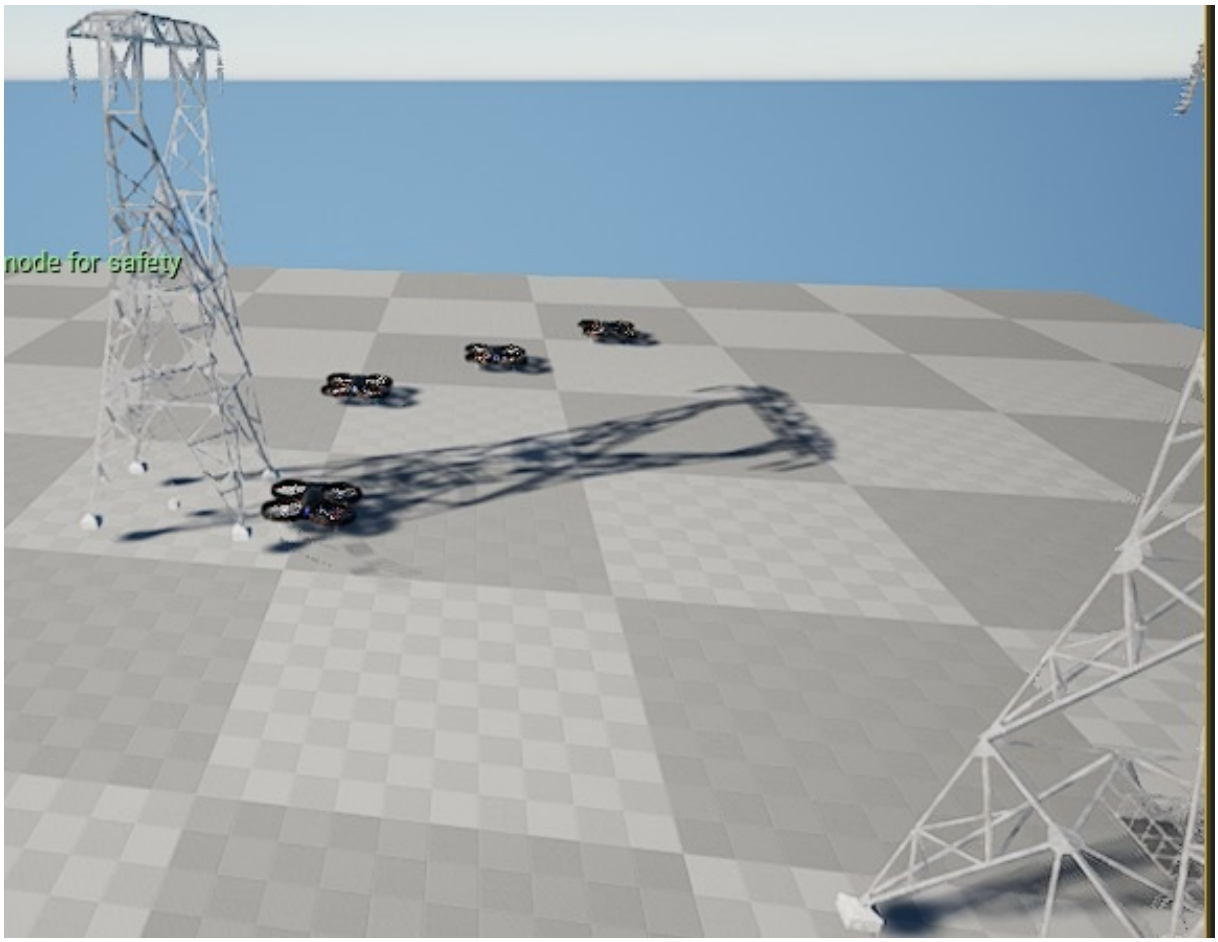

Figure 4.6 – Objects in simulation.
Source: Author

4.3 Image Dataset

It was necessary to produce a dataset with real and simulated images taking into account routes and positions during inspections of power transmission lines and towers. In total, 1005 images of 3 different types of towers were collected and labeled, in 3 real environments and 3 simulated environments. These images were labeled according to the position of the line represented in the image, both for the Real Image Dataset and for the Simulated Image Dataset, according to the discrete action to be performed by the UAV. A sample of these labeled images is presented in Figure 4.3.

Figure 4.7 – Sample datasets
(a) marked pictures; **(b)** view from above and **(c)** side vision.
Source: Author

When preparing the Dataset, the images were divided into 905 for training (90%), 80 images for validation (8%) and 20 images for testing (2%). With the intention of improving the model's learning, a contrast [-10%,+10%] and brightness [-10%,+10%] differentiation

reinforcement was generated, totaling 1,300 images for training, 116 for validation and 32 for testing.

Other forms of adding Datasets, such as rotation, cuts, occlusion, mosaic, and change of angulation, were not considered as they directly alter the result of the inference and contribute little. However, training tests were carried out using noise increment and blur, resulting in a small improvement compared to using only contrast and brightness in gray scale.

4.4 Edge Detection

Edge Detection (ED) in an image defines and stores the pixels that have some discontinuity or sudden change in relation to their neighbors. John F. Canny in (CANNY, 1986) proposed an algorithm, named after him, for detecting all edges of an image. The segmentation in this algorithm makes it easier to find straight shapes in images.

Its complete operation consists of applying a Gaussian filter to smooth the image and remove noise, finding the image's intensity gradients and determining potential edges by applying double Sobel [1], check if the pixel is part of a "strong" edge by suppressing all other edges that are weak and not connected to edges with a strong relationship of values between neighboring pixels (BRADSKI; KAEHLER, 2008). The figure 4.8 shows the application of the gradient filter in the Canny algorithm.

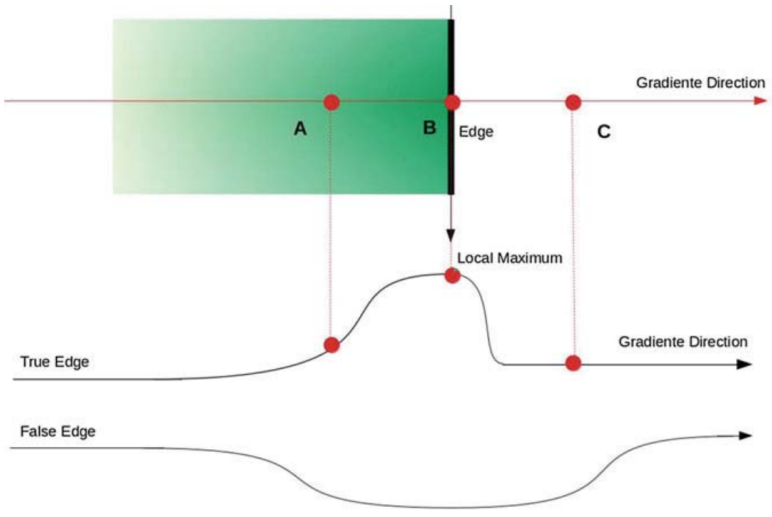

Figure 4.8 – Canny gradient filter. Source: (FILHO A. J. D.; RAMOS, 2020)

This section details the algorithm developed to track transmission lines using LSD, HT and PHT (described in Section 3.8). Initially, the system parameters are defined, such as the initial position of the UAV, availability and frequency of obtaining images, length of

[1] Operator used to determine potential edges through the gradient of the intensity function , obtaining the norm or horizontal and vertical gradient vector.

the path to be covered, and standard speed of the defined movements. After obtaining the first image, the image is resized and converted to gray scale, thus allowing the following processes to be optimized.

An image processing determined to be closest to the ideal for the general situation is carried out to facilitate the identification of straight line segments according to the images obtained, thus, the noise filter with a kernel size of 3 or 5 is applied for experiments. In edge detection, a threshold of [50,300] is used to classify any gradient edges with this range as valid. The edges are passed to a HT, PHT, and LSD (MARTINS, 2020).

These sets of real images will undergo manipulation processing, and the recognition techniques presented, considering n the number of instances, VP, FP and FN, their effectiveness will be evaluated with Precision, Recall, *F1 Score* and/or reward (GOUTTE; GAUSSIER, 2005).

The precision equation 4.1 measures the percentage of how correct a model's predictions are. This metric allows for a better assessment of when FPs are considered more harmful than FNs.

$$P = \frac{VP}{VP + FP} \tag{4.1}$$

The recall equation 4.2 measures how correct the results given as positive are. In this case, FNs are considered more harmful than FPs.

$$R = \frac{VP}{VP + FN} \tag{4.2}$$

The F1 Score equation 4.3 is a metric for the harmonic value between precision and recall. This metric allows quick evaluation of the model, indicating when precision or recall is low

$$F1 = 2.\frac{P * R}{P + R} \tag{4.3}$$

The criterion used in RL will be the maximum average reward achieved and average episode size of the total training, in relation to the total steps executed.

After these processes, all sets of accepted parallel lines are found. This restriction is defined by the minimum size defined by the average of the results obtained, to disregard small lines belonging to towers or external elements. If none are found, the process must be restarted, the selected set is the one with the largest straight line segment sizes. This value is used to determine the direction of rotation, or, Ascent and Descent to be carried out by the upper or lateral UAV respectively.

The angle formed between the central axis of the image with the central space of the parallel lines is obtained through the hyperbolic tangent function, as seen in Figure 21. It was chosen because it has a stable behavior to obtain a unique angle in the calculation from a point, in this case the end of the straight line.

Several experiments with Edge Detection were planned, and the results are presented in Table 4.1, where the grid, LL, and **UL** used in the Canny algorithm are presented, and then the average of the results referring to the number of potential lines are calculated using the HT, PHT and LSD algorithms in test images. Results with less than 5 valid lines for all algorithms were discarded, and results with more valid lines are highlighted in the table.

After defining the best parameters for each algorithm, experiments were carried out with images of real power TLs and the simulator, comparing them with the predictive actions according to the model established in the previous section. The values obtained are presented in Table 4.2.

Table 4.1 – Edge detection using test images with different parameters.

			Superior Drone			**Side Drone**		
Grid	**LL**[1]	**UL**[1]	**HT**	**PHT**	**LSD**	**HT**	**PHT**	**LSD**
3x3	0	100	13.0	10.75	0.0	21.0	21.75	0.0
3x3	100	100	3.0	5.75	2.0	16.0	16.0	19.0
5x5	50	100	29.5	**25.5**	**9.25**	61.0	19.25	29.75
5x5	50	200	28.25	26.5	**9.25**	53.75	18.5	21.75
5x5	50	300	27.25	23.0	**9.25**	50.5	**23.0**	21.75
5x5	100	100	29.25	24.25	**9.25**	60.0	18.5	26.25
5x5	100	200	27.75	23.75	**9.25**	53.25	18.25	21.5
5x5	100	300	26.5	23.0	**9.25**	50.0	20.5	21.25
5x5	150	100	28.25	24.5	9.0	56.0	24.0	24.75
5x5	150	200	26.5	24.25	9.05	53.75	22.25	21.25
5x5	150	300	26.5	22.25	9.05	49.5	19.5	21.25

[1]Considering an edge segment, for any value located above the UL, it is immediately accepted. For any value below the LL, it is immediately rejected. Points located between the two limits will be accepted if they are related to pixels that show strong responses.

Table 4.2 – Tests using the algorithms and determining the actions.

	Real life						**Simulated**					
	Superior Drone			**Side Drone**			**Superior Drone**			**Side Drone**		
	P	**R**	**F1**	**P**	**R**	**F1**	**P**	**R**	**F1**	**P**	**R**	**F1**
TH	0.29	**0.40**	0.33	0.17	**0.14**	0.15	0.17	**0.20**	0.18	0.29	0.40	0.33
THP	**0.31**	**0.40**	**0.35**	**0.18**	**0.14**	**0.16**	**0.22**	**0.20**	**0.21**	**0.36**	**0.40**	**0.38**
LSD	0.23	0.30	0.26	0.17	**0.14**	0.15	0.17	**0.20**	0.18	0.29	**0.40**	0.33

PHT was defined for comparison with other methods. The parameters selected for this algorithm have a 5x5 grid and threshold [0.100] for Canny Edge Detector, in identifying line segments.

4.5 Deep Learning

In this subsection, training of 6 popular high-performance Single Shot Multibox Detector (SSD) models used in the study is evaluated for training the developed Dataset. Some configurations and characteristics of the models are presented in Table 4.3.

Table 4.3 – Comparison of some popular SSD models.

Model	**FPN**[1]	**Batch**	**Optmizer**	**Parameters**
Inspection V2	NA[2]	24	RMS	10M
Mobilenet V1	NA[2]	24	RMS	3M
Mobilenet FPN	3.7	64	Momentum	4M
Mobilenet V2	NA[2]	24	RMS	3M
Resnet 101 FPN	2.7	64	Momentum	42M
Resnet 50 FPN	3.7	64	Momentum	25M

[1]Feature Pyramid Network (FPN). A feature extractor designed with feature pyramid concept to improve accuracy and speed.
[2]Not applicable

All these models use Rectified Linear Unit (RELU) activation and they are Residual Networks (ResNet) architecture based. They underwent training of 10,000 steps, with batch size 12, and 50 random images for each evaluation step. With training completed, the newly trained inference graph is extracted for later use in object detection. Furthermore, the export of trained weights is used for simple inference with the same raw images as the test set, for a quick empirical check of model quality.

4.6 Reinforcement Learning

In this section, the three RL algorithms and the reward mode will be evaluated for study in the proposed solution, using the clean world simulation environment and different towers.

To identify the best form of reward mathematical tests were carried out empirically, taking into account the main objective, adjusting the view of transmission lines and nearby surroundings in the search for identified problems. The straight line **AB** is the segment between two towers, one tower being point **A** and the next tower being point **B**, and the position of the UAV being point **P**.

Initially, the simple distance reward between two points **P** and **B** was determined, obtained by Equation 4.4. Despite the correct execution of the route throughout the training, the field of vision of the lines was compromised and the reward continued to grow, as the UAV only had to find one path to the next tower.

$$distance(P, B) = \sqrt{(P_x - B_x)^2 + (P_y - B_y)^2 + (P_z - B_z)^2} \tag{4.4}$$

A reward through the minimum distance from a point to the center of line segments was tested. Using vectors in modulus, the distance measured from **P** to **AB** given by negative Equation 4.5 is given as a reward, that is, the closer to zero the greater the reward.

$$distance(P, B) = \begin{cases} 0 & , if(P = A) or (P = B) \\ |P - A| & , if \Theta(AB, AP) > 90) \\ |P - B| & , if \Theta(AB, BP) > 90)) \\ \frac{|B - AxA - P|}{|B - A|} & , otherwise \end{cases} \tag{4.5}$$

The reward per episode during the training showed that the reward met the proposed solution, as it encourages the agent to center the field of vision on the lines. However, this reward mode encourages the execution of unnecessary movements that distance the agent from the next tower. In this way, a composition of rewards is proposed to accelerate the agent's learning. Equation 4.6 defines the relevance weight for each negative distance obtained.

$$reward = (distance(P, B) \star 0.1 + distance(P, AB) \star 0.9) \star (-1) \tag{4.6}$$

This reward format allows the agent to identify the best action to take to reach the next tower while remaining centered in the field of view of the power TLs. The values for the markers were then defined, -50 for the punitive marker and +20 for the target marker, defined in model section 45, and with no limit on both success and failure for reward accumulation.

4.6.1 Reinforcement Learning Algorithms

The Reinforcement Learning (RL) algorithms proposed in the materials and methods section were trained in a continuous space environment, with discrete actions and an individual acting agent. As hyperparameters, it was used a learning rate of 0.002, batch size 32, due to the number of steps, episodes and low discount, which help in long-term training. The training time was up to 15,000 steps, the graphs of episode size and average reward are presented in Figure 4.9.

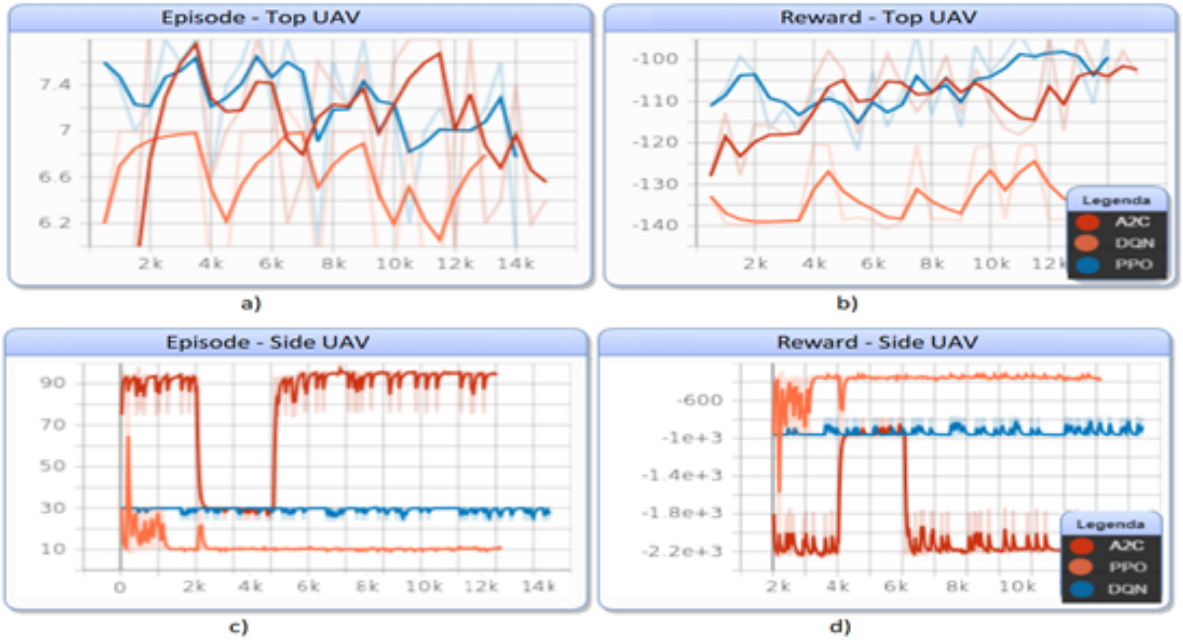

Figure 4.9 – Training and learning results for DRL.
Source: Author

According to the results presented, DRL performed better on the UAV positioned at the top of the structure, whereas the UAV positioned on the side, even with a low update rate, was unable to progress with the increase in reward.

4.7 Simulated Environments

4.7.1 Airsim Simulator

As shown in Figure 4.10, the route developed in the simulator was based exclusively on the set of towers whose images were taken in the field to assemble the Dataset, the use of all movements in the defined model was taken into account.

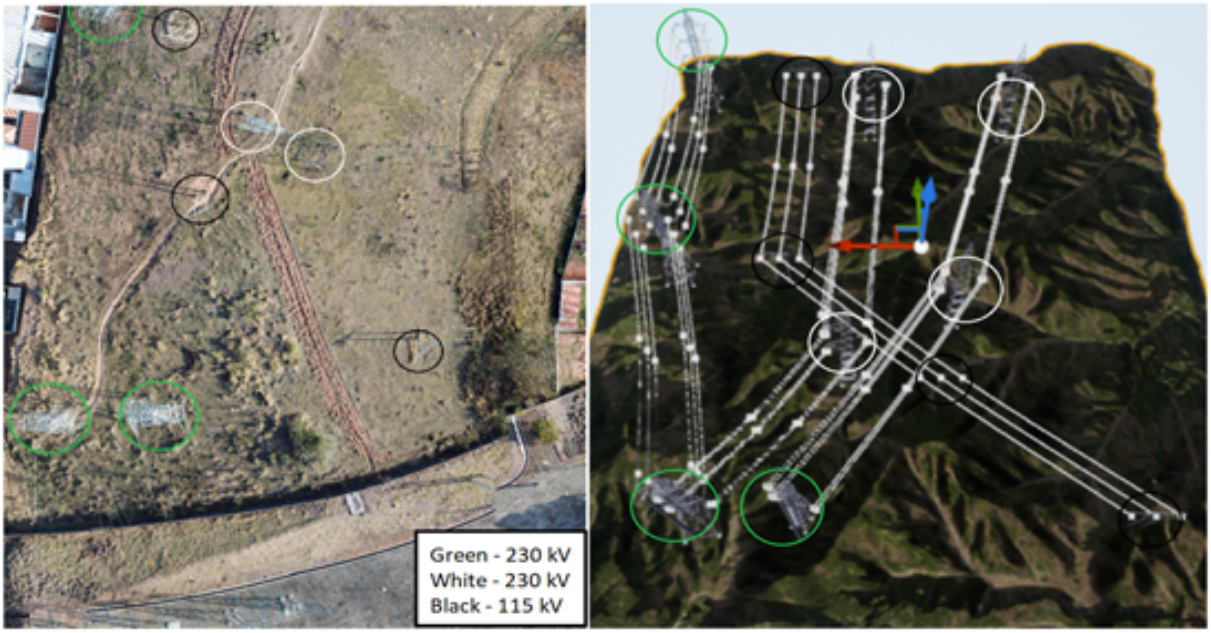

Figure 4.10 – The routes done by the UAV.
(a) real life, and **(b)** simulation.
Source: Author

Three algorithms was developed in the first moment, the Main Control Algorithm, the Buffer Control Algorithm, and the Simplified Inference Algorithm. This section explains each of these algorithms.

The Main Control Algorithm was developed to control UAVs in a discrete collaborative way, its pseudocode is presented in Algorithm 4.1. This ensures execution in a swarm system, where each UAV has its own function and works together. This Main Control Algorithm is executed for each proposed solution separately, initially the necessary packages are loaded and initialized, a control loop is executed until the final situation is reached, which may be a number of towers, a distance in meters, GPS position among others, the route results are displayed at the end of the program.

Algorithm 4.1 Main Control Algorithm

```
...                                                    ▷ Packets...
buffer ← []
UAV_up ← NewUAV()
UAV_side ← NewUAV()
...                                                    ▷ Initializations
while control do                                       ▷ Route
    buffer(UAV_up, UAV_side)
    buffer(UAV_side, UAV_up)
    ...                                                ▷ Results
end while
```

The Buffer Control Algorithm (Algorithm 4.2) is called by each UAV in the main program.

Its objective is to ensure that the UAV identifies and performs an action, so that the other UAV can also perform it.

Algorithm 4.2 Buffer Control Algorithm

```
function Buffer(UAV1,UAV2,buffer1,buffer2)                ▷ Cooperating
done ← false
while not done do
    Inference(UAV1)
    if (buffer) then
        RealAction(UAV2, buffer.pop)
        done ← true
    end if
end while
```

The Action Identification and Storage Algorithm (4.3) is responsible for determining the action that the UAV will perform based on the last image obtained by it, and the type of solution that wishes to be used, if identification is successful, the action is executed and stored in temporary memory (buffer).

Algorithm 4.3 Action Identification and Storage Algorithm

```
function Inference (UAV)                                  ▷ Action
movement ← identify_movement(UAV)
if (movement) then
    RealAction(UAV, movement)
    buffer.push(movement)
end if
```

4.7.1.1 Evaluation of the Selected Methods

In this subsection, comparative results of the selected techniques are presented, both for the upper UAV and the side UAV, in edge detection, deep learning and reinforcement techniques. Each of the experiment data is obtained from 10 runs of a given observation method and variable. Table 4.4 lists the average training and execution time for each method developed for the solution. The training time is understood from the beginning until the end of training or parameter definition (in the case of Edge Detectors) in each suggested model, that is, the time for the defined model to be ready for use in the main algorithm. The execution time is the interval between receiving the image and defining the action to use UAV in the simulator.

Table 4.4 – Average training and execution time.

Method	**Training (hours)**	**Executing (seconds)**
Edge Detecytor	2	0.3
Deep Learning mono class	20	2.72
Deep Learning multi class	22	3.10
Reinforcement Learning	90	0.87

It is possible to observe that Edge Detector maintains the highest execution speed, mainly due to the non-use of a neural network. Reinforcement Learning also has a fast execution despite having a neural network, this is mainly due to the fact that the reinforced trapping structure allows for a simplified network. The Deep Learning model has a considerably longer execution time, this is mainly due to the size of the neural network, and the identification and return structure using bounding boxes.

When comparing the variables in the experiments (Figure 4.11), it is possible to observe that the average error in Edge Detector and Deep Learning is smaller when compared to Reinforcement Learning, especially when noise is generated, such as in the storm and in the dark, and this shows a low detection rate. The best result was from Deep Learning, as the Edge Detector did not adapt well to the altitude variation. This result also shows that Reinforcement Learning can be trained more intensely in situations where the image received is unstable, since generally the learning rate used in deep neural networks is low, emphasizing long-term training. It is assumed that the results obtained in Deep Learning may reflect external elements that interfere in the identification of the action such as: trails, curbs, roads, objects, among others.

Regarding the total distance reached, Deep Learning and Edge Detector obtain similar results, with a small advantage to Deep Learning, at the same levels mentioned above, this is due to the generalization capacity of the technique used. The best result is obtained by Reinforcement Learning at most levels, it is understood that this occurs due to reinforcement training, which avoids the worst rewards obtained mainly when leaving the field of vision of the lines. This fact shows that different limit restrictions and training with images obtained in the field are necessary to be able to observe a real generalization of long-distance tracking of the transmission line corridor.

4.7.1.2 Environment variables

With the intention of broadly analyzing the trained models, test experiments were defined to examine how much certain factors affect the variables related to them. To inspect the exact effect of each factor and its combinations, factorial design was the model chosen for the experiments. The idea is to select levels for each chosen factor and see how each level impacts the experiment. Since the factorial design works with factors and variables,

3 factors with 2 levels and 3 variables each were defined, and are presented in Table **??**

Table 4.5 – Environment Variables for testing the models

Factor	Level	Variable
Bright (B)	Clear (C)$5\frac{lumens}{m2}$ Dark (D) $1\frac{lumens}{m2}$	Average Correct Distance [m]
Distance (D)	Near (N) $5m$ Far (F) $10m$	Total Distance Achieved [a]
Weather (W)	Good (G) *Limpo* Rainy (R) *Chuva e Vento*	Tempo médio de execução individual [t]

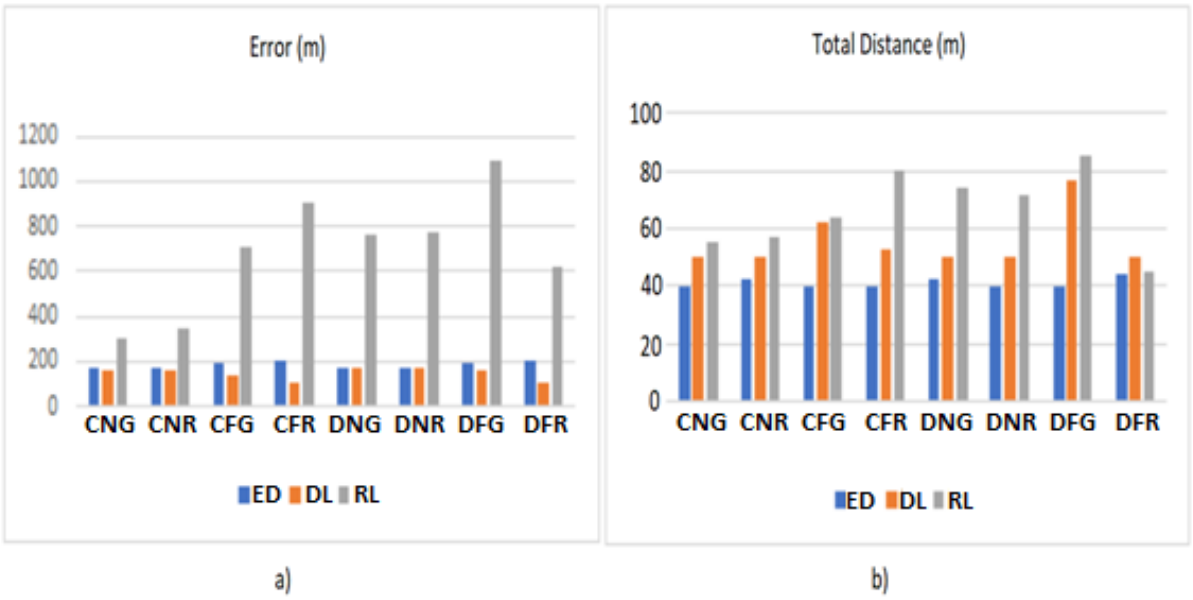

Figure 4.11 – Error and distance graphs.
(a) error and **(b)** distance.
Source: Author

4.7.2 Simulated UAVs and Real Images

As shown, initially the simulations were run in the Airsim simulator, a sophisticated development environment that is very realistic, but demanding an enormous amount of time and effort dedicated specifically to the simulator software, worlds and scenarios to be built to reflect the real world.

To minimize the time spent on these simulations, allowing greater dedication to the problem to be solved, in our case, in image processing, recognition of transmission lines, transmission towers and UAV trajectory control, a a simplified and dedicated simulator was developed in Python language, including a scenario with a variable and configurable number of UAVs represented by red dots, with behavior based on Reynolds flocking rules (REYNOLDS, 1987).

4.7.2.1 Reynolds Flocking Rules

(REYNOLDS, 1987) introduced a set of behavioral rules aiming to simulate the movement of groups of animals, such as flocks of birds or schools of fishes. He created a computer program in which entities called boids, the shortening of the expression *bird-oid object*, which refers to a *bird-like* object. These boids move following these rules. To best represent the behavior of real animals, was not created any central control, but instead programmed each boid to sense its own environment and decide where to move. This resulted in a fluid movement very similar to real bird flocks.

The flocking rules are represented in Figure 4.12 and can be described as the following: **(a)** Separation: boids try to move away from nearby flockmates to avoid collisions; **(b)** Alignment: boids try to match their heading with otherboids; and **(c)** Cohesion: boids try to move closer to the other boids to form a flock. (BRAGA et al., 2018b).

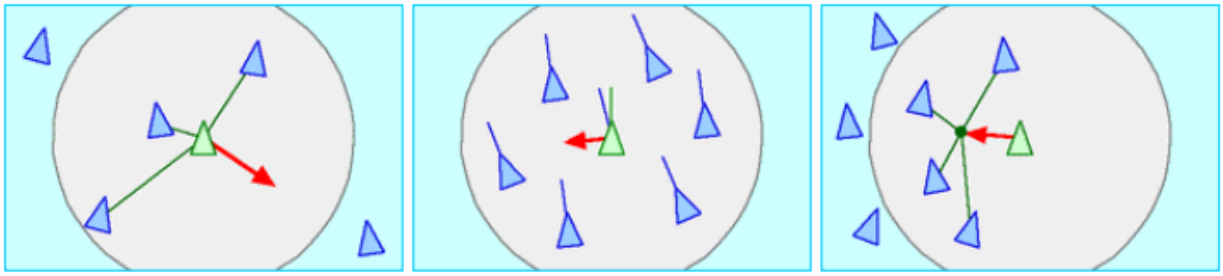

Figure 4.12 – Reynolds Flocking Rules.
Source: (REYNOLDS, 1987)

This solution allowed us to continue with the experiments without worrying about issues of collision and grouping of the UAVs, but only with the trajectory during the inspection of the TL.

To allow computers with less processing power to simulate the solution proposed in this thesis, a simulation environment written in Python language was developed.

Separation rule moves a boid away from the others, avoiding collisions. Vectors are created that point in the opposite direction of each detected neighbor, forming a single resulting vector. The code moves the boid in the direction of this resulting vector. Occasionally it is possible that the boid simply does not move, if the resulting vector has a value equal to zero. The implementation of these rules is shown in Algorithm 4.4.

Alignment rule moves a boid in the same direction as its neighbors based on the average direction they are moving. The implementation can be seen in Algorithm 4.5.

Cohesion rule moves the boid to the center of mass of the flock forming a swarm based on the average XYZ position of the neighbors. A vector pointing to this location is created and returned to the main program The implementation is shown in Algorithm 4.6.

Algorithm 4.4 Separation Rule Algorithm

```
1: procedure SEPARATION
2:     array V← 0
3:     for all n neighbors do
4:         V_n ← (this.position − n.position)
5:         V_n.normalize
6:         V_n ← (V_n ∗ distance(this, n))
7:         V ← (V − n)
8:         return V                          ▷ The array V is updated
9:     end for
10: end procedure
```

Algorithm 4.5 Alignment Rule Algorithm

```
1: procedure ALIGNMENT
2:     array V← 0
3:     for all n neighbors do
4:         V_n ← V_n + n.xyzVelocities
5:     end for
6:     V_n ← V_n/n
7:     return V                              ▷ The array V is updated
8: end procedure
```

Algorithm 4.6 Cohesion Rule Algorithm

```
1: procedure COHESION
2:     array V← 0
3:     for all n neighbors do
4:         V_n ← V_n + n.xyzPosition
5:     end for
6:     V_n ← V_n/n
7:     return V                              ▷ The array V is updated
8: end procedure
```

Migration rule moves the swarm to a destination point. In our case, the migration point is dynamically calculated in real time depending on the TL tracking task. The implementation is shown in Algorithm 4.7.

Algorithm 4.7 Migration Rule Algorithm

```
1: procedure MIGRATION
2:     array V← 0
3:     if MigrationPoint then
4:         V_n ← MigrationPoint + this.position
5:     end if
6:     return V                              ▷ The array V is updated
7: end procedure
```

Finally, a control algorithm is run independently on each UAV. In each loop, algorithm

(a). gets the pose of the boid based on the xy coordinates; (b) for each neighbor, obtain its pose relative to boid; (c) Apply Reynolds rules for Separation, Alignment, Cohesion and Migration and move the boid according to these rules. The algorithm is shown in Algorithm 4.8.

Algorithm 4.8 Swarm Control Algorithm

```
1: procedure MAIN
2:     getPose()
3:     getNeighbors()
4:     V1 ← Separation()
5:     V2 ← Alignment()
6:     V3 ← Cohesion()
7:     V4 ← Migration()
8:     Vres ← r1 * V1 + r2 * V2 + r3 * V3 + r4 * V4
9:     moveTo(Vres)
10: end procedure
```

Shown below are the results obtained using the developed environment that combines two simulated UAVs acting on video images captured in real flights.

Figure 4.13 shows a top view of five simulated UAVs flying over a transmission tower. All aircraft are grouped above the TL structures. The five red dots are the boids and represent the UAVs. The lead UAV starts positioned at the beginning of the mission via GPS geographic coordinates and the other aircraft position themselves autonomously, reacting to Reynolds rules and pre-defined parameters of minimum distance between each aircraft and the transmission lines, 10m above the tower.

Because the UAVs are under the effects of Reynolds' rules, they proved to be stable throughout the experiment, remaining cohesive and, at the same time, remaining a safe distance from each other, in a completely autonomous way. This was one of the biggest challenges to be overcome.

Figure 4.14 shows the side view of five simulated UAVs tracking a TL.

In all these images, the simulated aircraft interact with each other, keeping their distance from each other (dispersion rule) and follow the leader UAV and neighboring aircraft (alignment rule) and tend to go towards the group's center of mass (cohesion rule). They are still under the action of an intelligence (Section 4.7.1) that keeps them away from the lines and towers and on the path between one tower and another so as not to lose sight of the TLs.

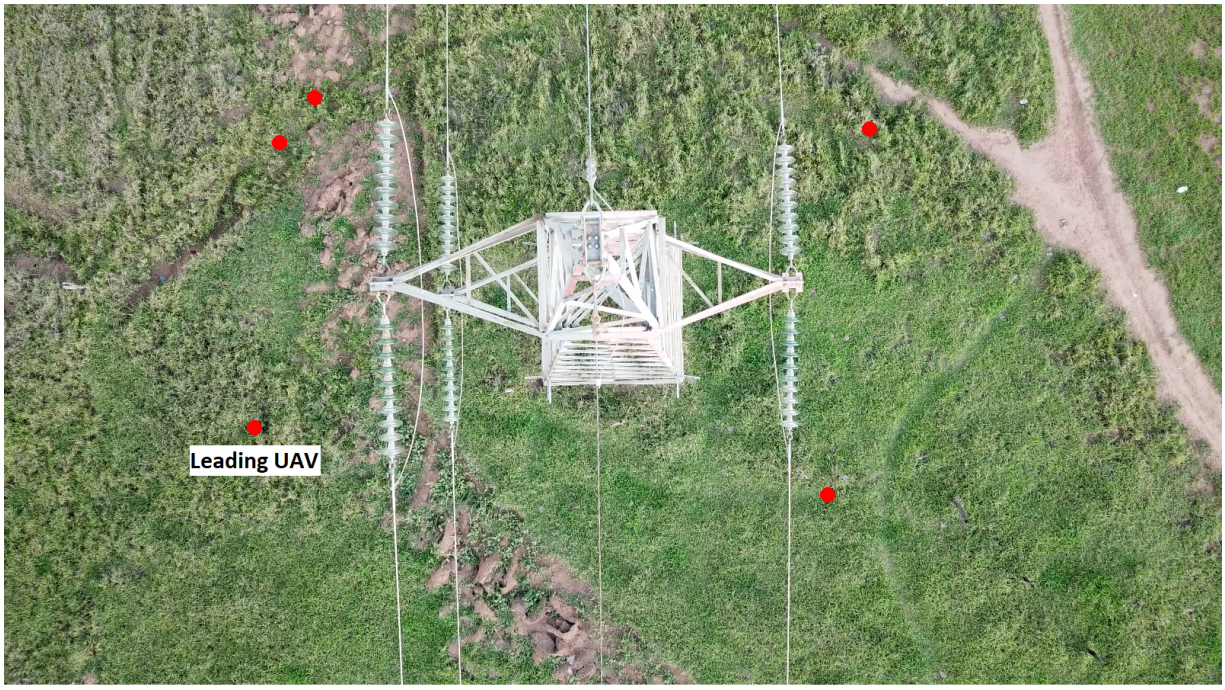

Figure 4.13 – Top view of five simulated UAVs flying over a transmission tower
Source: Author

Figure 4.14 – Five simulated UAVs tracking a TL (B)
Source: Author

4.8 Experiments with Real UAV

The developed algorithms were loaded into real UAVs and executed on the route belonging to tower A on the route shown in Figure 4.10, for a distance of 22 meters and 19 seconds, using the Mobilenet v1 Feature Pyramid Network (FPN) Single Shot Multibox Detector (SSD) model, in a section not belonging to the Training Dataset, Figure 4.15 shows an

aspect of the test carried out, in the upper right corner (a) shows a screen from the cameras of the upper UAV and the side UAV (d).

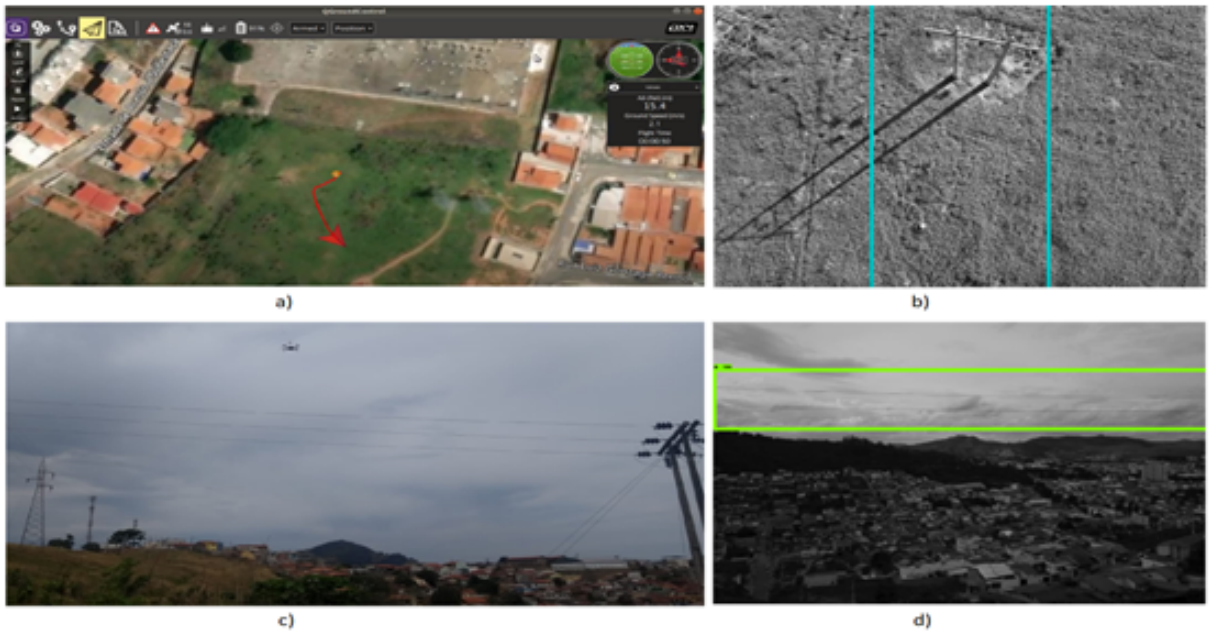

Figure 4.15 – Field test pictures
(a) GCS, **(b)** View of top UAV, **(c)** view of the UAV from operator, and **(d)** View of side UAV.
Source: Author

Although the weather conditions were not the best, it was possible to carry out the test in order to validate, even in a small section, the detection method for use in real environments. Results obtained were more successful in the simulated environment than in the real environment.

5 Conclusions

The experiments carried out and the results observed, both in a simulated environment and in a real environment, confirm the formulated hypothesis: "It is possible the integration of cooperative swarm algorithms with image inferences using deep learning for autonomous power TL tracking".

The solutions presented in this study refine computer vision algorithms, little discussed in applied form, for the function of autonomous tracking of power TLs in high voltage towers. The artifacts produced, such as Datasets and Simulators, reflect in the computational environment, in a realistic way, the challenge imposed in inspections of large extensions of energy transmission corridors throughout Brazil. All solutions obtained satisfactory results at a low cost, using only two UAVs equipped with a front camera, and a computer for image processing. Highlighting deep learning, which presents the best results, and allows widespread use in other environments and structures.

The UAV is capable of tracking at the top of the lines with the camera pointed downwards, or at the sides with the camera pointed at the side opposite to its relative position in the tower. Other positions such as diagonal, rotating at the top, or at the bottom of the tower, were not addressed in this study. The distance of the UAV in relation to the lines has a high impact on model detection, and a distance above 10m from the top of the target structure to the UAV is not recommended. Although it is possible to use the computer to process the trajectories, there is a small delay and limitation of distance from the UAV to the workstation, therefore, it is recommended to use it on board or using equipment with greater processing and range.

5.1 Main Difficulties

For Deep Learning training, finding a data set that contained the images necessary for the work proved to be a difficulty, in view of this, a specific dataset was developed. Training models that have Deep Learning are very expensive, especially Deep Reinforcement Learning, as each model required between 24 and 90 hours to be trained. The implementation of an autonomous image processing and decision-making system depends heavily on the performance of peripherals and frameworks, such as image data capture, hardware control, processing algorithms, among other external characteristics that directly influence the final implementation. The challenge of building and developing low-cost equipment has a direct impact on these issues.

There is a latency between detecting the model, updating the values, and executing the

actions, as all image frames were sent via video transmitter to a ground station, where the algorithm was stored, and, after processing the images, the Calculated values were sent back to the UAV via telemetry, which slows the movement with each detection.

5.2 Main Contributions

This work demonstrated the feasibility of applying cooperative swarm algorithms, with image inferences using deep learning for autonomous power TL tracking. This implementation, however, is still initial and many improvements can still be made in the future.

The bibliographical review of this work provides a vast modeling and demonstration of the possibilities and with well-defined methodological criteria, resulting in an analysis with relevant materials from different studies on autonomous tracking of power transmission lines.

The development of the work favored the production of its own dataset, an algorithm for image processing, and the integration of this algorithm with the UAV for identifying and tracking anomalies on the ground.

One of the merits of this work was to evaluate detection methods to identify discrete actions to track power TLs. These are the Edge Detector algorithms; Single-class and multi-class Deep Learning and Deep Reinforcement Learning, which produced a result with a promising future.

Complex simulated environments with different towers and ecosystems were created for simulation using an advanced 3D creation platform with photorealistic visuals. These environments enabled the validation of the best models proposed for each algorithm studied.

A simplified simulation environment was created capable of integrating real images obtained in flight with points simulating UAVs in order to allow testing computer vision algorithms and UAV trajectory control.

Three robust Datasets were developed with a collection of real and simulation images, which include different environments, transmission towers and power lines. The first consists only of identifying lines of the monoclass type, and the second for actions to be taken of the multiclass type. The original images were manually labeled (MARTINS, 2020; DANTAS, 2020) and made available with pixel-level annotation in the TFRecords format (DANTAS, 2020).

Operating in swarm mode allowed for a more precise and detailed inspection, maintaining low costs, highlighting the relevance of the work, especially in a country with large areas and limited financial resources in terms of investment in infrastructure.

6 Future Work

Given the burgeoning use of UAVs for electrical TL inspection and the application for fault detection and identification, the continuation of research is paramount across several domains.

First and foremost, it is essential to conduct studies in optimal or combinatorial optimization to integrate metaheuristic algorithms geared towards UAV route generation. Such an approach can catalyze both quantitative and qualitative enhancements in application efficiency and scope, minimizing redundancies and ensuring comprehensive problem coverage.

Moreover, adopting systematic Automatic region of interest (ROI) techniques in edge detection algorithms can refine the segmentation of TL components. From a data standpoint, incorporating imagery from intricate environments or integrating additional datasets is crucial to diversify and hone the Deep Learning models employed.

Another promising avenue is the exploration of Deep Reinforcement Learning (DRL) algorithms with continuous actions, tailoring reward constraints and episode termination criteria to the specific task of inspection.

Ultimately, the development and deployment of a dedicated onboard computer for UAVs could optimize real-time processing and analysis during inspections in external settings, rendering the procedure even more effective and secure.

As a proposal for future work, assemble a group with at least several UAVs following TL, each with a specific reconnaissance task. For example, a UAV specialist in identifying defects in the cable, at the junction of cables and cable-insulator, another UAVs specialist in identifying defects in insulators, another UAVs with the mission of identifying defect in the tower, another UAVs could identify erosion at the base of the tower, another UAVs identifying housing invasion, another UAVs identifying tree invasion.

Appendix

APPENDIX A – COMPONENTS OF A QUADCOPTER TYPE UAV [1]

A.1 Introduction

There are several types and subtypes of UAVs according to their aerodynamic characteristics, such as fixed-wings (airplanes) and rotary-wings (helicopters and multirotors) (ANGELOV, 2012).

It is possible to divide the *hardware* of a rotary wing UAV, such as the quadcopters used in this research, into two parts: the platform and the embedded systems. The function of the platform (white balloons in Figure A.1) is to transport those on board (yellow balloons) ensuring a stabilized and safe flight. The onboard system is the combined set of one or more equipment or sensors, such as cameras and video transmitters responsible for capturing and transmitting environmental information during the flight, and accessories such as propeller protectors, alarms, hooks, and small networks for the transport of objects.

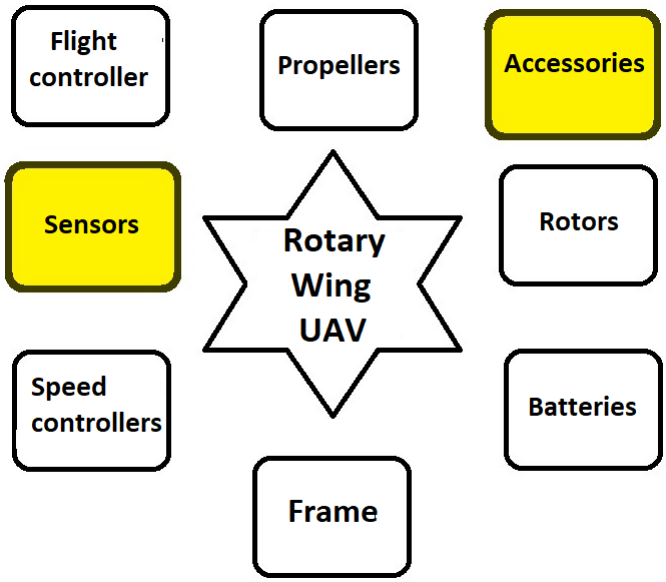

Figure A.1 – Components of a Rotary Wing UAV.
Source: Author

Some of the main components of a UAV are described below.

[1] This material is the updated and adapted version of that produced in the author's master's thesis(MARTINS, 2018).

A.2 Frame

The frame or "chassis" (Figure A.2), is the physical base of the UAV and it is on it that all other components are fixed.

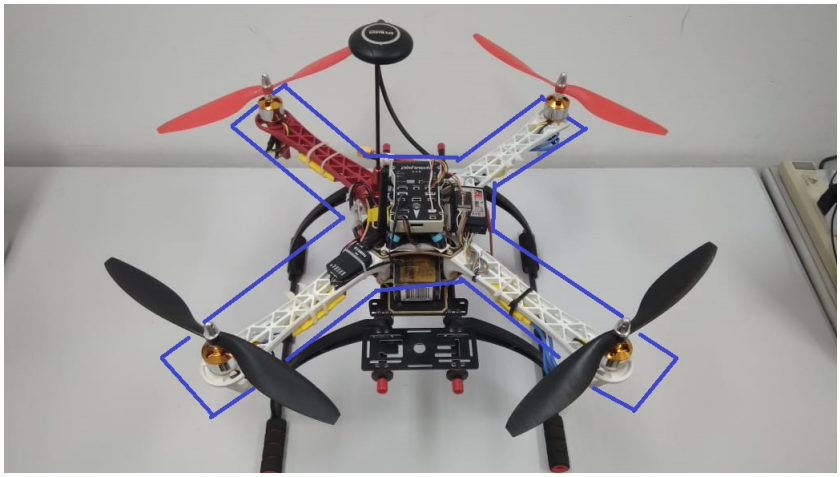

Figure A.2 – Frame of a Quadcopter UAV (highlighted in blue).
Source: Author.

There are several categories of frames, depending on the application of the UAV, such as aerial cinematography, capable of lifting heavier professional cameras, light sports frames to facilitate rapid and radical movements in acrobatics, First Person View (FPV) which allow to accommodate various accessories such as cameras, transmitters and antennas to give the operator the impression that he is flying on board the aircraft, and mini frames, which are much smaller and resistant to falls.

A.3 Batteries

The battery (Figure A.3) provides the energy for the operation of the engines and all electro-electronic components on board the UAV, and is therefore a vital item for your flight.

Figure A.3 – Tattu 5200 battery used in UAV.
Source: Author

Unfortunately, electrical power is still a critical point for all users of rotary-wing UAVs,

both for domestic and professional use, since practically no aircraft is currently able to offer autonomy greater than 30 minutes of flight, as shown in Table A.1.

Table A.1 – The ten commercial RPAs with the greatest flight range (2022)

UAV	Flight autonomy	Control Range
Blade Chroma Quadcopter Drone	30 min	2,500m
Sim Too Pro	30 min	1,000m
DJI Phatom 4	28 min	3,500m
DJI Mavic Pro	27 min	7,000m
DJI Inspire 2	27 min	7,000m
Parrot Bebop 2	25 min	3,200m
DJI Phantom 3 Standard	25 min	1,500m
DJI Phantom 3 Pro	23 min	3,000 m
3DR Solo	22 min	500m
Yuneec Q500+	22 min	2,000 m

According to the specifications of their manufacturers. Source: (LOPES, 2022)

Rain, fog, winds and even atmospheric pressure influence the energy consumption and flight time of the UAV. Furthermore, efforts to maneuver and stabilize the aircraft cost an extra battery charge. In the case of atmospheric pressure, the higher the altitude, the thinner the air becomes, implying a greater need for engine rotations to keep the ARP in flight, resulting in greater battery energy consumption.

To maximize flight autonomy, it is necessary to use a battery that satisfactorily combines its charge capacity, capacitance and consequently discharge capacity. The harmony between these characteristics will provide a lighter battery with better power capacity. The number of cycles (recharges) that a battery has already spent also influences flight time. Older batteries do not fully charge or balance their cells perfectly.

The size, shape and material from which the propellers are made are also items that influence the ARP's flight time. Very small propellers result in less load capacity, forcing the engines to make extra effort to keep the aircraft in flight, while very large propellers overload and overheat the engine, reducing its efficiency and flight time, with the risk of engine burnout and consequent crash of the UAV, which can cause accidents and damage with unpredictable consequences.

A.4 Rotors

The motors for UAVs (Fig. A.4) are of the brushless type (without brushes or outrunners).

Because they do not have brushes, they last longer than brushed motors. While in these the motor coil core rotates, in brushless ones the coil core remains stationary, while the entire exterior rotates. For this reason they are called outrunners.

Furthermore, brushless rotors are stepper motors, that is, the combination of several

Figure A.4 – Rotor for UAVs.
Source: Author

steps at high speed translates into the efficiency of this type of rotor. Professional or high-performance UAVs use brushless rotors.

A.5 Propellers

The propeller of a UAV consists of two or more blades (Fig. A.5) connected to the central hub at the root of the blade, to which these blades are attached. Each blade is essentially a rotating wing, and every blade is an aerodynamic profile capable of generating lift. This support force in the plane in which the blade moves is called traction or propulsion.

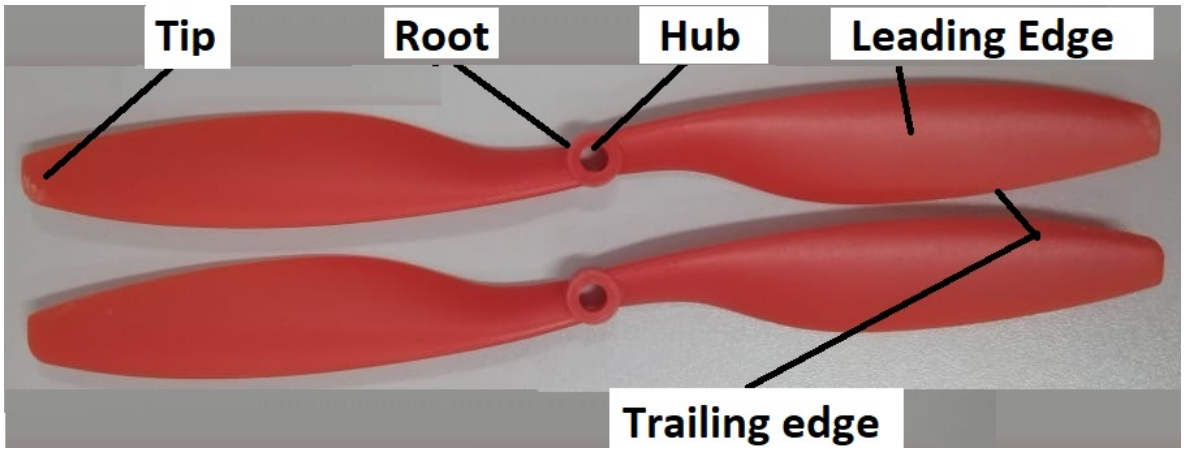

Figure A.5 – Components of a Propeller Blade
Source: Author

With the rotation, the propeller blades cut the air and create an aerodynamic effect, like that of the support of the wing or the aircraft structure, that is, the circular displacement

of the blade in the air will cause a low pressure on the back of the blade, and a high pressure on the face, causing traction.

The propellers are what make the aircraft leave the ground, fly and land, and the efficiency of a propeller is the direct ratio between the force exerted by the engines (input power) and the result obtained (output power). The force applied is the force that the engine will need to make to turn the propeller. The more force the engine exerts, the greater the battery consumption. The result obtained is the propeller's ability to produce thrust under a given air speed or wind speed.

Propellers can have one or more blades. The most common are those made of plastic (ABS, Nylon, etc.) and carbon fiber, while there are also those made of other materials, such as wood, which are more expensive and unusual.

In quadcopters, the most used propellers are plastic (various types of plastic materials) and are the cheapest and recommended for beginners, since at the beginning of learning how to drive a quadcopter it is very common for them to be damaged. Plastic propellers make more noise than carbon fiber propellers, have lower performance and vibrate more. Because they are flexible, they bend at high speed, which is clearly a disadvantage.

Carbon fiber propellers vibrate less, making them suitable for aerial filming. They make less noise, and are more stable. However, they are highly dangerous, as they transform into true cutting blades when at high speed. It is not recommended for beginners due to the cost, which is much higher than that of plastic propellers, and the danger of cutting. They are rigid, do not flex at high speeds, and demand more from the engines, and may consume a little more than plastic propellers. Because they are made of carbon fiber, they are lighter than plastic (MOLRC1, 2016).

There are hybrid plastic and carbon fiber propellers in an attempt to increase quality at a more affordable price.

A.6 ESC

Electronic Speed Controllers (ESCs) (Figure A.6) are mechanisms that transform the Pulses Width Modulation (PWMLs) received from the flight controller board in rotation of the engines, sending them electrical pulses making the engines rotate at a certain speed.

Figure A.6 – ESC for UAVs
Source: Author

ESCs are composed of power transistors and a microcontroller. For each rotor category there is a specific category of ESCs, as they vary in power, refresh rate in hertz, applications by type of rotor (brushless or brushed), support for certain types of batteries, and other features.

Figure A.7 illustrates the arrangement of ESCs mounted on an UAV, highlighted in blue.

Figure A.7 – ESCs mounted on a UAV.
Source: Author

ESCs are classified according to their powers in Ampere (A), there are 12A, 20A, 30A, etc ESCs.

The update frequency (update rates) in Hertz (Hz) directly implies the RPA's response speed to the commands sent to the motors. Older ESCs worked at 50Hz rates, while newer ones operate at 400Hz refresh rates (MOLRC2, 2016).

Some models have a reversal system, capable of making the engines/propellers rotate in reverse, allowing the aircraft to decelerate significantly, causing it to touch the ground gently at very low speed and in a reduced space (ECODRONES, 2018).

A.7 Transmitter Radio Control - TX

Radio controls (Figure A.8) are devices that allow an operator to control the flight and maneuvers of an UAV from the ground and can replace the control station if necessary.

Figure A.8 – Transmitter Radio Control - TX
Source: Author

They are made up of position switches and control levers called sticks, each of them generally linked to a channel of the operated frequency.

In multirotors, by manipulating the radio control (TX) commands, the operator transmits the information to the receiver (RX) on board the UAV, which takes it to the flight controller that interprets it and acts on the ESCs in order to change the speed. of motors producing remotely controlled movement (TX).

A.8 Automatic Pilot

The UAV's autopilot allows several operations, such as aircraft stabilization and some flight controls. Pixhawk is an example of an autopilot that has several pre-defined flight modes, such as those listed below, among others:

Stabilize Mode: This mode allows the automatic leveling of the UAV, so that the UAV operator (pilot) does not have to worry about the leveling of the aircraft, but only about

its altitude and direction.

Alt Hold Mode: Maintains the UAV's altitude. Altitude is automatically maintained by sensors such as barometer, sonar or another method, depending on the UAV. This mode is recommended for beginners as it makes operating the aircraft easier.

Loiter Mode: This mode is also known as GPS or Position Hold mode. It uses GPS to maintain position, barometer to maintain altitude, and compass to maintain direction. The UAV remains relatively fixed in the same position in space, relieving the operator of any need to interact with the radio control while the UAV remains practically stationary (immobile) in the air.

Return-to-Launch (RTL) mode: Also known as Return-to-Home (RTH) mode, this mode causes the UAV to return to the starting location (where it started the flight).

Auto mode: This mode executes a mission planned through a system or Mission Planner software.

Guided Mode: This function is only available through the use of a ground station running Mission Planner software and telemetry. Allows the operator to control the UAV by clicking on the Mission Planner map. The UAV will move to the location indicated by the operator.

To be able to perform the functions mentioned, the autopilot has some sensors of its own, namely:

A.8.1 IMU

Inertial Measurement Unit (IMU) is a device that brings together several sensors, such as an accelerometer, gyroscope and temperature sensor. The first two sensors with three measurement axes allow output response in six values, allowing six Degree of Freedom (DOF).

A.8.2 Barometer / Altimeter

Altimeter is a type of barometer, a tool that allows you to measure air pressure. The higher the aircraft is, the thinner the atmosphere and, therefore, the lower the air pressure, thus allowing an algorithm to estimate the UAV altitude (distance between the aircraft and sea level).

A.8.3 Accelerometer

The accelerometer is a device with sensors that, when moved from top to bottom or to the sides, in 3D axis space, by flight movements, perceives the direction and speed of displacement.

A.8.4 Gyroscope

The gyroscope measures angular velocity. An example measurement would be 1 revolution per second, which would represent 360 degrees or, 360/1. The direction in which the device is rotating is also recognized. But depending on the application, there may be no rotation, but just a shift in degrees, common in UAVs. By detecting small variations it is possible to stabilize the flight.

A.8.5 Compass

A gyroscopic compass has 3 axes, while a magnetic compass only and always points north. The mechanical gyro compass corrects for tilts caused by hills, sea influences and aircraft pitch. The digital compass or electronic compass uses magneto-inductive technology, reading variations in the Earth's magnetic field. As it is a device sensitive to magnetic fields, several peripheral precautions must be taken, such as considering the metallic mass close to the sensor, electromagnetic fields and interference caused by circuits or sources close to it (OPENCV, 2017).

A.8.6 Telemetry

Two-way communication system (both receives and transmits information) wirelessly via antennas (Figures A.9 and A.10) and which allows data exchange between the onboard flight controller and the control station (Figure A.8).

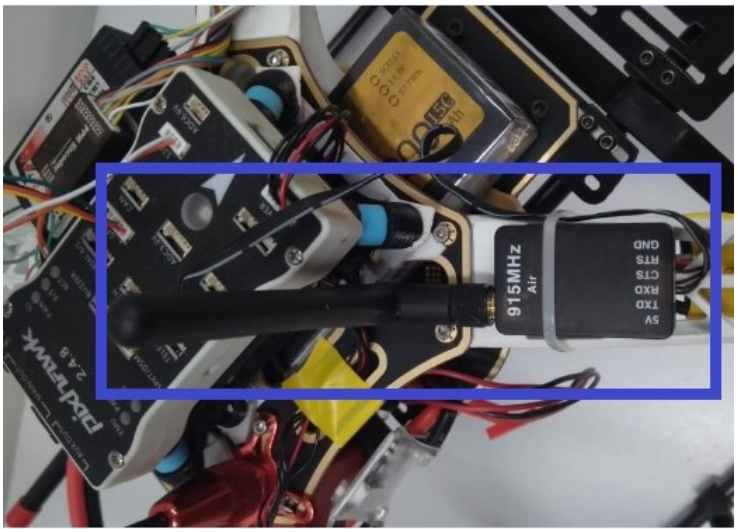

Figure A.9 – Embedded Wifi Antenna.
Source: Author

Telemetry provides the pilot with flight information and metrics by sending various types of information to a receiver on the ground.

One of the important pieces of information that telemetry provides to the ground controller is RSSI, which indicates the strength of the radio signal, useful for understanding when the aircraft is approaching the maximum radio control range limit, or the inclination is unfavorable. for data transmission via antennas.

The charging voltage of the batteries is another information transmitted by telemetry to the radio control, useful for estimating how much flight autonomy the UAV has left.

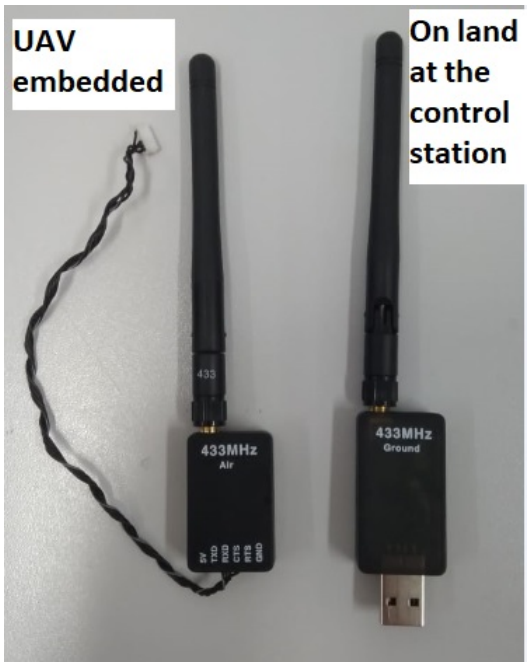

Figure A.10 – Wifi Antennas.
Source: Author

Although it is common to see operators using stopwatches to estimate the aircraft's flight time, factors such as the intensity of headwinds can require additional effort from the engines and a consequent increase in energy consumption from the batteries, reducing flight autonomy, which makes this practice inadvisable.

A.9 Sensors

To aid stability and allow free flight (when the GPS signal is unavailable), UAVs have a series of internal and external equipment such as compass, altimeter, gyroscope and barometer. An UAV can use multiple embedded sensors in many different ways.

A.9.1 Sonar

Sonar is an electronic device that allows detecting the distance between the UAV and the ground or between the UAV and obstacles in front of it, depending on where the device is

installed, below or in front of the aircraft. This sensor combined with the altimeter allows for greater accuracy in altitude detection.

A.9.2 Laser

Lasers are sensors or *scanners* and *laser* allow scanning on board UAVs, making it possible to perceive obstacles and reliefs during flight. This method of perceiving the environment is called a Light Detection and Ranging (LIDAR) system and uses pulsed laser emission with a high repetition frequency to measure distances by recording the reflection of these pulses, allowing three-dimensional information to be obtained. about surfaces by assembling a table of position (x, y) and elevation (z) data, generating a cloud of points.

A.9.3 Other Embedded Components

Other equipment and accessories can be embedded in an ARP, such as the GPS module/antenna (Figure A.11), the Raspberry PI system, the Pixhawk controller and others.

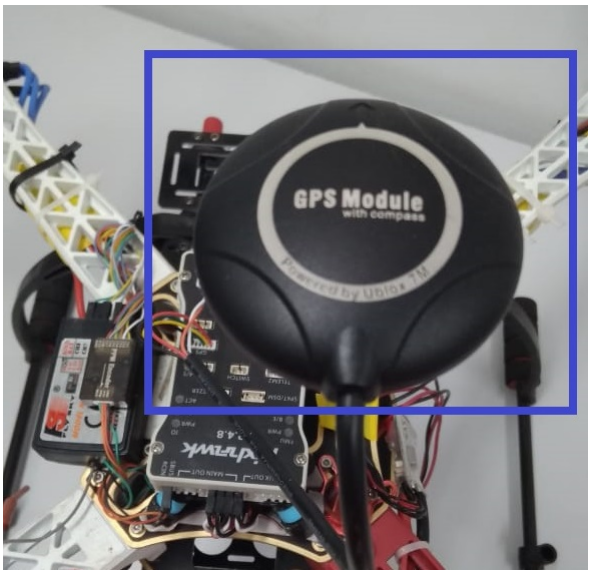

Figure A.11 – Onboard GPS module.
Source: Author

Raspberry Pi (Figure A.12) is a mini-microcomputer similar to the mother board found inside the case of a conventional Personal Computer (PC), containing processors, expansion slot, Universal Serial Bus (USB) interfaces, digital audio and video outputs High-Definition Multimedia Interface (HDMI), Random Access Memory (RAM), RJ45 connector for network cable and input for power supply.

Figure A.12 – RaspBerry Pi.
Source: Author

The Raspberry Pi computer was developed by the Raspberry Foundation, with the aim of bringing technology to teaching young people and children.

Pixhawk (Figure A.13) is a hardware and software device that implements an autopilot Open Source Hardware (OSHW) capable of controlling the basic operations of a UAV, such as stabilizing, taking off and landing, among many others .

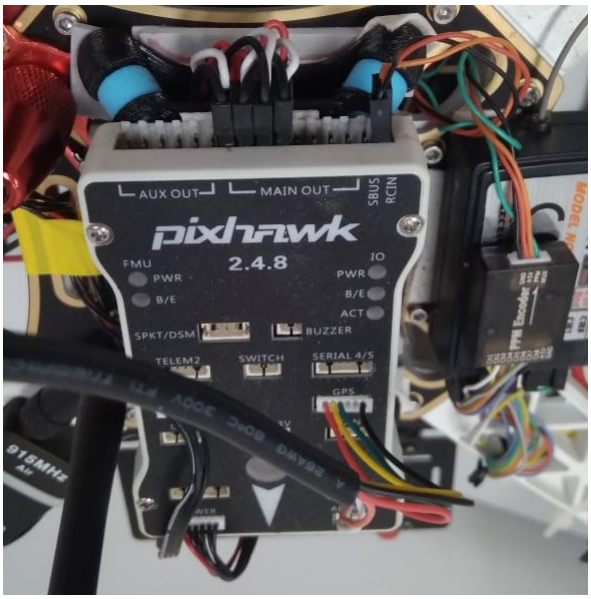

Figure A.13 – Pixhawk.
Source: Author

The Pixhawk system is multi-tasking and shares resources that can be performed together or individually.

It has a built-in software that implements the basic flight control functions.

It offers a programming environment compatible with Unix and Linux operating systems and integrated autopilot functions with detailed logs of missions and flight behavior. It is equipped with a gyroscope, accelerometer, magnetometer and barometer and can be connected to external accessories such as a GPS module.

A useful feature of Pixhawk is the ability to communicate with other devices through a protocol called MAVLink, which was developed specifically for UAV applications and can be used within remote control range of the autonomous aircraft, running the control algorithms in a small portable computer, such as a Raspberry Pi, which is embedded in UAV and sends commands to Pixhawk via messages in the MAVLink protocol.

Annex

ANNEX A – SOME TERMS IN DISTRIBUTION LINES

A.1 Introduction

There are several safety procedures when it comes to electrical energy, established by laws, standards and technical-operational procedures.

This appendix brings some of the concepts used in this thesis, contained in document 30.000-PE/LS-5621d - INTERFERENCE CRITERIA WITH DISTRIBUTION AND TRANSMISSION LINES BANDS, dated 05/30/2015, prepared by Companhia Energética de Minas Gerais Distribuição S.A. (CEMIG) (CEMIG, 2015) and on the Eletrobrás/Furnas website (FURNAS, 2022).

The original documents have not been fully transcribed here. However, the following definitions are faithful copies of the texts found in their original sources.

A.2 Definitions

A.2.1 Passing Lane

It is the strip of land along the axis of the overhead distribution and transmission lines, which may be domain or easement, whose width must be at least equal to the safety strip.

A.2.2 Domain Range

It is the strip of land along the axis of the overhead distribution lines and networks, declared of public utility, acquired by the owner of the line through an agreement through a public instrument extrajudicial, judicial decision or acquisitive prescription (acquisition of a property through peaceful and uninterrupted possession for a certain period of time), duly registered in the property registry office, with a width at least equal to that of the security strip.

A.2.3 Right of Way

It is the strip of land along the axis of the overhead distribution lines and networks, the domain of which remains with the owner, however with restrictions on its use. The aforementioned right over someone else's property can be established through a public or private instrument, acquisitive prescription over a period of time or even through a

judicial measure, by registering it separately from the respective real estate registration. In this case, the concessionaire, in addition to the right to pass the line, has free access to the respective facilities, with a width of at least the same as the safety lane.

Figure A.1 illustrates the Right of Way, where:

Area A: It is around the structure of the towers. Used for moving vehicles and equipment during maintenance work.

Area B: Corridor located well below the cables, along the line. Some improvements are permitted in this area (see table alongside).

Area C: Strip of land that complements the total width of the easement strip.

The use of these areas is not completely prohibited, however, any activities that may be carried out in these areas must first be analyzed and authorized by FURNAS.

Some activities, such as horticulture, fruit growing, floriculture, corn, wheat and rice plantations are permitted in areas B and C of the easement strip. The approval of improvements is related to their location on the strip.

In the following table, some examples of what can and cannot be done within the right-of-way. Table A.1 exemplifies some types of use of the Right of Way.

Type of use	Area A	Area B	Area C
Low plantings	YES	YES	YES
Small and medium-sized crops	NO	YES	YES
Medium and large-sized afforestation/reforestation	NO	NO	NO
Crops where burning is processed	NO	NO	NO
Agricultural vehicles	NO	YES	YES
Irrigation	YES*	YES*	YES*
Improvements to support agriculture Standard	NO	YES*	YES*
Electrical and mechanical installations	NO	NO	NO
Deposit of non-flammable materials	NO	NO	NO
Deposit of flammable materials	NO	NO	NO
Houses	NO	NO	NO
Wire fences, walkways and gates	YES*	YES*	YES*
Leisure, industry and commerce area	NO	NO	NO
Movement of people in the lane	YES	YES	YES

(*) Consult FURNAS before deploying.

Table A.1 – Examples of types of use in the Right of Way.
Source: Author with data extracted from (FURNAS, 2022)

There are some requirements imposed by Brazilian legislation so that these tracks are made correctly. One of the determinations implies that the strip must be 20 meters wide aligned according to the center of the duct or construction being monitored. The Right of Way cannot have any type of construction along its route, and only the strip and the ground must be kept free of any material or object.

It is also important to highlight that the Right of Way is still part of the property's land, being the property of the owner. These use restrictions are focused on the safety of the

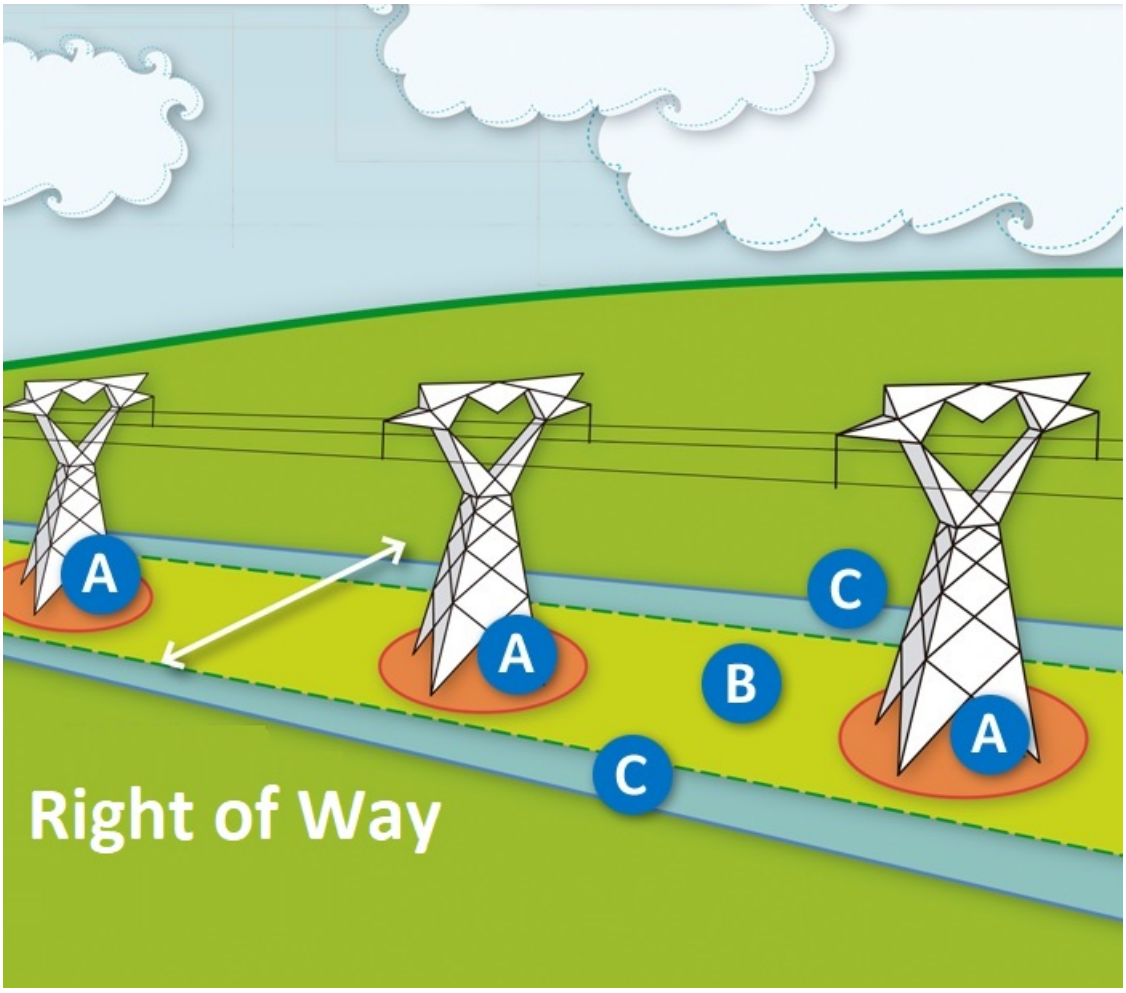

Figure A.1 – Right of Way
Source: (FURNAS, 2022)

work and transmission lines.

This entire reserve destined for the Right of Way is important for everyone's safety, especially if you take into account electromagnetic waves generated by these transmission lines.

When it comes to Right-of-Ways for monitoring gas pipelines, they aim to delimit and protect the entire pipeline area, in addition to identifying where the equipment will be installed.

Next to the support structures there is the right of way, which is the strip of land necessary for the construction, operation and maintenance of the transmission line. After crossing the line, landowners can use part of the easement, respecting restrictions that guarantee the safety of residents, the property and the project.

A.2.4 Safety Strip

It is the strip of land along the axis of overhead distribution lines and networks, necessary to guarantee its good performance, inspection, maintenance and the safety of installations and third parties. It is defined in accordance with the criteria established in NBR 5422, NBR 12304, in Law 11934 of May 5, 2009 and in ANATEL Resolution No. 442 of July 21, 2006.

A.2.5 Parallel track

It is a fictitious strip, parallel to the distribution line crossing lane necessary to ensure the operation of the line, taking into account the existence of large trees existing on the edge of the easement strip, whose pruning or tipping could affect the structures or the conductor cables and lightning arrester cables of the line.

A.2.6 Safety Distance

It is the minimum distance from the conductor and its energized accessories and any parts, energized or not, from the line itself to the ground or to obstacles close to the line, as prescribed by ABNT NBR 5422.

A.2.7 Counterweight wire

It is the conductor buried in the ground along the line's safety strip, with the objective of reducing the grounding resistance of the structure, tower or pole, to values compatible with the expected performance against short circuits, switching surges, atmospheric discharges and the security of third parties.

A.2.8 Dangerous potentials

In the event of phase-to-ground short circuits in a Line or in the substations at its ends, high currents are injected into the ground through the feet of the structures and the counterweight wires that make up the Line's grounding system. These currents, in turn, cause the appearance of electrical potential gradients on the ground surface that can impose impermissible potential differences (step voltage or touch voltage) on a person in the vicinity of structures.

A.2.9 Intersection or crossing

It is the transposition of a distribution line or network by another electrical line (higher, equal or lower voltage) or telecommunications, buried or overhead ducts, transport routes,

etc., complying with defined criteria and the regulatory requirements of the bodies involved.

A.2.10 Distribution Networks

It is an electrical installation with voltage between phases whose effective value is greater than 1kV and less than 69kV, also identified as DN.

A.2.11 Distribution Line

It is the line with voltage between phases whose effective value is equal to or greater than 69kV and less than 230kV, also identified as DL.

A.2.12 Transmission Line

It is the line with voltage between phases whose effective value is equal to or greater than 230kV, also identified as TL.

A.2.13 Convention

For simplicity, the overhead Distribution Lines (DL) and Transmission Lines (TL) will be referred to as Lines for short.

A.2.14 NBR 5422

Technical Standard for the Design of overhead electric power transmission lines, from ABNT, Brazilian Association of Technical Standards, which defines the minimum parameters for sizing the safety range.

A.2.15 NBR 12304

This Standard establishes the required conditions for measuring the levels of spurious signals generated by Information Technology Equipment (ETI) and establishes the corresponding limits permissible for the frequency range of 0.15MHz to 1,000MHz.

A.2.16 Law 11934 of May 5, 2009

This law provides for limits on human exposure to electric, magnetic and electromagnetic fields.

A.2.17 ANATEL Resolution No. 442 of July 21, 2006

This Regulation aims to establish electromagnetic compatibility requirements to be served by telecommunications products.

Bibliography

ADAMI, J. F. *Detecção e Identificação de Arcos de Contorno em Cadeias de Isoladores de Linhas de Transmissão Utilizando Técnicas de Processamento de Sinais. (in portuguese).* Tese (Doutorado) — Federal University of Itajubá, UNIFEI, 2008. 25

AL-ABRI, S.; MAXON, S.; ZHANG, F. Um modelo de controle de enxame multicamada para propagação de informações e multitarefa (in portuguese). In: *2019 Conferência Americana de Controle (ACC).* [S.l.: s.n.], 2019. p. 4653–4658. 36

ALKOUZ, B.; BOUGUETTAYA, A. Provider-centric allocation of drone swarm services. In: *2021 IEEE International Conference on Web Services (ICWS).* [S.l.: s.n.], 2021. p. 230–239. 36

ALKOUZ, B.; BOUGUETTAYA, A. Provider-centric allocation of drone swarm services. In: *2021 IEEE International Conference on Web Services (ICWS).* [S.l.: s.n.], 2021. p. 230–239. 36

ANAC. *aeronave remotamente pilotada (in portuguese).* 1999. Access date: 23 October 2023. Disponível em: <https://www2.anac.gov.br/anacpedia/por_ing/tr4132.htm>. 40, 41

ANAC. *Orientações para Usuários (in portuguese).* 2020. Access date: 23 October 2023. Disponível em: <https://www.gov.br/anac/pt-br/assuntos/drones/orientacoes_para_usuarios.pdf/view>. 40, 41, 42

ANGELOV, A. *Sense and avoid in UAS: research and applications.* 2012. First edition. United Kingdom: Wiley, 2012. 84

ARAAR, O.; AOUF, N. Visual servoing of a quadrotor uav for autonomous power lines inspection. In: IEEE. *22nd Mediterranean Conference on Control and Automation.* 2014. p. 1418–1424. Disponível em: <https://ieeexplore.ieee.org/abstract/document/6961575>. 33

BAYıNDıR, L. A review of swarm robotics tasks. *Neurocomputing*, v. 172, p. 292–321, 2016. ISSN 0925-2312. Disponível em: <https://www.sciencedirect.com/science/article/pii/S0925231215010486>. 45

BELTRAMETTI M.C., C. C. M. A. e. a. *Geometry of the Hough Transforms with Applications to Synthetic Data.* [S.l.]: Math.Comput.Sci., 2021. Available online: <https://doi.org/10.1007/s11786-020-00470-4>, accessed 17 October 2023. 57

BENI, G.; WANG, J. Swarm intelligence in cellular robotic systems. In: DARIO, P.; SANDINI, G.; AEBISCHER, P. (Ed.). *Robots and Biological Systems: Towards a New Bionics?* Berlin, Heidelberg: Springer Berlin Heidelberg, 1993. p. 703–712. ISBN 978-3-642-58069-7. 44

BIANCHETTI, M. *Cemig instalará 200 subestações com investimentos de R$5bi. (in portuguese).* [S.l.]: Diário do Comércio, 2021. Available online: <https://diariodocomercio.com.br/economia/cemig-fara-investimento-de-r-5-bi-em-subestacoes> (in portuguese), accessed 10 October 2023. 24

BORUAH, P. An immuno-inspired approach towards post-processing of ocr errors. In: *2023 Fifth International Conference on Electrical, Computer and Communication Technologies (ICECCT)*. [S.l.: s.n.], 2023. p. 1–8. 46

BRADSKI, G.; KAEHLER, A. *Learning OpenCV: Computer vision with the OpenCV library*. " O'Reilly Media, Inc.", 2008. Disponível em: <https://www.google.com.br/books/edition/Learning_OpenCV_3/SKy3DQAAQBAJ?hl=pt-BR&gbpv=1>. 65

BRAGA, R. G. et al. *Collision avoidance based on Reynolds Rules: a case study using quadrotors*. 2018. Information Technology-New Generations (ITNG). 773-780, 2018. 46

BRAGA, R. G. et al. *Collision avoidance based on Reynolds Rules: a case study using quadrotors*. 2018. Information Technology-New Generations (ITNG). 773-780, 2018. 75

BRITO, P. L. d. e. a. *A technique about neural network for passageway detection*. [S.l.]: SPRINGER. 16th International Conference on Information Technology-New Generations (ITNG 2019). [S.l.]. 2019. p. 465–470., 2019. Available online: <https://doi.org/10.1007/978-3-030-14070-0_64>, accessed 18 October 2023. 26

BRITO, P. L. d. e. a. *A technique about neural network for passageway detection*. [S.l.]: SPRINGER. 16th International Conference on Information Technology-New Generations (ITNG 2019). [6] (pp. 465–470), 2019. Available online: <https://link.springer.com/chapter/10.1007/978-3-030-14070-0_64>, accessed 17 October 2023. 54

BROWNLEE, J. *A Gentle Introduction to Object Recognition With Deep Learning*. 2021. Available at <https://machinelearningmastery.com/object-recognition-with-deep-learning/>, accessed at Dec 2023. 59

CAI, W.; ZHANG, M. Y.; ZHENG, Y. R. *Task Assignment and Path Planning for Multiple Autonomous Underwater Vehicles Using 3D Dubins Curves*. 2017. Sensors 2017, 17, 1607. 38

CANNY, J. A computational approach to edge detection. *IEEE Transactions on pattern analysis and machine intelligence*, Ieee, n. 6, p. 679–698, 1986. Disponível em: <https://ieeexplore.ieee.org/stamp/stamp.jsp?tp=&arnumber=4767851>. 65

CEMIG. *"CEMIG Informa (in portuguese)", howpublished= Disponível em <https://www.cemig.com.br/>, accessed 24 February 2023*. [S.l.]: CEMIG, 2015. 99

CENTER, S. I. A. I.; AGIN, G. *Real time control of a robot with a mobile camera*. SRI International, 1979. (Technical note). Disponível em: <https://books.google.com.br/books?id=XEAtGwAACAAJ>. 34

CHANG, W. et al. Development of a power line inspection robot with hybrid operation modes. In: IEEE. *2017 IEEE/RSJ International Conference on Intelligent Robots and Systems (IROS)*. 2017. p. 973–978. Disponível em: <https://ieeexplore.ieee.org/stamp/stamp.jsp?tp=&arnumber=8202263>. 33

COMMISSION, E. *Prevention, detection, response and mitigation of the combination of physical and cyber threats to the critical infrastructure of Europe*. [S.l.]: Horizon 2020 Framework Programme. CIP-01-2016-2017, 2017. Available online: <https://ec.europa.eu/info/funding-tenders/opportunities/portal/screen/opportunities/topic-details/cip-01-2016-2017>, accessed 18 October 2023. 24

DANTAS, A. *Artefatos produzidos na dissertação. (in portuguese)*. [S.l.]: DANTAS, 2020. Available online: <https://github.com/dantasunifei/artefatos_dissertacao>, accessed 17 October 2023. 81

DANTAS, A. J. *Algoritmos de processamento digital de imagens para rastreamento de linhas de transmissão de energia. (in portuguese)*. [S.l.]: Federal University of Itajuba - UNIFEI, 2021. Available online: <https://repositorio.unifei.edu.br/jspui/handle/123456789/2919> (in portuguese), accessed 17 October 2023. 25, 28

DECEA. *AERONAVES NÃO TRIPULADAS E O ACESSO AO ESPAÇO AÉREO BRASILEIRO. (in portuguese)*. 2023. Access date: 12 October 2023. Disponível em: <https://static.decea.mil.br/publicacoes/files/2023/1686848015-ica-100-40-2023.pdf?X-Amz-Content-Sha256=UNSIGNED-PAYLOAD&X-Amz-Algorithm=AWS4-HMAC-SHA256&X-Amz-Credential=pNf2JQbOhtSrsEzMW9aNRYAHfqzX2fnd%2F20231023%2Fus-east-1%2Fs3%2Faws4_request&X-Amz-Date=20231023T085145Z&X-Amz-SignedHeaders=host&X-Amz-Expires=900&X-Amz-Signature=a65a013927ee3dcd919bd3a8645fbbb5383a62369a48d5d1b8382f1673edb3bf>. 42

DECEA. *DECEA: Quem somos. (in portuguese)*. 2023. Access date: 12 October 2023. Disponível em: <https://www.decea.mil.br/?i=quem-somos&p=o-decea>. 41

DENG, C. et al. Real time autonomous transmission line following system for quadrotor helicopters. In: IEEE. *2016 International Conference on Smart Grid and Clean Energy Technologies (ICSGCE)*. 2016. p. 61–64. Disponível em: <https://ieeexplore.ieee.org/stamp/stamp.jsp?tp=&arnumber=7876026>. 32, 35

DENG(B), C. et al. Unmanned aerial vehicles for power line inspection a cooperative way in platforms and communications. *J. Commun.*, v. 9, n. 9, p. 687–692, 2014. Disponível em: <http://www.jocm.us/uploadfile/2014/0918/20140918110959273.pdf>. 33

DJI. *Naza-M Lite Features.* [S.l.]: DJI, 2019. Available online: <https://www.dji.com/naza-m-lite/feature>, accessed 17 October 2023. 51

ECODRONES. *E386 desenvolvido pela Event 38 Unmanned Systems (in portuguese)*. 2018. Disponivel em <https://store.ecodrones.com.br/rpas-e386-mapeamento-profissional-laser-rangefinder>, 2018, accessed 11 September 2018. 90

ESCHMANN, C. et al. *Unmanned aircraft systems for remote building inspection and monitoring*. 2012. 6th European workshop on structural health monitoring. 2012. 38

FELIZARDO, L. F.; RAMOS, A. C. B.; CAMINO, F. A. C. M. *Integration of ANN and UAV for Aerial Inspection*. 2015. International Micro Air Vehicles Conference and Flight Competition (IMAV). 2015. 38

FILHO A. J. D.; RAMOS, A. C. B. J. L. D. d. C. F. H. F. d. M.-C. F. D. *A General Low Cost UAV Solution for Power line Tracking*. [S.l.]: 17th International Conference on Information Technology–New Generations (ITNG 2020), 2020. Available online: <https://link.springer.com/chapter/10.1007/978-3-030-43020-7_69>, accessed 10 October 2023. 12, 47, 65

FLOREANO D., . W. R. J. Science, technology and the future of small autonomous drones. In: **Nature**. [S.l.: s.n.], 2015. v. 521, n. 7553, p. 460–466. 44

FURNAS. *"Cuidados com linhas de transmissão (in portuguese)", howpublished= Disponível em <https://www.furnas.com.br/cuidadoslt/?culture=pt>, accessed 24 February 2023.* [S.l.]: FURNAS, 2022. 99, 100, 101

G1. *Erosão coloca em risco torre de transmissão de energia em Belém. (in portiguese).* 2021. Disponível em: <https://g1.globo.com/pa/para/noticia/2021/06/29/erosao-coloca-em-risco-torre-de-transmissao-de-energia-em-belem.ghtml>. 26

GAO, F. et al. A novel inverse method for automatic uav line patrolling with magnetic sensors. In: IEEE. *2018 IEEE International Symposium on Electromagnetic Compatibility and 2018 IEEE Asia-Pacific Symposium on Electromagnetic Compatibility (EMC/APEMC).* 2018. p. 481–485. Disponível em: <https://ieeexplore.ieee.org/document/8393825>. 33

GERKE, M.; SEIBOLD, P. Visual inspection of power lines by uas. In: IEEE. *2014 International Conference and Exposition on Electrical and Power Engineering (EPE).* 2014. p. 1077–1082. Disponível em: <https://ieeexplore.ieee.org/document/6970074>. 33

GIOI R. G. VON; JAKUBOWICZ, J. M. J. R. G. *LSD: a Line Segment Detector.* [S.l.]: Image Processing On Line.[21] (pp. 35–55), 2012. Available online: <https://doi.org/10.5201/ipol.2012.gjmr-lsd>, accessed 17 October 2023. 57

GLOBO, R. T. *G1 Notícia (in portuguese).* 2019. Disponível em: <http://g1.globo.com/>. 26

GOLDBERG, D. E.; HOLLAND, J. H. Genetic algorithms and machine learning. In: *Machine learning.* [S.l.: s.n.], 1988. v. 3, p. 95–99. 45

GOLDBERG, D. E.; HOLLAND, J. H. Genetic algorithms and machine learning. *Machine Learning*, v. 3, p. 95–99, 1988. 45

GONZALES, I. *NGCP warns on dangers of trespassing on transmission areas.* [S.l.]: The Philippine Star., 2013. Available online: <https://www.philstar.com/business/2013/06/24/957412/ngcp-warns-dangers-trespassing-transmission-areas>, accessed 09 October 2023. 24

GOUTTE, C.; GAUSSIER, E. A probabilistic interpretation of precision, recall and f-score, with implication for evaluation. In: SPRINGER. *European conference on information retrieval.* 2005. p. 345–359. Disponível em: <https://link.springer.com/chapter/10.1007/978-3-540-31865-1_25>. 66

GUI, Y.; LI, D.; FANG, R. A fast adaptive algorithm for training deep neural networks. In: . Applied Intelligence, 2023. (Gui2023), p. 4099–4108. Disponível em: <https://doi.org/10.1007/s10489-022-03629-7>. 34

GUPTA, S. G. e. a. *Review of unmanned aircraft system (UAS).* [S.l.]: International journal of advanced research in computer engineering & technology (IJARCET) v. 2, n. 4, [13] (pp. 1646–1658), 2013. Available online: <https://papers.ssrn.com/sol3/papers.cfm?abstract_id=3451039>, accessed 17 October 2023. 48

GUZZONI, D. et al. Many robots make short work: Report of the sri international mobile robot team. *AI Magazine*, v. 18, n. 1, p. 55–63, 1997. Cited By :61. Disponível em: <www.scopus.com>. 44

HAMELIN, P. et al. Discrete-time control of linedrone: An assisted tracking and landing uav for live power line inspection and maintenance. In: IEEE. *2019 International Conference on Unmanned Aircraft Systems (ICUAS)*. 2019. p. 292–298. Disponível em: <https://ieeexplore.ieee.org/document/8798137>. 32, 35

HAQUE S. R.; KORMOKAR, R. Z. A. U. *Drone ground control station with enhanced safety features.* [S.l.]: IEEE. 2nd International Conference for Convergence in Technology (I2CT), 2017. Available online: <https://ieeexplore.ieee.org/abstract/document/8226318>, accessed 17 October 2023. 52

HARRELL, B. *Protecting vital electricity infrastructure.* [S.l.]: CSO, 2016. Available online: <https://www.csoonline.com/article/554857/protecting^vital-electricity-infrastructure.html>, accessed 09 October 2023. 24

HENTATI, A. I. e. a. *Simulation tools, environments and frameworks for uav systems performance analysis.* [S.l.]: IEEE. 14th International Wireless Communications & Mobile Computing Conference (IWCMC). **2018 [6] (pp. 1495–1500)., 2018. Available online: <https://ieeexplore.ieee.org/document/8450505>, accessed 17 October 2023.** 54

HERMíNIO, R. P. S. et al. *Visão Computacional aplicado a um Protótipo Elétrico (in portuguese)*. 2010. Mostra Nacional de Robótica - Instituto Federal de Educação, Ciência e Tecnologia da Bahia, Vitória da da Conquista, BA, 2010. 37

HRABAR, S.; MERZ, T.; FROUSHEGER, D. *Development of an autonomous helicopter for aerial powerline inspections*. 2010. 1st International Conference on Applied Robotics for the Power Industry (CARPI 2010). 1–6, 2010. 38

HUAMÁN, A. *Hough Line Transform.* [S.l.]: Math.Comput.Sci., 2019. Available online: <https://docs.opencv.org/3.4/d9/db0/tutorial_hough_lines.html>, accessed 17 October 2023. 57

HUI, X. et al. A monocular-based navigation approach for unmanned aerial vehicle safe and autonomous transmission-line inspection. *International Journal of Advanced Robotic Systems*, SAGE Publications Sage UK: London, England, v. 16, n. 1, p. 1729881419829941, 2019. Disponível em: <https://journals.sagepub.com/doi/full/10.1177/1729881419829941>. 32, 35

HUO, M.; DUAN, H.; FAN, Y. Pigeon-inspired circular formation control for multi-uav system with limited target information. *Guidance, Navigation and Control*, v. 01, n. 1, 2021. 38

JONES, S.; ANDRESEN, C.; CROWLEY, J. Appearance based process for visual navigation. In: *Proceedings of the 1997 IEEE/RSJ International Conference on Intelligent Robot and Systems. Innovative Robotics for Real-World Applications. IROS '97.* [S.l.: s.n.], 1997. v. 2, p. 551–557 vol.2. 37

JORGE, L. de C. *Determinação da cobertura de solo em fotografias aéreas do Projeto Arara (in portuguese)*. 2001. Dissertação (Mestrado em Ciências da Computação) - Universidade de São Paulo, São Carlos, 2001. 40

JÚNIOR, L. D. R. S. S.; NEDJAH, N. *Distributed strategy for robots recruitment in swarm-based systems (in portuguese).* [S.l.]: Revista Pesquisa FAPESP, 2016. International Journal of Bio-Inspired Computation, mai., 4, 2016, disponível em <https://revistapesquisa.fapesp.br/enxames-de-robos/>, accessed 13 May 2018. 44

KENNEDY, J.; EBERHART, R. Particle swarm optimization. In: *Proceedings of ICNN'95 - International Conference on Neural Networks*. [S.l.: s.n.], 1995. v. 4, p. 1942–1948 vol.4. 44

KIRTLEY JAMES L, T. *Electric power principles: sources, conversion, distribution and use*. [S.l.]: John Wiley & Sons, 2020. Available online: <https://onlinelibrary.wiley.com/doi/book/10.1002/9781119585305>, accessed 10 October 2023. 24, 25

KIRYATI N.; ELDAR, Y. B. A. M. *A Hough Probabilistic Hough Transform*. [S.l.]: Pattern recognition, Elsevier. v. 24, n. 4, [14] (pp. 303–316), 1991. Available online: <https://www.sciencedirect.com/science/article/abs/pii/003132039190073E>, accessed 17 October 2023. 57

LI, J.; CHEN, R. A distributed task scheduling method based on conflict prediction for ad hoc uav swarms. *Drones*, v. 6, n. 11, 2022. ISSN 2504-446X. Disponível em: <https://www.mdpi.com/2504-446X/6/11/356>. 37

LI, Y. et al. A method for autonomous navigation and positioning of uav based on electric field array detection. *Sensors*, MDPI AG, v. 21, n. 4, p. 1146, Feb 2021. ISSN 1424-8220. Disponível em: <http://dx.doi.org/10.3390/s21041146>. 36

LOPES, S. *Os 10 Melhores Drones com Maior Tempo de Voo de 2022 (in portuguese)*. 2022. Disponivel em <https://filmora.wondershare.com.br/drones/drones-with-longest-flight-time.html?gad_source=1&gclid=CjwKCAiAu9yqBhBmEiwAHTx5pxrw-8IjqgE-9J3IQpk86jzB6c36ZBEDBdeyVd1-If9xksbuK10HbhoBwE>, 2022, accessed 17 November 2023. 86

LUO, P. et al. An ultrasmall bolt defect detection method for transmission line inspection. *IEEE Transactions on Instrumentation and Measurement*, v. 72, p. 1–12, 2023. 39

LUO, Y.; BAI, A.; ZHANG, H. Distributed formation control of uavs for circumnavigating a moving target in three-dimensional space. *Guidance, Navigation and Control*, v. 01, n. 3, 2021. 38

LUQUE-VEGA, L. F. et al. Power line inspection via an unmanned aerial system based on the quadrotor helicopter. In: *MELECON 2014 - 2014 17th IEEE Mediterranean Electrotechnical Conference*. [S.l.: s.n.], 2014. p. 393–397. 32, 34

MAANYU K. N.; RAJ, D. G. C. S. B. *A study on drone autonomy*. 2020. Available online: <http://www.ijater.com/Files/5fd7d25b-b3a9-49b8-89fc-5b00f81b082e_IJATER_51_04.pdf>, accessed 10 October 2023. 47, 48

MACHADO G, V. *Resenha Janeiro 21 - Claro Final. (in portuguese)*. [S.l.]: Empresa de Pesquisa Energética (EPE), 2021. Available online: <https://www.epe.gov.br/sites-pt/publicacoes-dados-abertos/publicacoes/PublicacoesArquivos/publicacao-153/topico-574/Resenha%20Mensal%20-%20Dezembro%202021%20(base%20Novembro).pdf>, accessed 10 October 2023. 24

MARTINS, W. M. *Estudo de Algoritmos de Visão Computacional para Identificação e Desvio de Objetos em Tempo Real: Uma aplicação para quadrotores (in portuguese)*. 2018. Dissertação (Mestrado em Ciência e Tecnologia da Computação - Programa de Pós-graduação em Ciência e Tecnologia da Computação, POSCOMP, Universidade Federal de Itajubá - UNIFEI, Itajubá, MG, 2018. Disponível em: <https://repositorio.unifei.edu.br/xmlui/bitstream/handle/123456789/1874/dissertacao_2019009.pdf?sequence=1&isAllowed=y>. 84

MARTINS, W. M. *Percentage of certainty that the trained network achieved in each identified object*. 2023. Disponível em: <https://youtu.be/uPFJpB3_DFg?si=kGcDYxsCPKdIVnIE>. 60

MARTINS, W. M. et al. Low-cost uav for medical delivery. *IAES International Journal of Robotics and Automation*, IAES Institute of Advanced Engineering and Science, v. 9, n. 4, p. 233, 2020. 29

MARTINS, W. M. e. a. *Tracking for inspection in energy transmission power lines using unmanned aerial vehicles: a systematic review of current and specific literature*. [S.l.]: IAES International Journal of Robotics and Automation, IAES Institute of Advanced Engineering and Science. v. 9, n. 4, [1] (p. 233), 2020. Available online: <https://ijra.iaescore.com/index.php/IJRA/article/view/2029>, accessed 17 October 2023. 57, 66, 81

MATARIĆ, M. J. *The Robotics Primer*. [S.l.]: Massachusetts Institute of Technology, 2007. ISBN 978-3-662-48847-8. 45

MAZA, I. et al. Multi-uav cooperation and control for load transportation and deployment. In: _____. *Selected papers from the 2nd International Symposium on UAVs, Reno, Nevada, U.S.A. June 8–10, 2009*. Dordrecht: Springer Netherlands, 2010. p. 417–449. ISBN 978-90-481-8764-5. Disponível em: <https://doi.org/10.1007/978-90-481-8764-5_22>. 36

MEDEIROS, F. A. *Desenvolvimento de um veículo aéreo não tripulado para aplicação em agricultura de precisão (in portuguese)*. 2017. Dissertação (Mestrado em Engenharia Agrícola) - Universidade Federal de Santa Maria, Santa Maria, 2007. 40

MENENDEZ, O. A. et al. Vision based inspection of transmission lines using unmanned aerial vehicles. In: IEEE. *2016 IEEE International Conference on Multisensor Fusion and Integration for Intelligent Systems (MFI)*. 2016. p. 412–417. Disponível em: <https://ieeexplore.ieee.org/document/7849523>. 33

MICROSOFT. *Welcome to AirSim*. 2019. Disponível em: <https://microsoft.github.io/AirSim/>. 54

MOLRC1. *Hélices: plástico e fibra de carbono*. 2016. Disponivel em <https://www.molrc.com/?p=888>, 2016, accessed 10 September 2018. 88

MOLRC2. *Como montar um drone você mesmo: ESCs (in portuguese)*. 2016. Disponivel em <https://www.molrc.com/?p=1119>, 2016, accessed 10 September 2018. 90

MOSCATO, P. Una introducción a los algoritmos meméticos. *Inteligencia Artificial, Revista Iberoamericana de Inteligencia Artificial*, n. 19, p. 131–148, 2003. 46

MOTA, R. L. M. et al. *Expanding Small UAV Capabilities with ANN: A Case Study for Urban Areas Inspection*. 2014. British Journal of Applied Science Technology, 4(2), 387-398, 2014. 38

NETO, A. de M. *Navegação de robôs autônomos baseada em monovisão (in portuguese)*. 2017. Dissertação (mestrado) - Universidade Estadual de Campinas, Faculdade de Engenharia Mecanica, Campinas, SP, 2017. 38

NETO, M. da S. *Agricultura de Precisão com Drones (in portuguese)*. 2016. Disponivel em <http://blog.droneng.com.br/agricultura-de-precisao-com-drones/>, 2016, accessed 05 September 2018. 38

NISTER, D.; NARODITSKY, O.; BERGEN, J. *Visual Odometry for Ground Vehicle Applications*. 2006. Princeton NJ 08530 USA, 2006. 37

OES. *Introdução Guia MAVSDK. (in portuguese)*. [S.l.]: OES, 2019. Available online: <https://mavsdk.mavlink.io/main/en/index.html> (in portuguese), accessed 17 October 2023. 52

OLSSON, E. e. a. *Using a Drone Swarm/Team for Safety, Security and Protection Against Unauthorized Drones*. [S.l.]: Lect.Notes Mechanical Engineering, Uday Kumar et al. (Eds): International Congress and Workshop on Industrial AI and eMaintenance., 2023. Available online: <https://ec.europa.eu/info/funding-tenders/opportunities/portal/screen/opportunities/topic-details/cip-01-2016-2017>, accessed 18 October 2023. 39

OPENCV. *Embarcados, Linux, programação e IoT (in portuguese)*. 2017. <https://www.dobitaobyte.com.br/acelerometro-giroscopio-bussola-altimetro-barometro-imu/>, accessed 27 Abr. 2017. 93

PANIGRAHI, B. K.; SHI, Y.; LIM, M.-H. *Handbook of Swarm Intelligence: Concepts, Principles and Application*. [S.l.]: Springer-Verlag, Berlin Heidelberg, 2011. v. 8. 45, 46

PAUL, C. R. *Introduction to electromagnetic compatibility*. 2006. Available online: <https://books.google.com.br/books?id=A-eLEAAAQBAJ&printsec=frontcover&hl=pt-BR#v=onepage&q&f=false>, accessed 10 October 2023. 26

QGC. *qgroundcontrol web site*. 2023. Disponível em: <http://qgroundcontrol.com/>. 53

RANGEL, R. K.; KIENITZ, K. H.; BRANDÃO, M. P. Sistema de inspecao de linhas de transmissao de energia electrica utilizando veiculos aereos nao-tripulados (in portuguese). Sep, 2009. Disponível em: <http://www.cta-dlr2009.ita.br/Proceedings/PDF/59018.pdf>. 27

RESENDE, G. V. d. *Segurança na manutenção de linhas de alta tensão. (in portuguese)*. [S.l.]: APTEL / PETROBRAS. XVI Seminário Nacional de Telecomunicações - Painel: Segurança, Meio Ambiente e Saúde – Rio de Janeiro -RJ, Brazil., 2017. Available online: <https://dokumen.tips/documents/seguranca-na-manutencao-de-linhas-de-alta-tensao-seguranca-em-linhas-de.html?page=1> (in portuguese), accessed 18 October 2023. 26

RESENDE, G. V. de. Segurança na manutenção de linhas de alta tensão (in portuguese). In: APTEL / PETROBRAS. *XVI Seminário Nacional de Telecomunicações – Rio de Janeiro -RJ*. 2017. Painel: Segurança, Meio Ambiente e Saúde. Disponível em: <https://www.aptel.com.br/event/92/home-93>. 27

REYNOLDS, C. W. Flocks, herds and schools: A distributed behavioral model. In: *Proceedings of the 14th Annual Conference on Computer Graphics and Interactive Techniques*. New York, NY, USA: Association for Computing Machinery, 1987. (SIGGRAPH '87), p. 25–34. ISBN 0897912276. Disponível em: <https://doi.org/10.1145/37401.37406>. 74, 75

RIBEIRO, L. do V. *Estudo de Algoritmos de Visão Computacional para Identificação e Rastreamento de Linhas de Transmissão de Energia Elétrica com Multirotores. (in portuguese)*. 2019. 25

ROBOFLOW. *Faster-R-CNN*. 2022. Disponível em: <https://roboflow.com/model/faster-r-cnn>. 60

SAHIN, E. Swarm robotics: From sources of inspiration to domains of application. In: . [S.l.: s.n.], 2004. p. 10–20. 44

SAUNDERS, J.; BEARD, R.; MCLAIN, T. *Obstacle Avoidance Using Circular Paths*. 2007. AIAA Guidance, Navigation and Control Conference and Exhibit, 2007. 37

SHAH, S. e. a. *Airsim: High-fidelity visual and physical simulation for autonomous vehicles*. [S.l.]: SPRINGER. Field and service robotics. [15] (pp. 621–635)., 2018. Available online: <https://arxiv.org/abs/1705.05065>, accessed 17 October 2023. 53

SHIGUEMORI, E. H.; MARTINS, M. P.; MONTEIRO, M. V. T. *Landmarks recognition for autonomous aerial navigation by neural networks and Gabor transform*. 2007. IPAS, v. 6497, n. 12, p. 1–9, 2007. 37

SHIMA, T.; RASMUSSEN, S. *UAV Cooperative Decision and Control: Challenges and Practical Approaches*. [S.l.]: Springer, Society for Industrial and Applied Mathematics, Philadelphia, PA,USA., 2009. v. 1. 45

SHRIT, O. e. a. *A new approach to realize drone swarm using ad-hoc network*. [S.l.]: IEEE 16th Annual Mediterranean Ad Hoc Networking Workshop (Med-Hoc-Net). [6] (pp. 1-5), 2017. Available online: <https://hal.archives-ouvertes.fr/hal-01696735>, accessed 17 October 2023. 49

SILVA, A. F.; LEMONGE, A. C. C.; LIMA, B. S. L. P. Algoritmo de otimização com enxame de particulas auxiliado por metamodelos (in portuguese). In: *SIMMEC/EMMCOMP 2014: XI Simpósio de Mecânica Computacional e II Encontro Mineiro de Modelagem Computacional*. [S.l.: s.n.], 2014. 45

SILVA G. C. DA; MUNARO, M. *Especificações de um sistema adequado para postes de escalada (in portuguese)*. [S.l.]: Seminário Nacional de Distribuição de Energia Elétrica (SENDI) in Olinda-Pernambuco, Brazil., 2008. Available online: <https://www.cgti.org.br/publicacoes/wp-content/uploads/2016/01/Especificac%CC%A7o%CC%83es-de-Um-Adequado-Sistema-Para-Escalada-em-Postes.pdf> (in portuguese), accessed 18 October 2023. 26

SILVA, R. L. da. *Defeitos e falhas nas linhas de transmissão. (in portiguese)*. 2011. 26

SMITH, J.; SIMONS, C. L. A comparison of two memetic algorithms for software class modelling. In: *Proceeding of the fifteenth annual conference on Genetic and evolutionary computation conference (GECCO 2013)*. [S.l.: s.n.], 2013. p. 1485–1492. 45

SPATA, M. O. et al. *Deep Learning Algorithm for Advanced Level-3 Inverse-Modeling of Silicon-Carbide Power MOSFET Devices*. 2023. 34

STUBBLEBINE, A. et al. *Laser-Guided Quadrotor Obstacle Avoidance*. 2015. AIAA Infotech @ Aerospace. 2015. 38

THONG-IA, S.; CHAMPRASERT, P. Gene-ants: Ant colony optimization with genetic algorithm for traveling salesman problem solving. In: *2023 International Technical Conference on Circuits/Systems, Computers, and Communications (ITC-CSCC)*. [S.l.: s.n.], 2023. p. 1–5. 46

TOROK, M. M.; GOLVARPAR-FARD, M.; KOCHERSBERGER, K. B. *Image-Based Automated 3D Crack Detection for Post-disaster Building Assessment*. 2014. Journal of Computing in Civil Engineering, v. 28, n.5, 2014. 38

TRIVEDI, N. B. e. a. *Geomagnetically induced currents–gic in electric power system at low latitudes in brazil: A case study. [161] (pp. cp–160).* [S.l.]: EUROPEAN ASSOCIATION OF GEOSCIENTISTS & ENGINEERS. 9th International Congress of the Brazilian Geophysical Society., 2005. Available online: <https://sbgf.org.br/mysbgf/eventos/expanded_abstracts/9th_CISBGf/SBGF402.pdf>, accessed 10 October 2023. 27

VARGAS, A. C. G. C. A. M. P. V. C. N. *Um estudo sobre redes neurais convolucionais e sua aplicação em detecção de pedestres. (in portuguese).* [S.l.]: SIBGRAPI—Conference on Graphics, Patterns and Images., 2016. 55

WAGSTER, J. et al. *Obstacle Avoidance System for a Quadrotor UAV.* 2012. Infotech@Aerospace 2012, Infotech@Aerospace Conferences, 2012. 38

WEISS, A. et al. *Safe Positively Invariant Sets for Spacecraft Obstacle Avoidance.* 2014. Journal of Guidance, Control, and Dynamics, Vol. 38, No. 4 : pp. 720-732, 2014. 38

WILLEE, H. *Choosing a Ground Station.* 2019. Available online: <https://ardupilot.org/copter/docs/common-choosing-a-ground-station.html>, accessed 17 October 2023. 52

WU, Y. et al. Swarm-based 4d path planning for drone operations in urban environments. *IEEE Transactions on Vehicular Technology*, v. 70, n. 8, p. 7464–7479, 2021. 36

WU, Y. et al. Overhead transmission line parameter reconstruction for uav inspection based on tunneling magnetoresistive sensors and inverse models. *IEEE Transactions on Power Delivery*, IEEE, v. 34, n. 3, p. 819–827, 2019. Disponível em: <https://ieeexplore.ieee.org/document/8603761>. 33, 35

XIE, X. et al. A multiple sensors platform method for power line inspection based on a large unmanned helicopter. *Sensors*, Multidisciplinary Digital Publishing Institute, v. 17, n. 6, p. 1222, 2017. Disponível em: <https://www.mdpi.com/1424-8220/17/6/1222>. 33, 35

YAN, Z. et al. *A Real-Time Reaction Obstacle Avoidance Algorithm for Autonomous Underwater Vehicles in Unknown Environments.* 2018. Sensors 2018, 18, 438; doi:10.3390/s18020438. 38

YAN, Z. P. et al. *Globally Finite-Time Stable Tracking Control of Underactuated UUVs.* 2015. Ocean Eng. 2015, 107, 132–146. 38

YANG Z.; LIN, F. C. B. M. *Survey of autopilot for multi-rotor unmanned aerial vehicles.* [S.l.]: IEEE. IECON 2016-42nd Annual Conference of the IEEE Industrial Electronics Society. [6] (pp. 6122–6127)., 2016. Available online: <https://ieeexplore.ieee.org/document/7793820>, accessed 17 October 2023. 51

ZAVALA-RIO; SOERENSEN, C. A. G. An introduction to swarm robotics. *ISRN Robotics*, v. 2013, n. 1, p. 2356–7872, 2013. Cited By :61. Disponível em: <https://doi.org/10.5402/2013/608164>. 44

ZEILER M. D.; FERGUS, R. *Visualizing and understanding convolutional networks.* [S.l.]: SPRINGER. European conference on computer vision. [16] (pp. 818–833, 2014. Available online: <https://arxiv.org/abs/1311.2901>, accessed 17 October 2023. 55

ZHANG, X. et al. A binocular vision based auxiliary navigation system of the unmanned aerial vehicle for power line inspection. In: IEEE. *2016 3rd International Conference on Systems and Informatics (ICSAI).* 2016. p. 291–296. Disponível em: <https://ieeexplore.ieee.org/abstract/document/7810970?> 32, 34

ZHOU, G. et al. Robust real-time uav based power line detection and tracking. In: IEEE. *2016 IEEE International Conference on Image Processing (ICIP)*. 2016. p. 744–748. Disponível em: <https://ieeexplore.ieee.org/document/7532456>. 33, 35

ZORMPAS, A. et al. Power transmission lines inspection using properly equipped unmanned aerial vehicle (uav). In: IEEE. *2018 IEEE International Conference on Imaging Systems and Techniques (IST)*. 2018. p. 1–5. Disponível em: <https://ieeexplore.ieee.org/document/8577142>. 32, 35